スメクティック液晶に於ける電気傾斜効果

The Electroclinic Effect in Smectic Liquid Crystal

楊　映保

Yang Ying Bao

March, 1992

学位論文

(1)

論文題目

The Electroclinic Effect in Smectic Liquid Crystal

スメクティック液晶に於ける電気傾斜効果

工学研究科博士後期課程　電子情報工学専攻

平成元年度入学

学籍番号　89823013

氏名　　楊　映保

The Electroclinic Effect in Smectic Liquid Crystal

by

Yang Ying Bao
M.S.Yamanashi University

Thesis directed by
Professor Shunsuke Kobayashi

A Thesis Submitted to
the Faculty of the Graduate School of
Tokyo University of Agriculture and Technology
in Partial Fulfillment of the Reguirements
for the Degree of Doctor of Engineering
Division of Electronic and Information Engineering
12 November, 1991

ACKNOWLEDGMENT

The author would like to acknowledge to Mr.LCD-Professor Shunsuke Kobayashi for his continuing guidance and encouragement throughout the present work. The author also would like to express his appreciation to Prof. Katsuaki Sato, Prof. Nobuyoshi Koshida, Prof. Yoshiyuki Suda, and Takeshi Shiina for their invaluable advice and encouragement. The present work is essentially made in collaboration with them through freqent, stimulating and fruitful discussions.

The author wishes to thank Mr.Ehara, the manager of EHC Co.,Ltd, for his warm support in these three years. The author also thank Prof. K.Hiroshima of Yamanashi Univ. for his helpful advice in these years.

The author is indebted to Mr.A.Mochizuki for the preparation of electrclinic material, to Mr.Kimura for the preparation of software in the measurement. The author is also grateful to Mr.N.Nakamura and Mr.T.Ban for his cooparation throughout this research. The author would also like to thank to Dr.C.M.Gomes and other colleagues of Kobayashi Lab. for their cooparation in these years.

Finally, the author would like to thank his wife and his family for their continuous understanding and encouragement.

Abstract

The electroclinic (EC) effect , which appears in smectic A phase near the transition temperature, is one kind of tunable optical transmission variation resulted from the tilting of LC director perpendicular to the applied electric field. EC is known as the most fast electro optical (E-O) effect in the E-O effects which have been found in liquid crystal, of a typical response time approaching to 1μs. This effect is expected to find wide application in the optical computing and optical processing.

EC effect was discoveried by R.B.Meyer in 1975, as a critical behavior in the phase transition process from the smectic A (SmA) phase to chiral smectic C (SmC*) phase. Recently, because large transmission variation has been realised with the improvement of materials, EC effect attracts wide attention in the aspect of optical computing. But the basic property of EC effect remains almostly unknown. To make effective use of EC in optical computing practically, it is necessary to made the basic property of EC clear.

In this thesis we have investigated the origin and the basic property of electroclinic effect. As a conclusion, it has been made clear by this thesis, that the electroclinic effect appears not only in chiral SmA phase, but also in the chiral SmC* phase, even in chiral nematic phase. The amptitude of EC effect is found to show divergent increase when the sample temperature approaches to the transition point, the temperature dependence of EC coefficient (the tilt angle via the electric field strength) is shown to be $K_o(T-Tc)^{-1}$, where Tc represents the transition point, and ratio of K_{oA}, for SmA phase, and K_{oC} for

SmC* is measured to be 2.3. This value is near to the predicated factor 2 of analyzation by modefied Landau phase transition theory. The dielectric properties of EC effect were also studied, the dielectric constant, corresponding to EC, at a frequency of 2KHZ, show a divergence at Tc. The smectic layer deformation where the LC director tilts has been studied. It has been made clear that the smectic layer change its direction together with modulation in the planes parallel to the substrate to keep its thickness, when the LC director was tilted by electric field.

We modified Landau phase transition theory to interpret electroclinic effect discovered in SmC* phase, with using an order parameter which was defined as the tilt angle which describe the symmetry difference between SmA (belong to point group $D_{\infty h}$) and SmC* (belong to C_{2h}), and the polarization P induced by the electric field. The analyzation predicts that the temperature dependences of electroclinic coefficient K, dielectric constant ε , and response time τ vary as $(T-T_c)^{-1}$, where T_c is the transition point between SmA and SmC* phase. These results have been verified experimently, good agreement has been found.

In addation to the research on the material property, the EC device properties have also been studied. We have discovered, for the first time, the EC effect show strong surface orientation dependence. The amplitude of EC effect decrease with the rubbing number of orientation film, and decrease with the decrease of sample thickness. we have found that the transition point Tc between SmA and SmC* phase measured from the divergent peak of dielectric constant, is largely influenced by the surface orientation. The transition point Tc shift to low

temperature when the sample thickness decreases, but to high temperature when the rubbing number of orientation increases.

The surface dependence of EC effects were discussed by introducing an surface potential, at the physical surface, which was consisted of an two term polynomial of the tilt angle of LC director, a linear term corresponding to the polar interaction, and square term for nonpolar interaction between the surface and LC layer. From analyzation, we found that non polar part contributes only to modify the phase transition point, While the polar part not only change the transition point, but also change the curve of the phase transition.

The analysed results where the surface influence was considered, has been verified experimently. It is shown that the theoretical model interpreted the experimental results sucessfully.

CONTENTS

ACKNOWLEDGMENT page

ABSTRACT <1>

TABLE OF CONTENT <4>

CHAPTER I INTRODUCTION 1

§1.1 Preface 1

§1.2 Electroclinic Effect 2

§1.3 The research of the electroclinic effect 3

§1.4 The content of this thesis 4

CHAPTER II THE ELECTRO OPTICAL EFFECTS IN LIQUID CRYSTAL 7

§2.1 Introduction 7

§2.2 The basic property of liquid crystal 9

§2.3 The continuum theory for liquid crystal 13

§2.4 The electroclinic effects in liquid crystal 14

CHAPTER III THE FERROELECTRICITY IN LIQUID CRYSTAL 19

§3.1 General discussion of ferroelectricity in LCs 19

§3.2 A general discussion of ferroelectricity in chiral smectic phase 24

§3.3 The experimental results of ferroelectric liquid crystal 27

§3.4 Conclusion 39

CHAPTER IV ELECTROCLINIC EFFECT 40

§4.1 The phenomenal theory of electroclinic effect 40

§4.2 The electroclinic effect in chiral smectic-A phase 43

§4.3 The experimental results on electroclinic effect 46

§4.4 Conclusion 59

CHAPTER V SEVERAL PROPERTY OF ELECTROCLINIC EFFECT 60

§5.1 The dielectric property of electroclinic effect ····· 60
§5.2 The dynamic behavior of electroclinic effect ····· 72
§5.3 The layer response in electroclinic effect ····· 77
§5.4 Conclusion ····· 81

CHAPTER VI THE SURFACE ANCHORING DEPENDENCE OF ELECTROCLINIC EFFCET ····· 83
§6.1 The optical variation of electroclinic effect result from surface anchoring potential ····· 85
§6.2 The influence of surface anchoring strength on dielectric constant ····· 95
§6.3 Conclusion ····· 104

CHAPTER VII THE PHENOMENAL THEORY FOR SURFACE ANCHORING EFFECTS IN ELECTROCLINIC EFFECT ····· 105
§7.1 The surface potential energy ····· 105
§7.2 The electroclinic coefficient and dielectric constant in smectic A phase ····· 111
§7.3 The electroclinic effect in smectic C phase ····· 113
§7.4 The surface potential dependence of the transition point ····· 118
§7.5 Conclusion ····· 122

CHAPTER VIII CONCLUSION ····· 123

REFERENCE ····· 126
LIST OF PUBLICATION ····· 128

Chapter I INTRODUCTION

§1.1 Preface

The development of liquid crystals (LCs) as basic electronic materials similar to semiconductors and insulators, is now an active and viable field. Liquid crystals exhibit good electro-optical properties due to their anisotropic nature and therefor have wide display applications. Liquid crystal displays (LCDs) are known for their flexible sizing properties, flatness, low power consumption and high information storage capacity, making them competitive with cathode ray tubes (CRTs) and other flat panel displays.

The most widely used LC materials in electro-optic devices today are the nematic liquid crystals (NLCs). The response time of NLCs, which is dependent on the dielectric anisotropy ($\Delta\varepsilon$), is in the millisecond range. The slow response time decreases the potential utilization of NLCs in video TV and optical computers. Such a problem was answered with the discovery of ferroelectric effects in chiral smectic C liquid crystals by R.B.Meyer[2].

The ferroelectric effect exhibits a direct coupling between the electric field **E** and the spontaneous polarization **P** in the form of **P*E**. This gives rise to very high switching speeds near the microsecond order. N.A. Clarck and S.T. Lagerwall[3] further improved the use of ferroelectric liquid crystals (FLCs) in electro-optical devices through the surface stabilized ferroelectric liquid crystal (SSFLC) which has a high response speed and show memory effect.

Today, a new electro-optic phenomenon, the electroclinic (EC) effect[4-9] has been found. The EC effect gives switching

time below the microsecond range, approaching the solid device capability[10].

§1.2 Electroclinic Effect[4-9]

The electroclinic effect appears in the smectic A phase, in the vicinity of the phase transition temperature range from smectic A (SmA) to chiral smectic C (SmC*) phase. Considered as a pretransition effect, it is a weaker director tilt induced by an external electric field.

The smectic A phase exhibits a layered structure with the LC director perpendicular to it. However, for the smectic C phase, the director is orientated at an angle θ with respect to the normal to the layer.

The molecules are free to rotate about their long axis in SmA phase. So the smectic A phase is uniaxial with the long molecular axis or the normal to the smectic layers, and a twofold axis perpendicular to the molecules. All of the planes containing the molecular long axis and the twofold axis are mirror planes. If an electric field **E** is applied parallel to the smectic layers, the free rotation is biased due to the tendency of the traverse component of the permanent molecular dipole **P** to orient parallel to the field. All of the symmetry elemants are destroyed, only one twofold axis along the electric field and one mirror plane containing electric field **E** and molecular long axis **n**(**Pn** plane) are maintained. The mirror plane corresponds to a free energy minimum, so no tilting of LC director appears in a non chiral system.

However, for the smectic A phase consisted of optical active molecules (chiral molecules), the chirality of the phase destroys all mirror symmetries, the **Pn** plane does not

maintain as a minimum for free energy, therefor, the molecules tilt away from **Pn**. For small field, the rotation bias and the induced polarization are linear to the field strength; the induced tilt angle is proportional to the field strength. The electric field induced tilting of LC director of the chiral smectic A phase is referred to as the electroclinic effect (EC) effect.

The rotation of LC molecules around their long axis show an relaxation frequency of tens MHZ in the SmA phase, so the EC effect shows response time even below microsecond. This high speed, together with the linearity, low power consumption, flexible size and high capability for storage information make EC to be the most promising E-O effect in the area of optical processing and optical computing.

§1.3 The research of electroclinic effect

The EC effect was predicated by R.B.Meyer[4], theoretically, Garoff and Meyer[5] confirmed the predication experimentally by using the dectloxybenzylidene-p'-amino -2-methlybutyleinamate (DOBAMBC). They used the sample structure where the smectic layers were parallel to the substrate. The electric field was applied in the traverse direction and the tilt of the LC director was determined by the measurements of induced birefringence. This system is not practical due to the limitations in the applied field and the difficulty in producing a monodomain smectic A phase. G. Anderson[6] et.al., improved the Garoff geometry and developed the ECE to a applicable level. Instead of a planer alignment, they used one in which the smectic layer perpendicular to the substrate. Such geometry produced a uniform director alignment, hence a

strong electric field and a smectic A monodomain could be easily realized. An optical modulation of 6% or a 5-degree variation range of tilt angle was obtained. Moreover the Anderson group piled up several pieces of electroclinic cells for larger optical variations. Experimental work is complemented by the research on the synthesis of materials where Y.Ouchi[11], et. al. reported a giant ECE in the smectic A phase.

The theoretical basis for the existence of the ECE and its relation to other material properties remain unknown. The only interpretion of the electrolcinc effect in given by the modified Landau-de Gennes theory[11-15]. Sin Doo Lee and Patel[8,9] discussed the nonlinear behavior of ECE in the vicinity of the transition. The existence of the ECE in other phases as well as magnetism-induced effects[16] have also been reported.

From dielectric point of view, the electroclinic effect corresponds to the soft mode in SmA [17,18] or SmC* which contains chiral dopants, with respect to the Goldstone mode. In the SmA phase, only the soft mode exists, however, in the SmC* phase, besides the soft mode, another much stronger response, resulted from Goldstone mode exists. In smectic C phase, the two dielectric response were distinguished from the temperature and frequency dependence of the dielectric constants[19-22]. However, it is difficulty to separate the two modes as no sufficient results have been obtained before the utilization of bias electric field parallel to the smectic layer, to suppress the Goldstone mode.

§1.4 The content of this thesis

The purpose of this research is to study the electroclinic effect systematically, including external field and temperature dependence, optical and dielectric properties and symmetry conditions of liquid crystal phases that exhibit such effect.

This thesis consists of the introduction and seven other chapters. In chapter 2, the basic properties of liquid crystal phases and sub-phase electro-optical effects will be discussed. The phenomenal theory of ferroelectric LC and the ferroelectric effect, which are closely related to the EC effect will be the topic of chapter 3. Chapter 4 is a theoretical study of the electroclinic effect, confirming its exitence in the smectic A phase and the possibility of observing it even in the ferroelectric phase. Some experimental results in support of the above discussion will be shown. Chapter 5 and 6 will give a thorough discussion of the experiments done and the major conclusions drawn. The confirmation of a temperature dependence of the form $(T-T_c)^{-1}$ and a divergent behavior of the dielectric constant in the vicinity of the phase transition will be discussed. Some dynamic feature of the EC effect, i.e., divergent decrease of switching time, for EC effect, above and below the transition point i.e. for the smectic A and the ferroelectric phase respectively are included.

For the first time, the dependence of phase transition point on surface anchoring based on measurements of the dielectric constant and the ECE coefficient was demonstrated. Such phenomenon could be explained by introducing a surface potential at the physical surface which is consisted of polynomial of the tilting angle, a linear term, corresponding

to the polar interaction, and a square term, corresponding to the non-polar interaction between surface and LC layer. Chapter 7 gives the conclusions.

Chapter II ELECTRO OPTICAL EFFECTs IN LIQUID CRYSTAL

§ 2.1 Liquid crystal phase

Liquid crystal is a type of state, similar to the solid, liquid and gaseous states, observed in organic compounds and other materails with rod-like and disc-shaped molecules (Fig.2.1). The discovery of liquid crystals dates back to 1888 when Reiniter observed optical anisotropies in molten cholesteryl benzoate under the polarizing microscope to a Liquid Crystalline mesophase. It was called liquid crystal because of properties intermediate between the solid crystalline and the ordinary isotropic liquid crystal phases.

Based on symmetry considerations, there are two types of liquid crystals: the nematic phase (Fig.2.2a) with an anisotropic structure due to the orientation of the long molecular axis; and the smectic phase (Fig.2.2b) which exhibits both long molecular axis orientation and layered structure of the molecular centers. Depending on the order of the layered structure, the smectic phase may be classified as SmA (Smectic A), SmB,....SmI. Liquid crystals may also be classified as chiral (the consistent molecules is different from its mirror image) or non-chiral systems. An ordinary nematic can be changed to a chiral nematic phase (N*) by dissolving a chiral material in it, resulting in a helical structure. A chiral smectic phase may also be obtained by doping with a chiral or opticall active material. The most widelyknown of these is the chiral smectic C.

The orientation of liquid crystal molecules is described

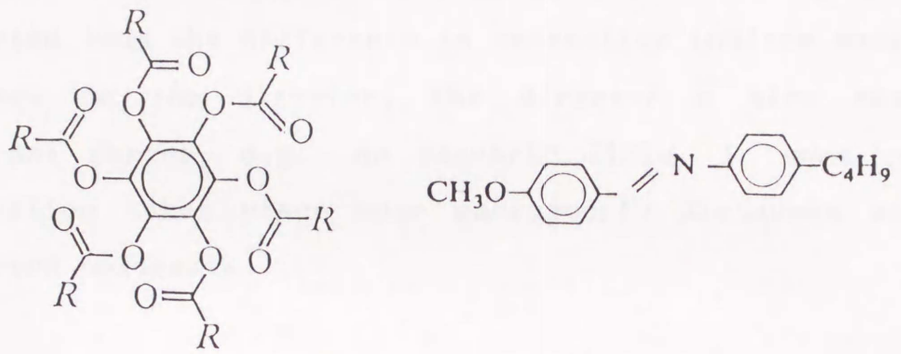

Fig.1-1. The structures of two typical organic compounds which show liquid crystal phase.

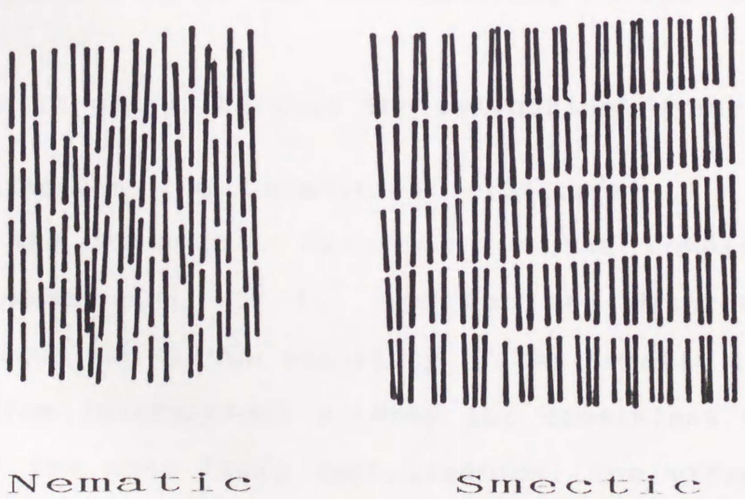

Fig.1-2. The orderring of molecules in the nematic phase and smectic phase.

in terms of the director $\bar{n}$. Many physical properties may be described in terms of $\bar{n}$. The dielectric anisotropy, $\Delta\varepsilon = \varepsilon - \varepsilon$, is the difference between the permittivity, parallel and perpendicular to $\bar{n}$. The birefringence, $\Delta n = n - n$, is likewise computed from the difference in refractive indices measured with respect to the director. The director $\bar{n}$ also responds to external forces, e.g., an electric field. In some cases, its distortion takes place over macroscopic distances and may be observed optically.

§2.2 The mean molecule-field theory for liquid crysta

The anisotropy of liquid crystals arises because of the tendency of the rod-like molecules in the fluid to align their long axis parallel to the director. At finite temperatures, the thermal motion of the molecules prevents perfect alignment with n; the orientations of the molecules are in fact distributed in angle.

For nematic phase, because the cylindrical symmetry, only one order parameter, by tradition $\frac{1}{2}(3\langle\cos^2\Theta\rangle-1)$, is used to describe the structure. Clearly, for the completely ordered nematic phase equal to 1, and for the disorderd isotropic phase, S equal to 0. The stability of the nematic liquid crystal results from interactions between the consistent molecules. In spirit of the mean field approximation, the effective single-molecule potential function v is used to mimic these intermolecular interaction. It is clear that the potential should be dependent on the angle between molecules. Ordinary, a

form of (2.2) is used.

$$V(\cos\Theta) = -\upsilon P2(\cos\Theta)\cdot S \qquad (2.1)$$

where P2() represents the second-order Legendre polynominal. In the mean field discussion, the interactions between individual molecules are represented by a potential of average force ignoring the fact that the individual behaviors and interactions of molecules may be widely distributed about the average.

The rules of classical statistical mechanics give the orientational distribution function $\rho(\cos\Theta)$ in terms of the potential function υ as

$$\rho(\cos\Theta) = Z^{-1}\exp\{\beta V(\cos\Theta)\} \qquad (2.2)$$

$$Z = \int_0^1 \exp\{\beta V(\cos\Theta)\}d(\cos\Theta) \qquad (2.3)$$

where Z is the single-molecular partition function and $\beta=1/KT$. The order parameter is just the average value of the second Legendre function for given molecule, therefor

$$S = \int_0^1 P2(\cos\Theta)\rho(\cos\Theta)d(\cos\Theta) \qquad (2.4)$$

substuting (2.3) into (2.5), it gives

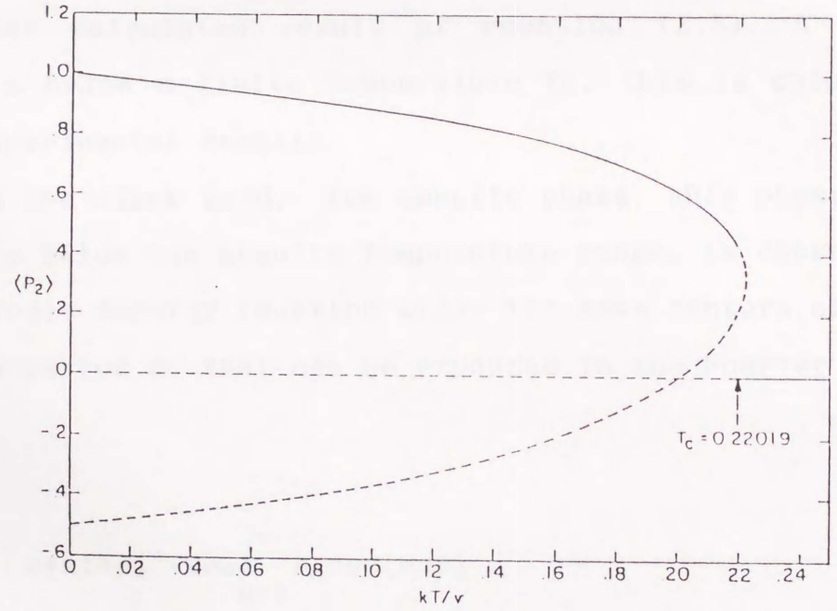

Fig. 2—Temperature dependence of the order parameter obtained from solving the self-consistency Equation, Eq. 2.5 . The stable equilibrium solutions are shown as the solid lines.

$$S=\frac{\int_0^1 P2(\cos\Theta)\exp\{\beta vP2(\cos\Theta)\cdot S\}\rho(\cos\Theta)d(\cos\Theta)}{\int_0^1 \exp\{\beta vP2(\cos\Theta)\cdot S\}d(\cos\Theta)} \qquad (2.5)$$

This is a self-consistent equation for the determination of the temperrature dependence of the order parameter S. Fig.2.1 shows computer calculated result of equation (2.5). A non zero S appears below a finite temperature Tc, this is coincident with the experimental results.

On the other hand, for smectic phase, this phase ordinarily appears below the nematic temperature range, is characterized by a periodic density function $\rho(Z)$, for mass centers of molecules, with a period d, that can be expanded in the Fourier series,

$$\rho(z)=\rho_o+2\rho_o\sum_{n=1}^{\infty}\rho_n\cos(nqz) \qquad (2.6)$$

z is the layer normal direction, $q=2\Pi/d$. In smectic phase, the interaction between two arbitrary planes, situated at z and z', is assumed to be

$$-U(z)=-\int_{-\infty}^{+\infty}A(K)\cos\{(z-z')\}dK \qquad (2.7)$$

where

$$A(K)=-\int_{-\infty}^{+\infty}U(z)\cos(kz)dK \qquad (2.9)$$

similar to the discussion for nematic phase, a self-consistent equation for ρ can obtained as

$$\rho = \frac{1}{z}\int_0^{2\Pi} \cos(n\phi)\exp\{-\beta Mt(\phi)\}d\phi \tag{5.10}$$

with

$$z = \int_0^{2\Pi} \exp\{-\beta Mt(\phi)\}d\phi \tag{5.11}$$

$$Mt(\phi) = \sum_{n=1}^{\infty} U_n \rho_n \cos(nqz) \tag{5.12}$$

The computer calculation of equation (2.$) shows that below transition point Tc, layer structure, with a period d, appears.

§2.3 The continuum theory for liquid crystal

Liquid crystals are elastic-like materials which can respond to distortions due to surface containts and external fields. Such distortions result in alignment deformations. The deformation is best described using the continuum theory first postulated by Osee-Zocher and put in mor complete form by Frank. This theory describes the distorted state in terms of a vector field n of variable orientation. The fundamental equation of the continuum theory is the free energy density, Fd, which in its simplest form is given by

$$f = \frac{1}{2} K_{11}(\nabla.n)^2 + \frac{1}{2} K_{22}(n.\nabla\times n)^2 + \frac{1}{2} K_{33}(n\times\nabla\times n)^2 \qquad (2.13)$$

where K_{11}, K_{22} and K_{33} are the splay, twist and bend elastic constants. In the chiral phase where a helical structure exists, the second term is modified to the form

$$\frac{1}{2} K_{33}(n\times\nabla\times n+p0)^2 \qquad (2.14)$$

It is possible to analyze all macroscopic orientations under the condition that the distortion energy must have a minimum in the stable state.

For smectic liquid crystals, the deformation of the layers must be considered. In general, twist deformation is not possible; but for chiral smectic C if small variations of layer thickness are negleted, a spontaneous bend and twist deformation may be introduced and equation 2.1 takes the form

$$f = \frac{1}{2} K_{11}(\nabla.n)^2 + \frac{1}{2} K_{22}(n.\nabla\times n+p)^2 + \frac{1}{2} K_{33}(n\times\nabla\times n+p)^2 . \qquad (2.15)$$

§2.4 The electro-optical (E-O) effect in liquid crystal

Optical variations induced by an external electric field is known as the electro-optical effect. Liquid crystals exhibit different types of electro-optical effect.

In nematic LCs, three types of electro-optical effects have

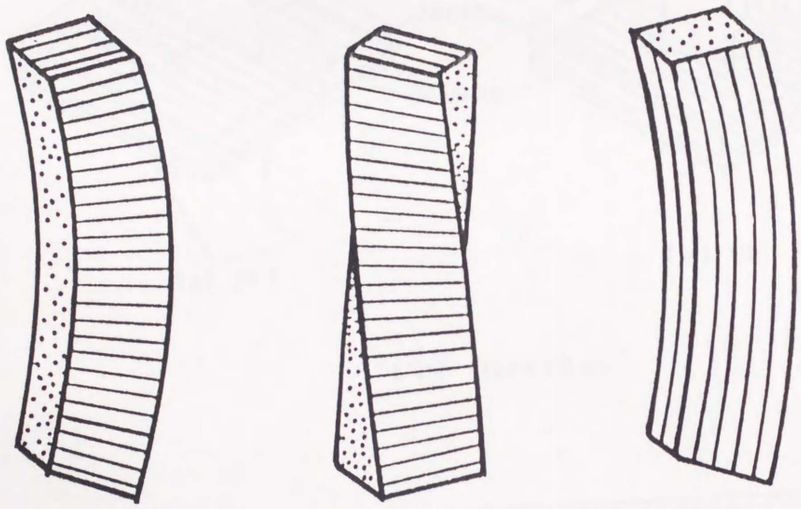

Fig.3. The director deformation in the nematic liquid crystal.

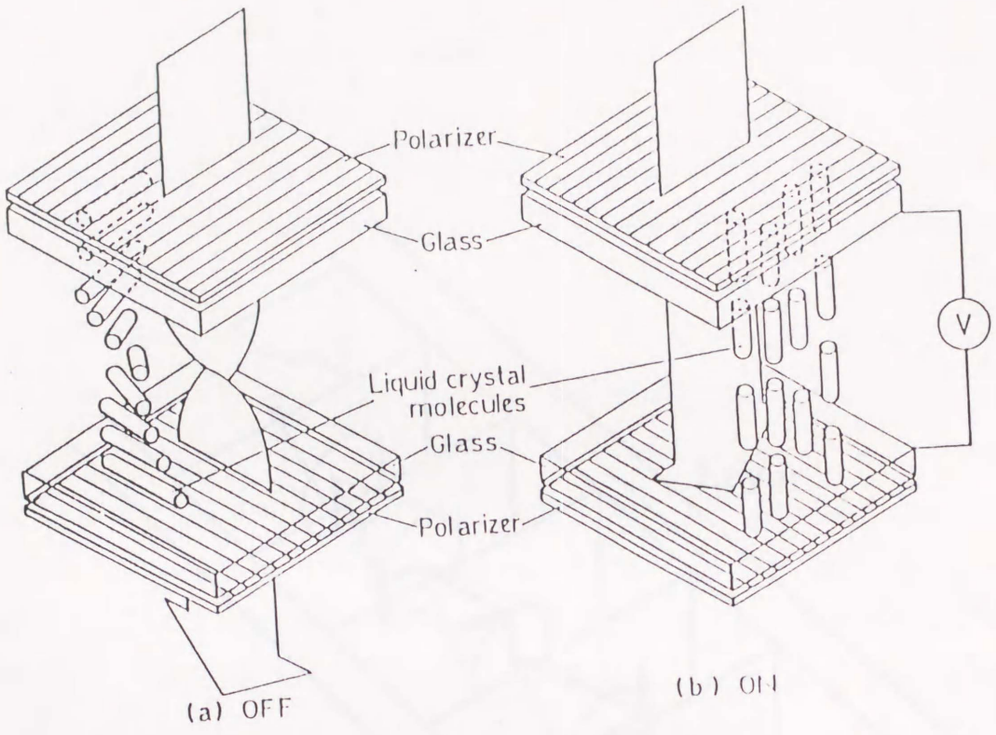

TN mode

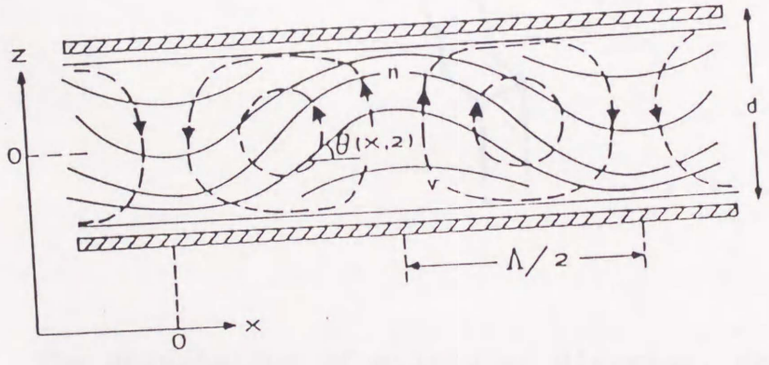

DSM mode

Fig.4. The electro optical effects in nematic liquid crystal

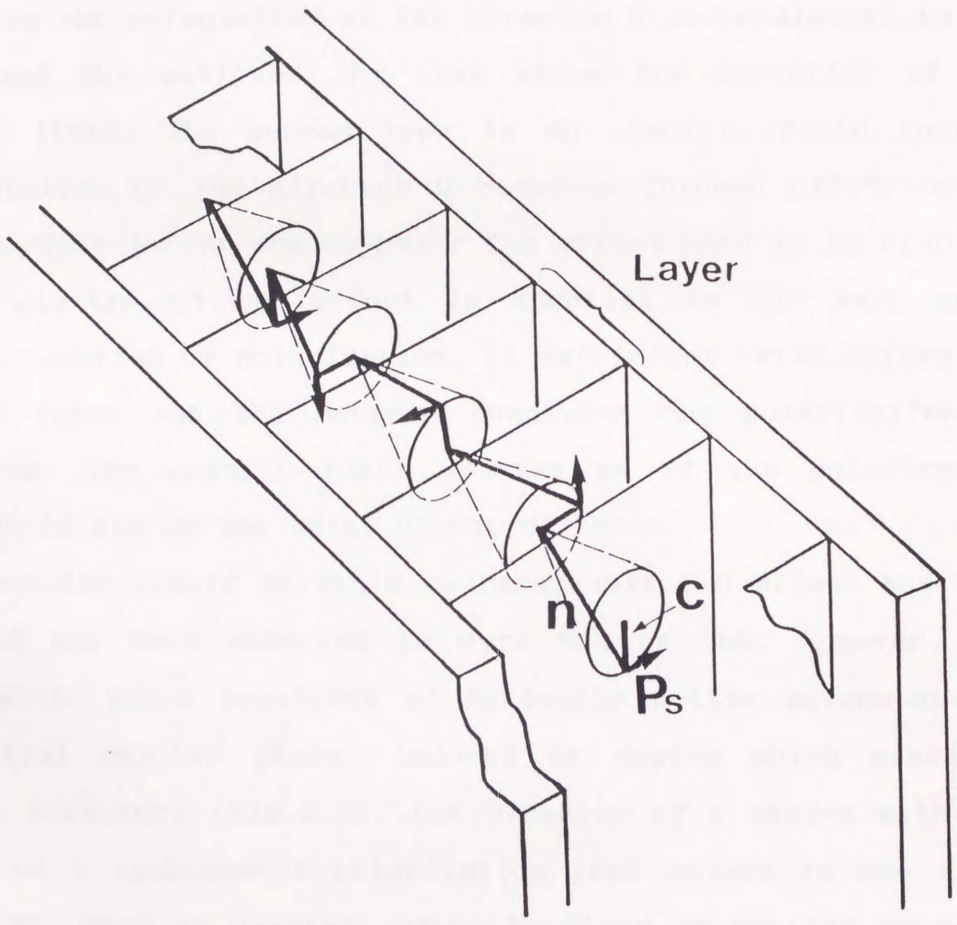

Fig.5. The orientation of molecular director, and spontaneous polarization of ferroelectric liquid crystal in thick sample.

been observed. The first is ion-current-induced perturbation of the director n which produces a strong scttering of light. For LC systems with negative dielectric anisotropy, the perturbation is due to the orientation of the director n perpendicular to the field and the motionof the ions along the direction of the applied field. The second type is an electric field induced reorientation of the director n observed through birefringence effects. This is the most popular E-O effect used in LC display. Athird electro-optical effect in nematics is the wave guide reduced rotation of polarization. If sufficient twist defors the nematic layer and the Mauguin condition for polarization is satisfied. the nematic layer bahaves as if the polarization rotation is due to the twist of the director.

In smectic liquid crystals no remarkable E-O effect has been observed has been observed in pure SmA or SmC. However, for the smectic phase consisted of optically active molecules, or the chiral smectic phase induced by doping which assume a helical structure (Fig.2.6), the director of n varies with the layer and a spontaneous polarization (Ps) exists in the layer direction. When an external electric field is applied to SmC*, Ps will result in an orientation parallel to the field. The torque experienced by n is PE. For this reason, a thick sandwich sample may be found in three states: the helical structure and two homogeneous states, with the Ps directed upwards or downwards depending on the field direction. This type of E-O effect has also been observed in other chiral smectic phases.In the chiral smectic A phase, a unique electro-optical effect known as the electroclinic effect has been found and this is the topic of this research.

Chapter III THE INTRODUCTION TO FERROELECTRICITY IN LC

The topics of theis thesis is electroclinic effect in smectic liquid crystals. In particular, we consider the electroclinic (EC) effect as a fluctuation of the ferroelectric behavior. Anomalous variations of ferroelectric properties, in the SmC* phase, leading to very large EC effect for special materials will also be discussed.

§3.1 General Discussion of Ferroelectricicty in LCs

R.B Mayer[2] pointed out that it is possible to observe ferroelectricity in a chiral smectic phase. Fig.6 shows a structure of smectic C and its high-temperature A phase. The molecules of smectic C exhibit monoclinic symmetry. In general, monoclinic cell contains three symmetry elements: a two-fold axis normal to the tilt direction and in the plane of the layer, a mirror plane normal to the two-fold axis, and a center of inversion. However, for a chiral molecule, no mirror planes or center of inversion exist. The molecular and environmental symmetry leaves the structure with only a two-fold axis. Therefore, it is necessary to have a spontaneous polarization parallel to the two-fold axis. On the other hand, in the high-temperature smectic A phase, the molecules rotatie freely about their long axes, which are perpendicular to the smectic layer. If each layer corresponds to the group D_∞, spontaneous polarization is not possible.

At temperature near the transition point, the behavior of the

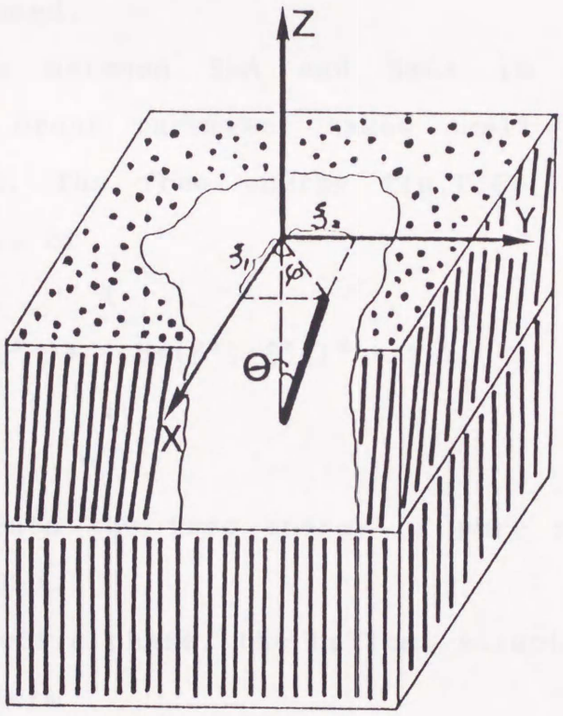

Fig.6. The coordinate for treating the fluctuation of the tilt angle Θ in the smectic phase in the vicinity of the transition point.

material may be described by the Landau-de Gennes phase transition theory. The order parameter of the transition are the components of the in-plane spontaneous polarization Px and Py which describe the order of the dipoles tranverse to the long axis. The quardratic combinations $\xi 1=nznx$ and $\xi 2=nzny$ of the molecular director n for the tilt-type description is also necessary to be used.

The transition between SmA and SmC* is a second order transition. The order parameter takes small values near the transition point. The free energy $f(p,T,\xi 1,\xi 2,Px,Py)$ may be expanded in powers of

$$f = \frac{1}{2} A^*(\xi_1^2+\xi_2^2) + \frac{1}{4} B^*(\xi^2_1+\xi^2_2)^2 + f_o \qquad (3.1)$$

where f_o represents the free energy of pure smectic A phase, $A=a(T-T_c)$, $a>0$, $B>0$.

In a chiral smectic phase, the helical structure is described by the Lifshifz term

$$\xi_1 \frac{d\xi_2}{dz} - \xi_2 \frac{d\xi_1}{dz} \quad . \qquad (3.2)$$

$$P_x \frac{dP_y}{dZ} - \frac{dP_x}{dZ} Py \quad . \qquad (3.2)$$

The symmetry of the high temperature SmA phase, allows two coupling terms between the molecular tilt and dipole ordering, i.e.

1 "Piezoelectriclike" coupling[35 37]

$$P_x\xi_2 - P_y\xi_1 \tag{3.4}$$

2 "Flexoelectric" term

$$P_x\frac{d\xi_1}{dz} + P_y\frac{d\xi_2}{dz} \tag{3.5}$$

Therefore the total free energy of the smectic phase in the neighborhood of the transition point is given by

$$f = \frac{1}{2}A*(\xi_1^2+\xi_2^2) + \Lambda*(\xi_1\frac{d\xi_2}{dz} - \xi_2\frac{d\xi_1}{dz})$$

$$+ \frac{1}{2}K_{33}\left[(\frac{d\xi_1}{dz})^2+(\frac{d\xi_2}{dz})^2\right] + \eta(\xi_1^2+\xi_2^2)(\xi_1\frac{d\xi_2}{dz} - \xi_2\frac{d\xi_1}{dz})$$

$$+ \frac{1}{2}\chi^{-1}(P_x^2 + P_y^2) - \mu(P_x\frac{d\xi_1}{dz} + P_y\frac{d\xi_2}{dz}) + C(P_x\xi_2 - P_y\xi_1) \tag{3.6}$$

In the coordinate system shown in Fig.6, the components of director n ξ_1, ξ_2 and the traverse components of the spontaneous polarization P_x, P_y can be described by

$$\xi_1 = \sin\Theta\cdot\cos(qz) \qquad \xi_2 = \sin\Theta\cdot\sin(qz)$$

$$P_x = -P_o\cdot\sin(qz) \qquad P_y = P_o\cdot\cos(qz) \tag{3.7}$$

In the smectic A phase, the magnitude of the fluctuation Θ is determined by the temperature, for small amplitudes of Θ, $\sin\Theta$ may be approximated by Θ. If we substitute (3.7) into (3.6) and take the average over the helix, we can write (3.8) as

$$
\begin{aligned}
Fg^{A} &= \frac{1}{2}\int_0^L f\cdot dz \\
&= \frac{1}{2}\cdot A\Theta^2 + \Lambda q\Theta^2 + \frac{1}{2}\cdot K_{33}q^2\Theta^2 + \frac{1}{2\chi}\cdot P^2 - (\mu q + C)\Theta P \\
&= A'\Theta^2 + \frac{1}{2\chi}\cdot P^2 - C\Theta P
\end{aligned}
\qquad (3.8)
$$

In the smectic C phase, Θ shows spontaneous tilting, hence higher order terms must be considered, Eq.(3.6) becomes

$$
\begin{aligned}
f &= \frac{1}{2}A^*(\xi_1^2+\xi_2^2) + \frac{1}{4}B^*(\xi^2{}_1+\xi^2{}_2)^2 + \Lambda^*\left(\xi_1\frac{d\xi_2}{dz} - \xi_2\frac{d\xi_1}{dz}\right) \\
&+ \frac{1}{2}K_{33}\left[\left(\frac{d\xi_1}{dz}\right)^2+\left(\frac{d\xi_2}{dz}\right)^2\right] + \eta(\xi_1^2+\xi_2^2)\left(\xi_1\frac{d\xi_2}{dz} - \xi_2\frac{d\xi_1}{dz}\right) \\
&+ \frac{1}{2}\chi^{-1}(P_x^2 + P_y^2) - \mu\left(P_x\frac{d\xi_1}{dz} + P_y\frac{d\xi_2}{dz}\right) + C(P_x\xi_2 - P_y\xi_1)
\end{aligned}
\qquad (3.8)
$$

similar averaging over one helical period gives

$$
Fg^{C} = \frac{1}{2}\int_0^L f\cdot dz
$$

$$= \frac{1}{2}\cdot A\Theta^2 + \frac{1}{4}B\Theta^4 + \Lambda q\Theta^2 + \frac{1}{2}\cdot K_{33}q^2\Theta^2 + \frac{1}{2\chi}\cdot P^2 - (\mu q + C)\Theta P$$

$$= \frac{1}{2}\ A`\Theta^2 + \frac{1}{4}B\Theta^4 + \frac{1}{2\chi}\cdot P^2 - C\Theta P \qquad (3.10)$$

If an electric field is applied, the coupling energy of the polarization and the field, E·P, must be integratedinto the total energy, so the Eq. (3.10) yields

$$F_{gce} = \frac{1}{2}\ A`\Theta^2 + \frac{1}{4}B\Theta^4 + \frac{1}{2\chi}\cdot P^2 - C\Theta P - E\cdot P \qquad (3.11)$$

where $A` = a*(T - T_o')$.

§3.2 A General Discussion of Ferroelectricity in SmC* phase for a material showing ECE

In the last section we have given the descriptions for the free energy of a chiral smectic liquid crystal. In this section, the possibility of ferroelectricity in two smectic phases, the SmC* and SmA phase, will be discussed.

The free energy of the chiral smectic C phase in the neighborhood of the transition point is given by

$$F_{gce} = \frac{1}{2}\ A`\Theta^2 + \frac{1}{4}B\Theta^4 + \frac{1}{2\chi}\cdot P^2 - C\Theta P \qquad (3.12)$$

The values of the variables Θ and P can be determined by imposing the condition that the free energy takes a minimum,

i.e. setting the first derivatives equal to zero

$$\frac{\partial F_{\varepsilon}^{c}}{\partial \Theta} = A`\Theta + B\Theta^3 - C\cdot P = 0 \qquad (3.13a)$$

$$\frac{\partial F_{\varepsilon}^{c}}{\partial P} = \chi^{-1}\cdot P - C\cdot\Theta = 0 \qquad (3.13b)$$

From (3.13b), P is described in terms of Θ as

$$P = \chi\cdot C\cdot\Theta. \qquad (3.14)$$

Substituting of (3.14) into (3.13a) results in

$$(A` - \chi C^2)\cdot\Theta + B\cdot\Theta^3 = 0 \quad . \qquad (3.15)$$

There are two solutions to equation (3.15). One is Θ =0.The other is a temperature-dependent one which can be written as

$$\Theta_o = - \left(\frac{A` - \chi C^2}{B} \right)^2 \qquad (3.16)$$

For simplicity, we write $A`-\chi C^2$ as $A^1 = a(T-Tc)$, $Tc=T0` + \chi C^2/a$. The incremental part of the transition point is due to the coupling of the polarization and the tilt of the chiral molecules.

The acceptable solution is the Eq.(3.16), because satisfies the minimum free energy condition.

Substituting (3.16) into (3.14), yields a non-zero value of the polarization at a temperature below the transition point which is given by

$$Ps = \chi \cdot t \cdot \Theta_o \ . \qquad (3.17)$$

Ps is the spontaneous polarization, which depends on temperature$(T - Tc)^{-1/2}$.

From above discussion, it has been shown that chiral molecules produce a linear coupling of polarization and molecular tilt. The chiral smectic C phase shows a ferroelectricity.

We now consider the situation of smectic A phase. From above section the free energy for smectis A phase has been described as,

$$F_{g}{}^{c}{}_{e} = \frac{1}{2} A' \Theta^2 + \frac{1}{2\chi} \cdot P^2 - C\Theta P \qquad (3.18)$$

The simultaneous state equations are written

$$\frac{\partial F_{g}{}^{c}}{\partial \Theta} = A' \Theta - C \cdot P = 0 \qquad (3.19a)$$

$$\frac{\partial F_{g}{}^{c}}{\partial P} = \chi^{-1} \cdot P - C \cdot \Theta = 0 \qquad (3.19b)$$

One solution of these equations is $\Theta = 0$, $P = 0$. In smectic A phase, $A > 0$, hence this solution corresponds the minimum of the free energy, it describes the real situation of smectic A phase. It is clear that the smectic A pahse is impossible to be a ferroelectric phase.

§3.3 The Experimental Results of Ferroelectric Liquid Crystals

The experimental results on the ferroelectric behavior in the chiral smectic C phasewill be introduced in this section. A comparison of two materials which exhibt and do not show the electroclinic effect will also be discussed.

① Layer structure of the smectic C phase

Smectic liquid crystals are characterized by layer structures. The thickness is temperature-dependent. Such dependence is very important for the smectic phase, since it explains the formation of the chevron layer structure in the SmC* phase. Fig.7 illustrates the X-ray diffraction result of 764E. The fact that only first order diffraction appears means that the layer smectic phase is only a density distribution. Hence, no real lattice exists. In (b) and (c), a comparison of two materails with and without the EC effect, was done. For an ordinary FLC only spontaneous tilting is resulted, resulting in a decrease of layer thickness. However EC effect materials show a divergent decrease of layer thickness, which is related to the anomalous tilt of FLCs.

We now consider another situation where the FLC material is sandwiched between cells with a homogeneous alignment. In the SmA phase, the layer is perpendicular to the substrate. After the transition, the thickness decreases. In order to maintain constant volume, the layer become tilted with respect to the substrates. To find the direction of the layer, the counter of diffractometer is fixed, when the sample is turned. Fig.10,11

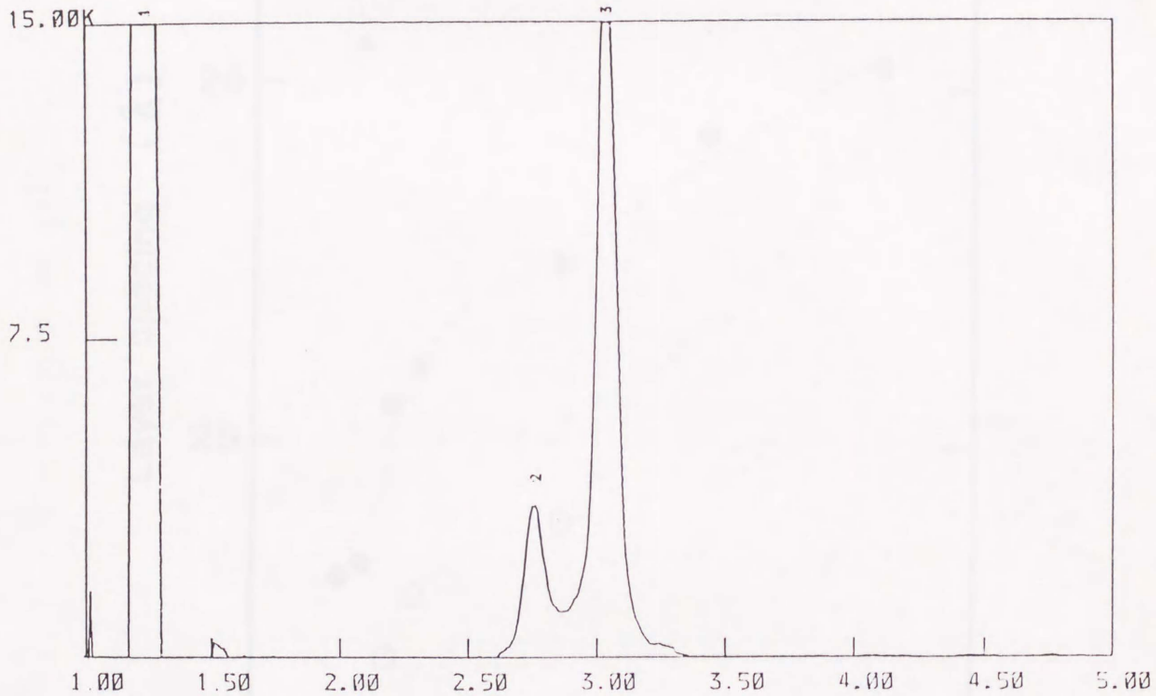

Fig.7. The result of X-ray diffraction of 764E which shows electroclinic effect was measured at 25℃ (Tc:28℃).

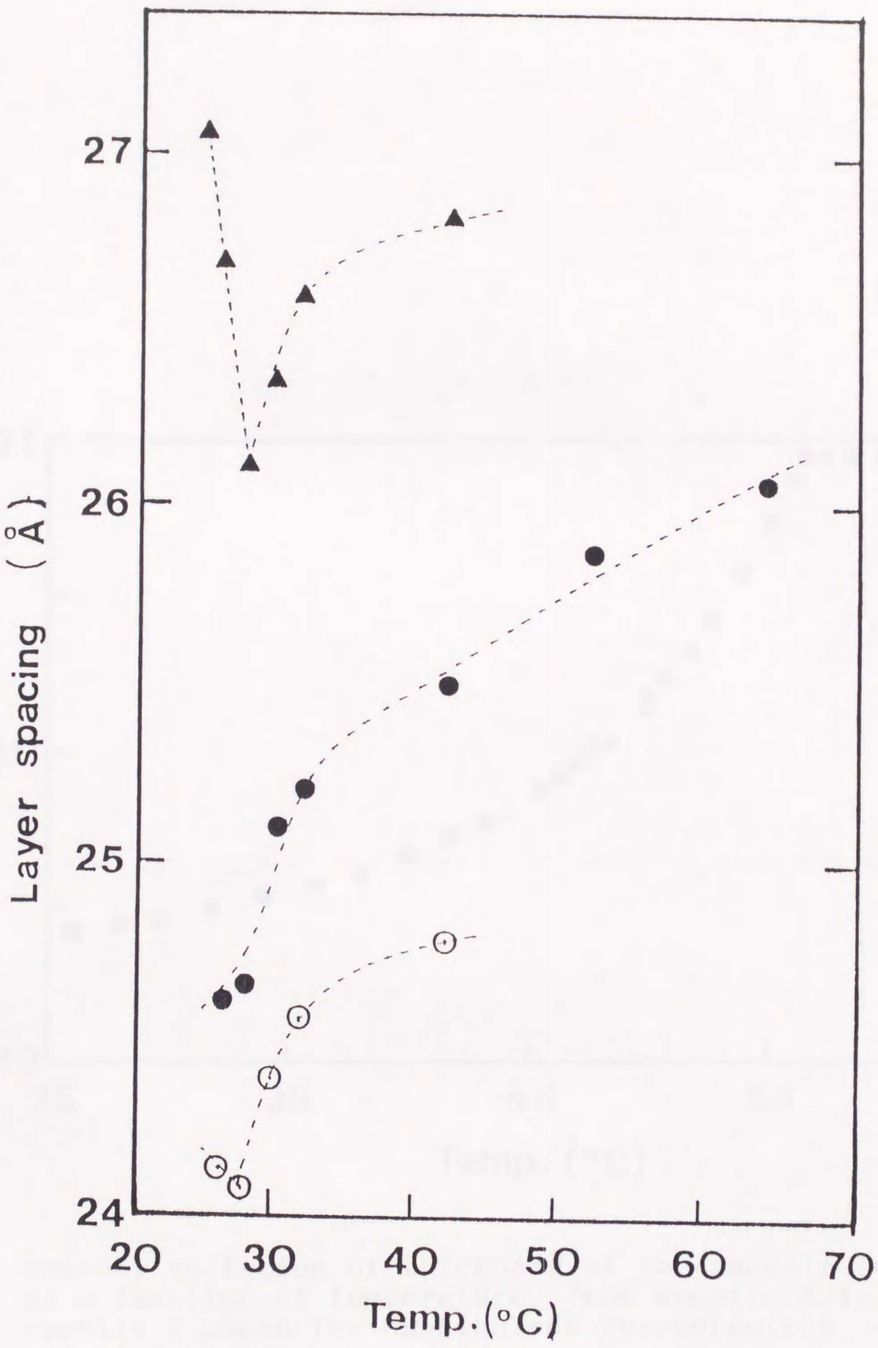

Fig.8. The temperature dependence of the layer thickness of 764E, three kinds of symbols represent the three types of layer thickness observed in this material

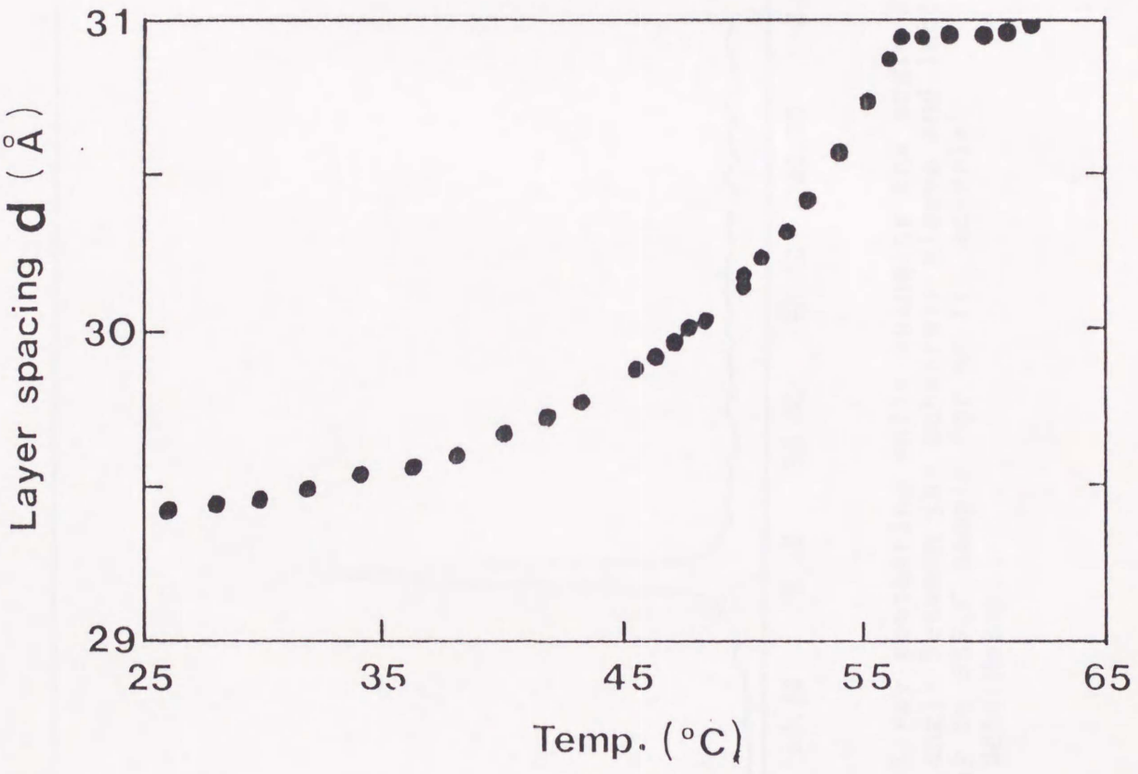

Fig.9. Typical variation of thickness of the smectic layer as a function of temperature, from smectic A to smectic C phase for naphthalene ferroelectric material

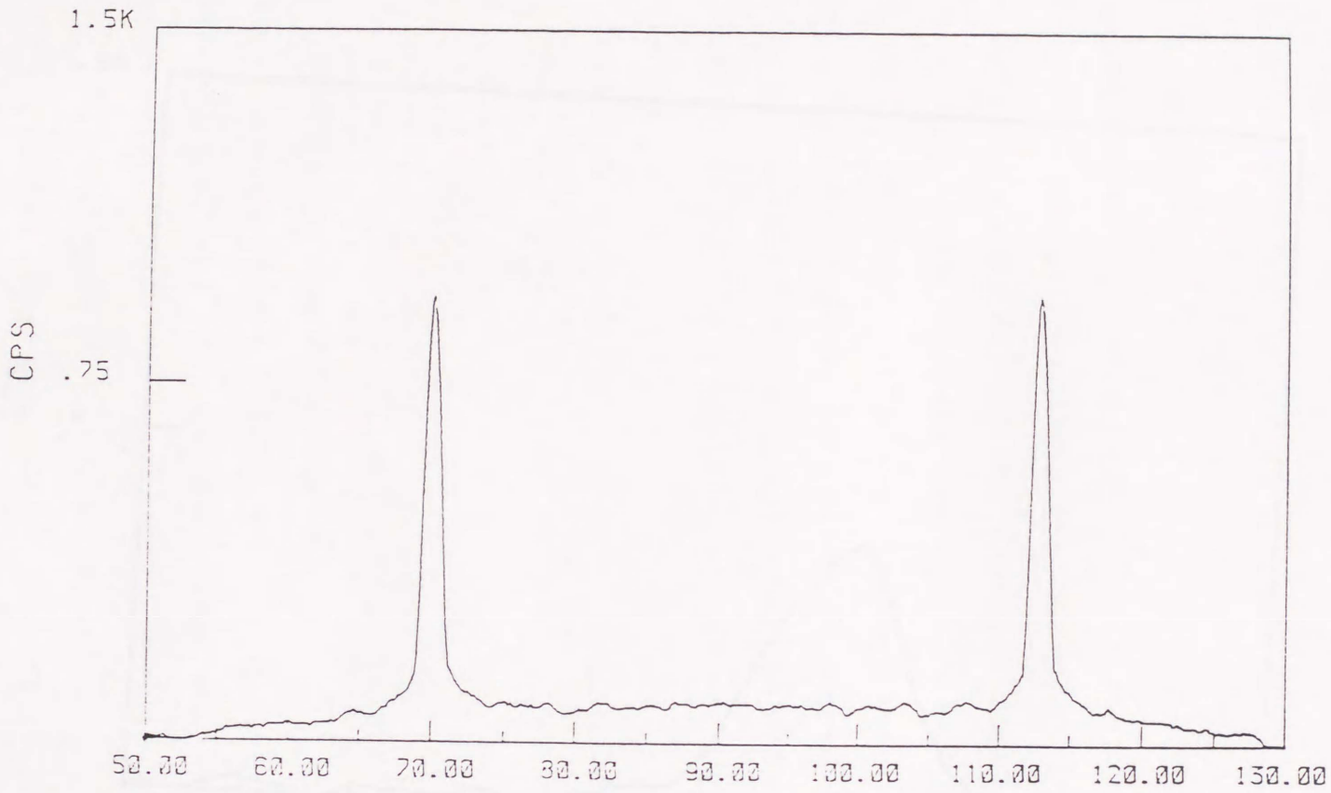

Fig.10. The X-ray scattering while changing the angle β, the angle between the substrate planes and incident X-ray in SSFLC sample for an FLC material ZLI-3654(Merck).

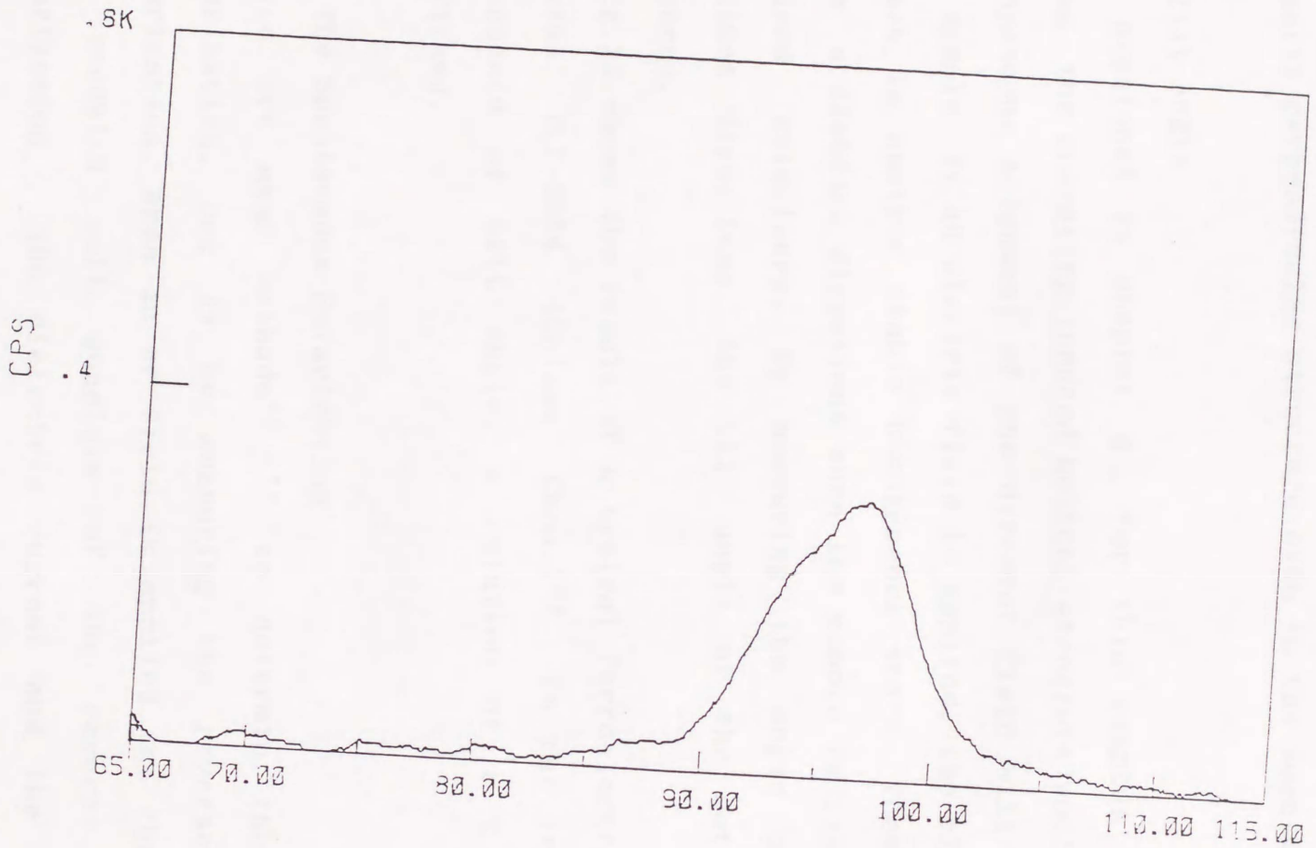

Fig.11. The X-ray scattering while changing the angle β, the angle between the substrate planes and incident X-ray in SSFLC sample for an FLC material 764(BDH) showing EC effect.

show the results. An ordinary FLC material shows a chevron structure[38] while 764E, which shows a strong EC effect , shows a nearly perpendicular structure even in the smectic C phase.

① .Tilt Angle.

As mentioned in chapter Ⅱ , for thin samples in smectic C phase, the chirality-induced helical structure would unwind and a homogeneous alignment of the director field will be formed in the sample. If an electric field is applied, the alignment would switch to another stable homogeneous state. These two states show a distinct directions when the sample is placed between crossed polarizers. By measuring the angle of these two distinct directions, the tilt angle of the material can be measured.

Fig.13 shows the result of a typical ferroelectric liquid crystal ZLI-3654 (Chisso Chem.)[39]. In the temperature dependence of tilt angle, a relation of $(T - Tc)^{1/2}$ was confirmed.

② . The Spontaneous Polarization

There are many methods[40 43] to determin the spontaneous polarization. One is by measuring the reverse current of polarization. When an ac field is applied the current through the sandwich cell consists of the reverse current of polarization , the dielectric current and the ion current, These can be written as

$$I_{to} = I_{re} + I_{die} + I_{ion} \qquad (3.20)$$

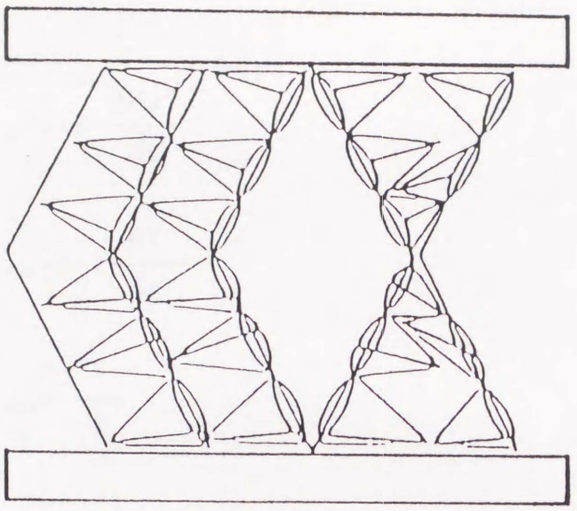

Shevron

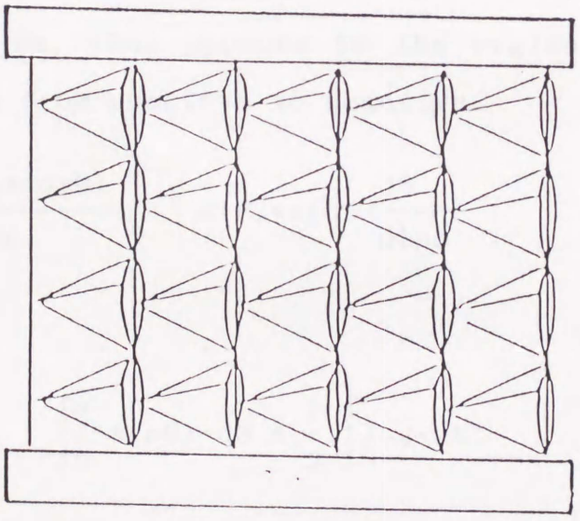

Bookshelf

Fig.12. The director orientation and layer conformation in the SSFLC samples.

$$I_{re} = S \cdot \frac{dP_s^2}{dt} \tag{3.21}$$

$$I_{die} = S \cdot \varepsilon \frac{dV}{dt} \tag{3.22}$$

$$I_{ion} = \frac{V}{R} \tag{3.23}$$

The response speed of I_{ion} is much more slow than the other two terms in Eq.(3.20). At the proper frequency, the totalcurrent I_{to} may be approximated by I_{die} and I_{ion}. Ordinarily, a square or triangular wave voltage was used in the measurement, so I_{die} remainedconstant in the reverse process of Ps. A current pick resulting from Ps, then appears in the region where the field change its sign from positive to negative.

$$I_{re} = S * \frac{d(P_s * \cos\Theta)}{dt} = -S * P_s * \sin\Theta \cdot \frac{d\Theta}{dtso} \tag{3.24}$$

Hence

$$P_s = \int I_{re} dt \div \int_0^{\pi} (-\sin\Theta) \cdot d\Theta = \frac{1}{2} \int I_{re} \cdot dt \tag{3.25}$$

Fig.13 indicates the Ps for ZLI-3654 obtained by the triangular wave method. A $(T-Tc)^{1/2}$ behavior was found for the tilt angle. similar to the behavior of tilt angle. Fig.15 shows the Ps of a FLC which shows strong electroclinic effect in the smectic A phase as a function of temperature. Deviations, between the

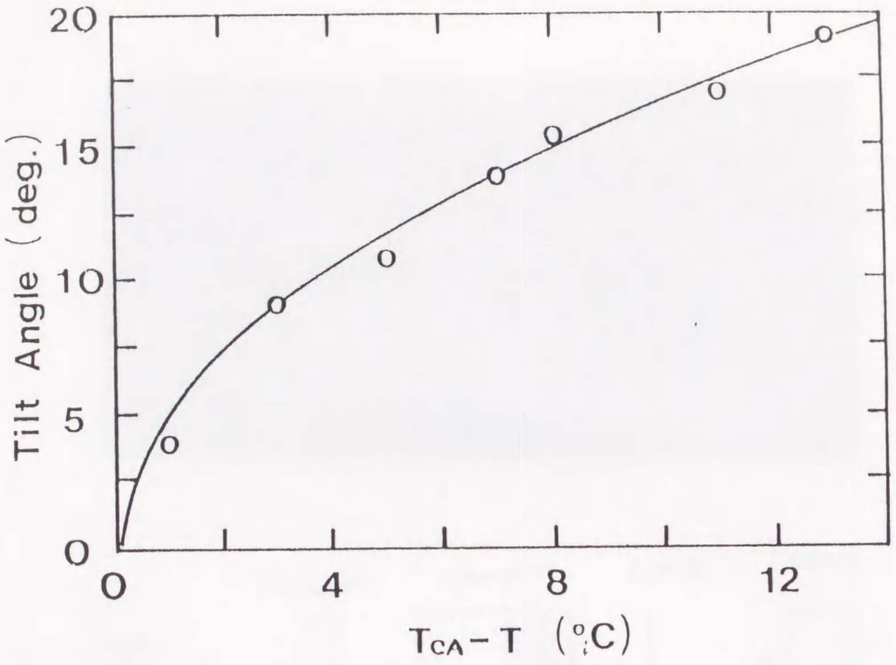

Fig.13. Typical temperature dependence of the tilt angle. The circles represent the experimental result, the solid line represents the theoretical result of Landau phase transition theory.

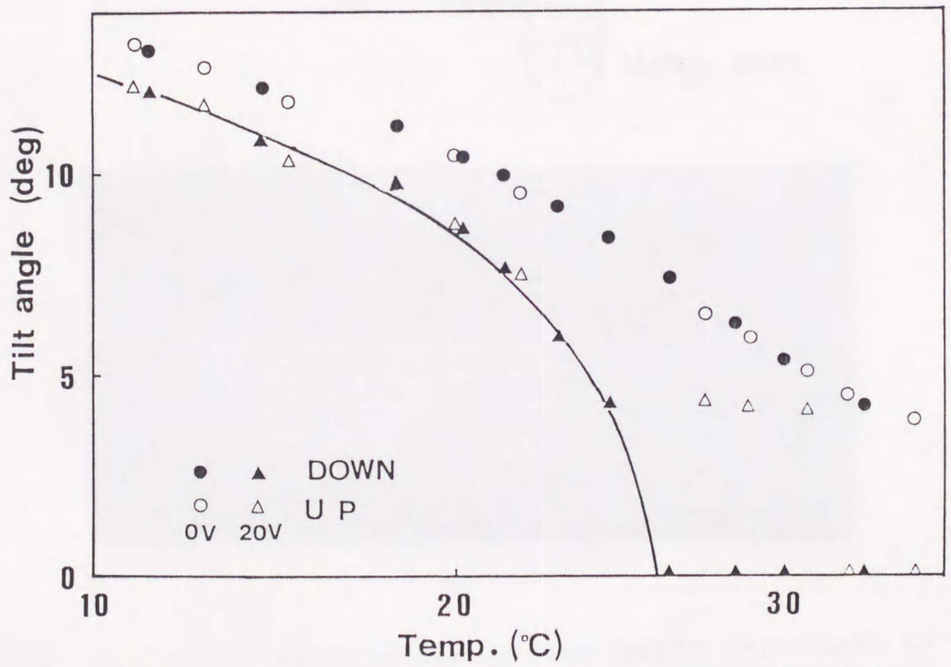

Fig.15. The temperature dependence of the tilt angle for the materials showing EC effect. The triangles, and circles represent the tilt angle for V_{DC}=0 and V_{DC}=20v, respectively. The open and closed symbols represent the results for heating and cooling process, respectively. The solid line represent the result calculated from Landau theory. The sample thickness was 1.8 μm.

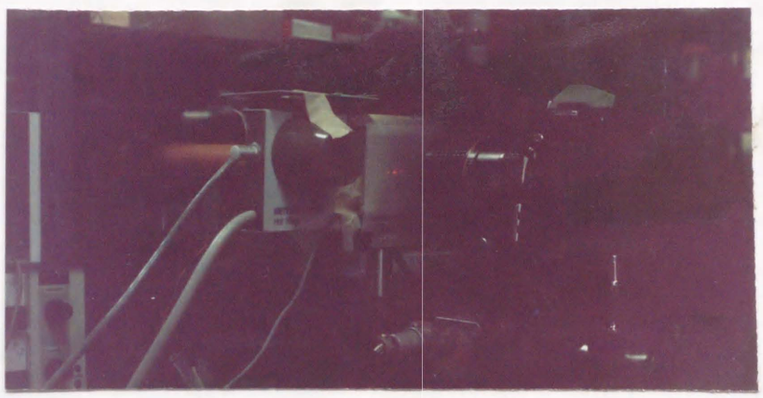

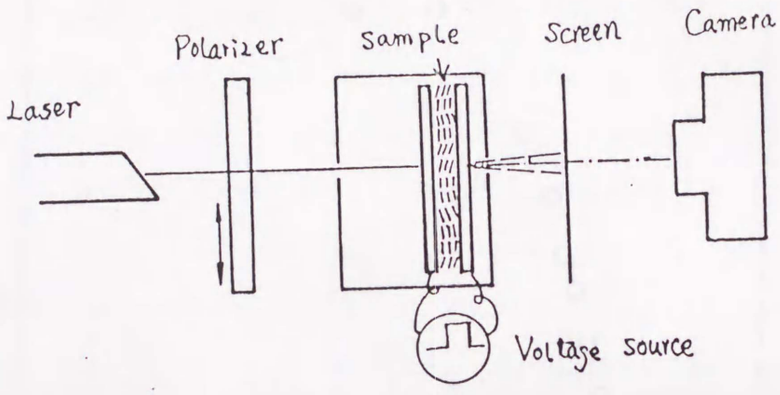

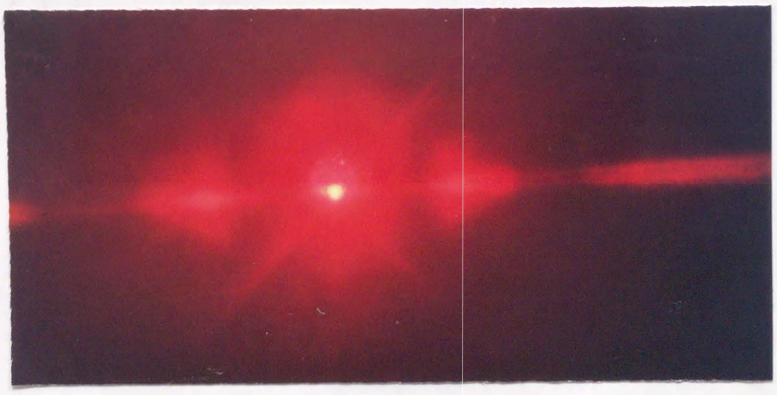

Fig.16a. The laser diffraction of the helix structure of the chiral smectic C phase in thick sample. (a) is a picture of the measuring system, (b) is its layout, (c) is an example of the diffraction pattern.

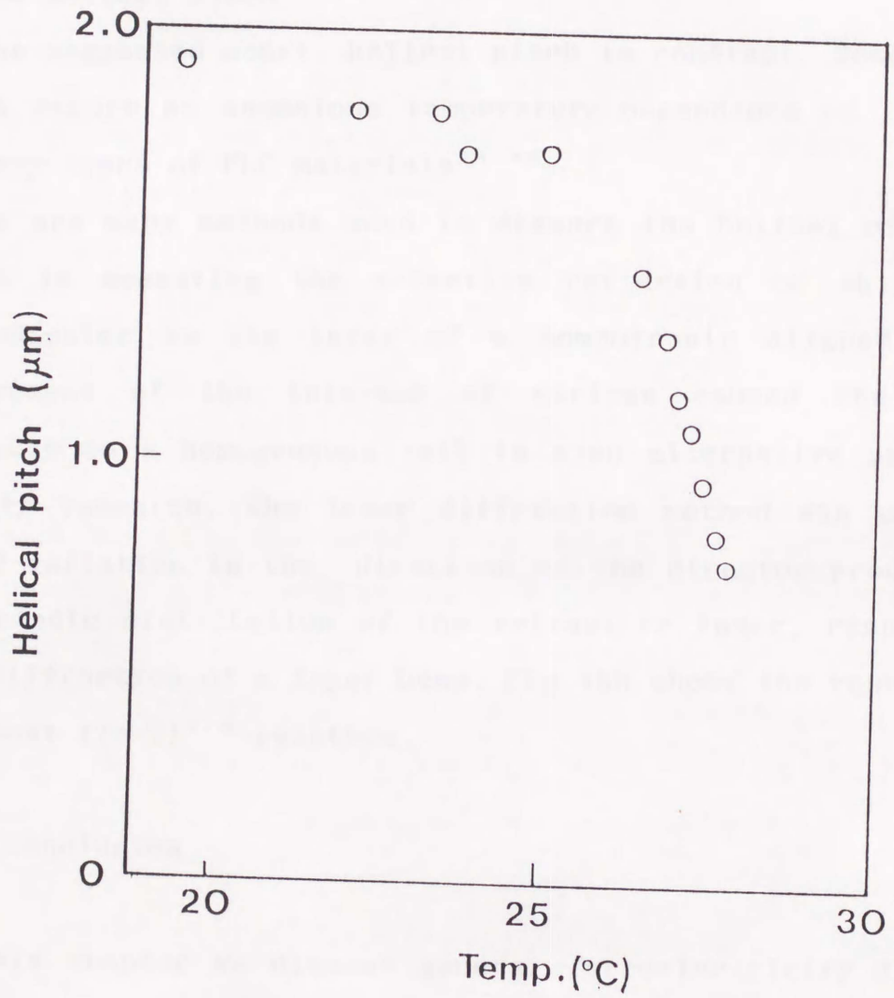

Fig.16b. The temperature dependence of the helical pitch of the chiral smectic C of 764E .

experimental results and the relation $(Tc-T)^{1/2}$, especially in the vicinity below transition point is attributed to the electroclinic effect in the smectic C Phase. This will be discussed in the next chapter.

④ . The helical pitch

In the suggested model, helical pitch is constant. However many groups report an anomalous temperature-dependence of the pitch for many types of FLC materials[44 46].

There are many methods used to measure the helical pitch. One method is measuring the selective reflection of white light perpendicular to the layer of a homeotropic aligned cell[48]. Measurement of the internal of stripes caused the helical structure in a homogeneous cell is also alternative procedure. In this research, the laser diffraction method was used. The period variation in the direction of the director produces a[49 50] periodic distribution of the refractive index, resulting in the diffraction of a layer beam. Fig.16b shows the result. with an almost $(Tc-T)^{1/2}$ relation.

§3.4 Conclusion

In this chapter we discuss general ferroelectricity in liquid crystals, with emphasis on electroclinic effect. An EC effect material exhibits a special behavior in its ferroelectric LC phase. The next chapter will deal more extensively with the electroclinic effect.

ChapterIV ELECTROCLINIC EFFECT

From this chapter, the center topic of this thesis, i.e., the electroclinic (EC) effect will be discussed. In chiral smectic phase, because of the existance of the coupling of polarization and tilt angle, the electric field which is parallel to the smectic layers induces tilting of LC director. This phenomenon is the electroclinic effect. In this chapter, the possibilities of EC effect in the chiral smectic C phase and smectic A phase will be discussed in terms of discussing the free energy, similarily to the last chapter. Also the theoretical calculations will be compared with the experimental results.

§4.1 The electroclinic effect in smectic A phase

① .The argument on the symmetry of the smectic A phase

The smectic A phase exhibits a layered structure with the LC director perpendicular to it. The molecules are free to rotate about their long axis in SmA phase. So the smectic A phase is uniaxial with the long molecular axis, and a twofold axis perpendicular to the molecules. All of the planes containing the molecular long axis and the twofold axis are mirror planes. If an electric field E is applied parallel to the smectic layers, the free rotation is biased due to the tendency of the traverse component of the permanent molecular dipole P to orient parallel to the field. All of the symmetry elemants are destroyed, only one twofold axis along the electric field and one mirror plane containing electric field $\mathbf{E}$ and molecular long axis $\mathbf{n}$($\mathbf{Pn}$ plane) are maintained. The mirror plane corresponds to a free energy minimum, so no tilting of LC director appears

in a non chiral system. However, for the smectic A phase consisted of optical active molecules (chiral molecules), the chirality of the phase destroys all mirror symmetries, the Pn plane don't maintain as a minimum for free energy, therefor, the molecules tilt away from Pn. For small field, the rotation bias and the induced polarization are linear to the field strength; the induced tilt angle is proportional to the field strength. The electric field induced tilting of LC director of the chiral smectic A phase is referred to as the electroclinic effect (EC effect).

② . The phenomenal theory of EC effect

The discussions in the last chapter has shown that the ferroelectricity in LC materials is resulted from the linear coupling of the polarization and the director tilting. The electroctinic effect is also caused by the coupling of these two factors. To consider the EC effect, it is necessary to deal with the state variables, i.e., the tilt angle and the polarization underelectric field.

The free energy descriptions for the smectic C and smectic A phase, where no external electric field is applied, have been obtained in the last chapter. The total energy where electric field exists consists of the summition of the free energy and the electric energy. Two kinds of electric energy must be considered in the LC materials. One is a coupling between polarization and the field $P \cdot E$. The other is results from the dielectric anisotropy of LC materials, which can be written as $1/2\Delta\varepsilon E^2\sin^2\Theta\sin^2\Phi$. This term is very small contrast to $P \cdot E$, it will be ignored in later discussion.

The situation of the smectic A phase containing chiral

molecules where the EC effect is the only response for an applied electric field will be considered at first.

The total energy for the smectic A phase which contains chiral molecules can be written as

$$F_g\hat{}_E = A`\Theta^2 + \frac{1}{2\chi}\cdot P^2 - P\cdot E - C\Theta P \qquad (4.1)$$

The variables P and Θ can be calculate from the similtaneous eq.(4.2)

$$\frac{\partial F_g\hat{}_E}{\partial \Theta} = A`\Theta - C\cdot P = 0 \qquad (4.2a)$$

$$\frac{\partial F_g\hat{}_E}{\partial P} = \chi^{-1}\cdot P - E - C\cdot\Theta = 0 \qquad (4.2b)$$

It is easy to get the polarization P from (4.2b),

$$P = \chi\cdot(C\cdot\Theta + E) \qquad (4.3)$$

substitutiing (4.3) into (4.2a) gives

$$(A` - \chi C^2)\cdot\Theta = \chi C\cdot E \qquad (4.4)$$

The solution of (4.4) is

$$\Theta = \frac{\chi C}{A` - \chi C^2}\cdot E \qquad (4.5)$$

like what has been done in the last chapter, a new form (4.6) for Θ can be obtained by writting $A` - \chi C^2$ as $a(T-Tc)$,

$$\Theta = \frac{\chi C}{a(T - Tc)} \cdot E \qquad (4.6)$$

It is clear that the tilt angle of LC director is proportional to the field strength in smectic A phase. This shows the EC effect of smectic A phase. For convenice, a new parameter K, the electroclinic coefficient will be introduce to describ the EC effect later.

$$K^{\wedge} = \frac{\chi C}{a(T - Tc)} \qquad (4.7)$$

As can be understood, the electroclinic coefficient shows divergent increase when the sample approaches the transition point.

§4.2 The Electroclinic effect in the SmC* phase

The usual EC effect which appears in smectic A phase has been reviewed in the last section. In this section, the possibility of the existance of EC effect in chiral smectic C phase will be discussed by considering the symmetry of the phase, and the coupling between the polarization and tilting of the director.

In smectic C phase, the free rotation of LC molecules is biased by the spontaneous tilting of the long axis of the molecules. If the phase transition from the SmA to SmC* is the first type, the rotation of the LC molecules in smectic C phase is hard to be changed, no further tilting of the director can be induced by the external field. However, if the transition is

the second type, the anisotropy of the molecular rotations in smectic C phase is very small, and is easy to be changed by the electric field perpendicular to the molecular long axis. The further biasing of the molecular rotations would induce further tilting of the LC director. For approximation, the tilting is proportional to the biasing, i.e., the polarization or the filed strength, hence the tilt angle would be proportional to field strength.

On the other hand, the EC effect in SmC* may also be discussed using the total free energy of LC materials. According to the last chapter, the free energy of the chiral smectic C phase is

$$F_{\varepsilon}{}^{C}{}_{E} = \frac{1}{2} A'\Theta^2 + \frac{1}{4} B\Theta^4 + \frac{1}{2\chi}\cdot P^2 - E\cdot P - C\Theta P \qquad (4.8)$$

The state equation is

$$\frac{\partial F_{\varepsilon}{}^{C}}{\partial \Theta} = A'\Theta + B\cdot\Theta^3 - C\cdot P = 0 \qquad (4.9a)$$

$$\frac{\partial F_{\varepsilon}{}^{C}}{\partial P} = \chi^{-1}\cdot P - E - C\cdot\Theta = 0 \qquad (4.9b)$$

Reminding the solution Θ_o for eq.(4.9) where E =0 in the last chapter, taking account of the fact that the electric field gives only small fluctuation of the tilt angle, $\Theta = \Theta_o + \delta\Theta$ will be presumed as a new form for Θ, where $\delta\Theta$ is a incremental part because of the existance of the electric field. Then the equation changes to

$$A'(\Theta_o + \delta\Theta) + B\cdot(\Theta_o + \delta\Theta)^3 - C\cdot P = 0 \qquad (4.10a)$$

$$\chi^{-1}\cdot P - E - C\cdot(\Theta_o + \delta\Theta) = 0 \qquad (4.10b)$$

Eq.(4.10b) gives

$$P = \chi \{ E + C\cdot(\Theta_o + \delta\Theta)\} \qquad (4.11)$$

A new equation about Θ_o and $\delta\Theta$ can be obtained by substituting (4.11) into (4.10a) as

$$A`(\Theta_o + \delta\Theta) + B\cdot(\Theta_o + \delta\Theta)^3 - C\cdot\chi \{ E + C\cdot(\Theta_o + \delta\Theta)\} = 0 \qquad (4.12)$$

In this equation, the higher order of $\delta\Theta$ can be omitted because $\delta\Theta$ is small for a real field. Then (4.12) changes to

$$\{A`\Theta_o + B\Theta_o^3 - \chi C^2\Theta_o\} + \{A`\delta\Theta + 3B\Theta_o\delta\Theta - \chi C^2\delta\Theta - \chi CE\} = 0 \qquad (4.13)$$

It has been clear that

$$A`\Theta_o + B\Theta_o^3 - \chi C^2\Theta_o = 0 \qquad (4.14)$$

in the last chapter. Eq.(4.13) changes to (4.15) by substituting (4.14) into (4.13).

$$A`\delta\Theta + 3B\Theta_o^2\delta\Theta - \chi C^2\delta\Theta - \chi CE = 0 \qquad (4.15)$$

The solution is

$$\delta\Theta = \frac{\chi C}{A`+3B\Theta_o^2-\chi C^2}\cdot E \qquad (4.16)$$

Considering $\Theta_o^2 = -(A`-\chi C^2)/B$, (4.16) can be written as

$$\delta\Theta = \frac{\chi C}{-2(A`-\chi C^2)}\cdot E = -\frac{\chi C}{2a(T-Tc)}\cdot E \qquad (4.17)$$

Clearly this is the electroclinic effect in chiral smectic C phase. Similarly, the electroclinic coefficient for the SmC* phase can be defined.

$$K_c^E = \frac{\chi C}{2a(T-Tc)} \qquad (4.18)$$

§4.3 The Electroclinic Effect

The possibility of the electroclinic effect both in smectic A and C phase has been shown. The electroclinic coefficient show divergence at the transition point from the SmA to SmC* phase. However, the absolute value of EC coefficients for SmA and SmC* are different by a factor 2.

The theoretical results will be confirmed experimentally in the following.

① The structure of the smectic A phase

The monodomain structure for SmA phase is very important for the optical measurement of tilt angle in EC effect. However, stripe defects are induced in the SmA sample where the surface aligning of LC director is realised by rubbing the substrate surface, because that the smectic layer always keeps its thickness constant. The rubbing treatment produce one direction alignment of LC director at surface only in average, actually, the investigations with using SEM or STM have shown that the rubbing porcess produces grooves on the surface[51] [52] with interval of near 4μ m. This grooves induce the alignment of LC molecules at the surface.

Fig.17 shows the stripe defects which appear in the rubbing cell. The stripes is parallel to the rubbing direction. The molecular director is nearly parallel to the rubbing direction. The interval between the stripes decreases with the decreasing of the sample thickness in reverse proportion relation as in Fig.18. The reciprocal of the interval is shown in Fig.18. This relation can be interpreted by using the elastic theory of the

Fig.17. The polarizing microscope pictures of the smectic A structure of 764E. (a), (b) and (c) show the results for the samples of 1.8μm, 8μm and 20μm, respectively.

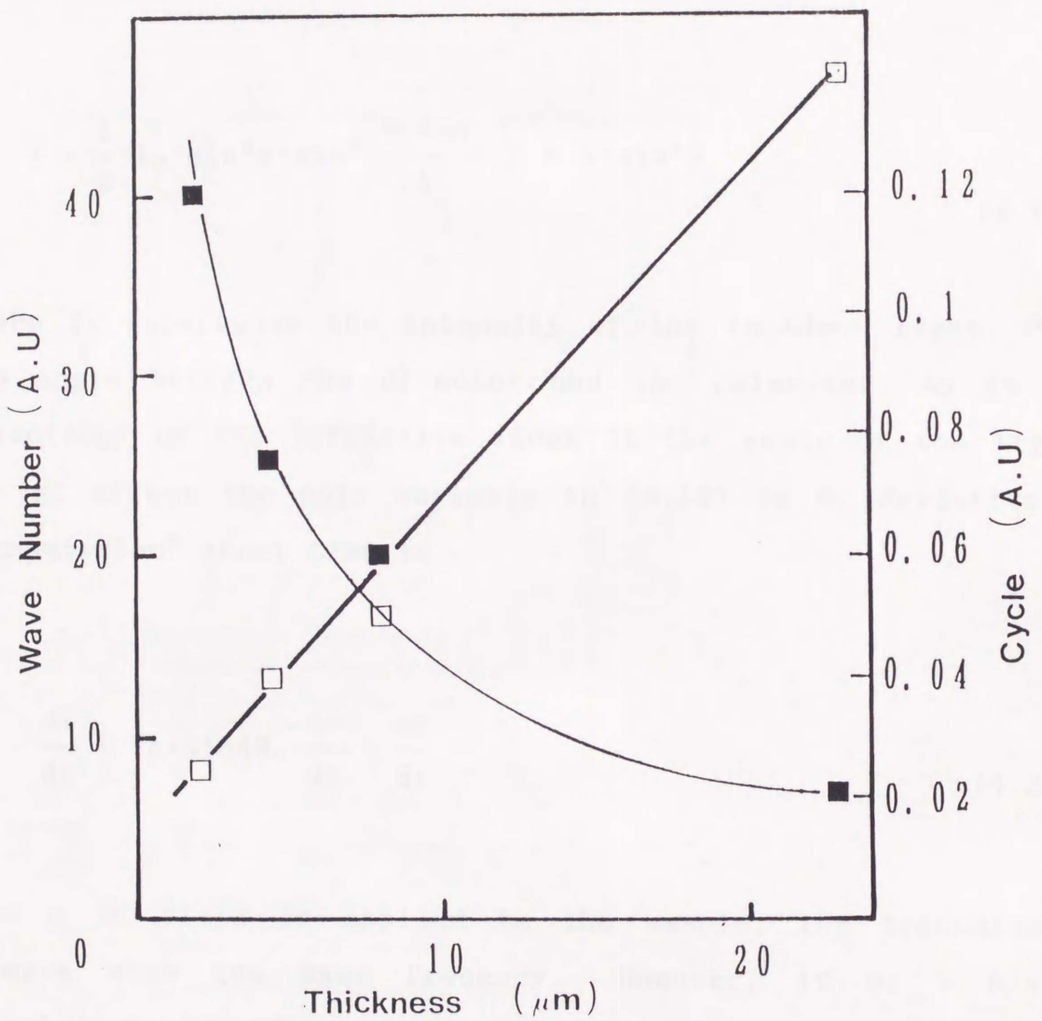

Fig.18. The relation between the intervals and their reciprocal of stripes and the thickness of the samples, temperature 30℃ .

smectic A phase.

The electric field induced tilt is measured by measuring the transmission of the sample between crossed polarizers. The transmission of a uniformly homogeneous liquid crystal layer can be written as

$$I = \frac{1}{2}\cdot I_o \cdot \sin^2\Theta \cdot \sin^2\{\frac{\pi \cdot d\Delta n}{\lambda}\} = A\cdot\sin^2\Theta \qquad (4.19)$$

Where I_o repersents the intensity of the incident light, Θ is the angle between the director and the polarizer, Δn is the anisotropy of the refractive index in the route of the light. For EC effect the only variable in (4.19) is Θ, deviative of transmission[6] about time is

$$\frac{dI}{dt} = A\cdot\sin 4\Theta_o \cdot \frac{d\Theta}{dE}\cdot\frac{dE}{dt} \qquad (4.20)$$

When a AC field is applied to the sample, the transmission changes with the same freqency. However, if $\Theta_o = n\cdot\pi/4$, transimission I takes the maximum, but dI/dt take its minimum, zero. The tilt angle is determined as the angle between two directions where the ac components of transmission are zero, when an DC field with a small AC undulation is applied over the sample. Fig.19 shows an example of the electroclinic effect in smectic A phase. A lear relation between Θ and E is confirmed.

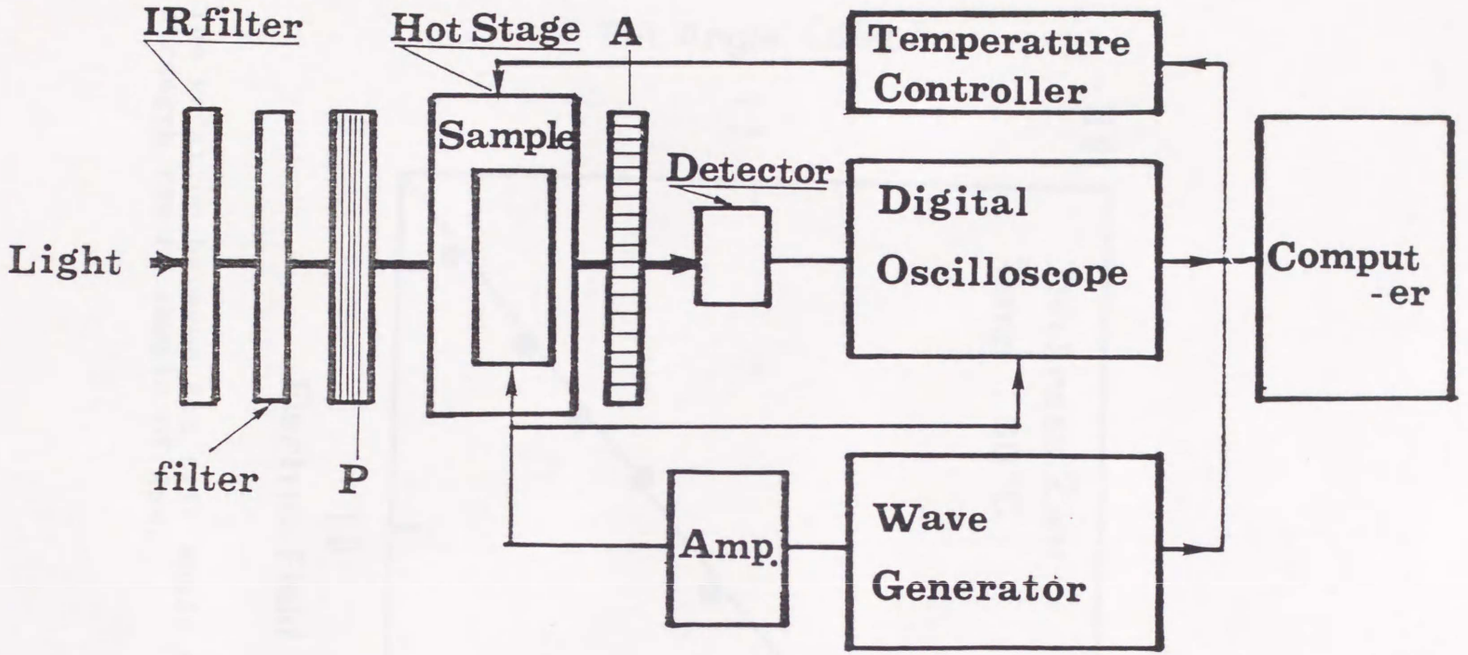

Fig.19. The layout for the measuring system of EC effect.

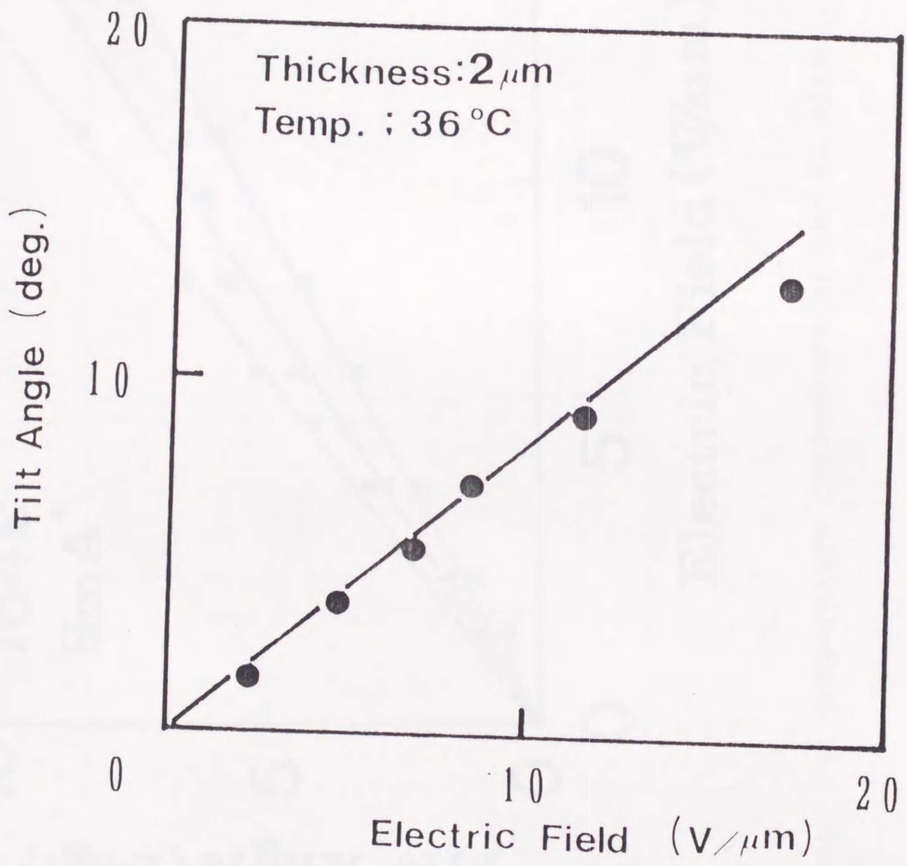

Fig.20a. The relation between the tilt angle and the field strength the EC sample of 2μm.

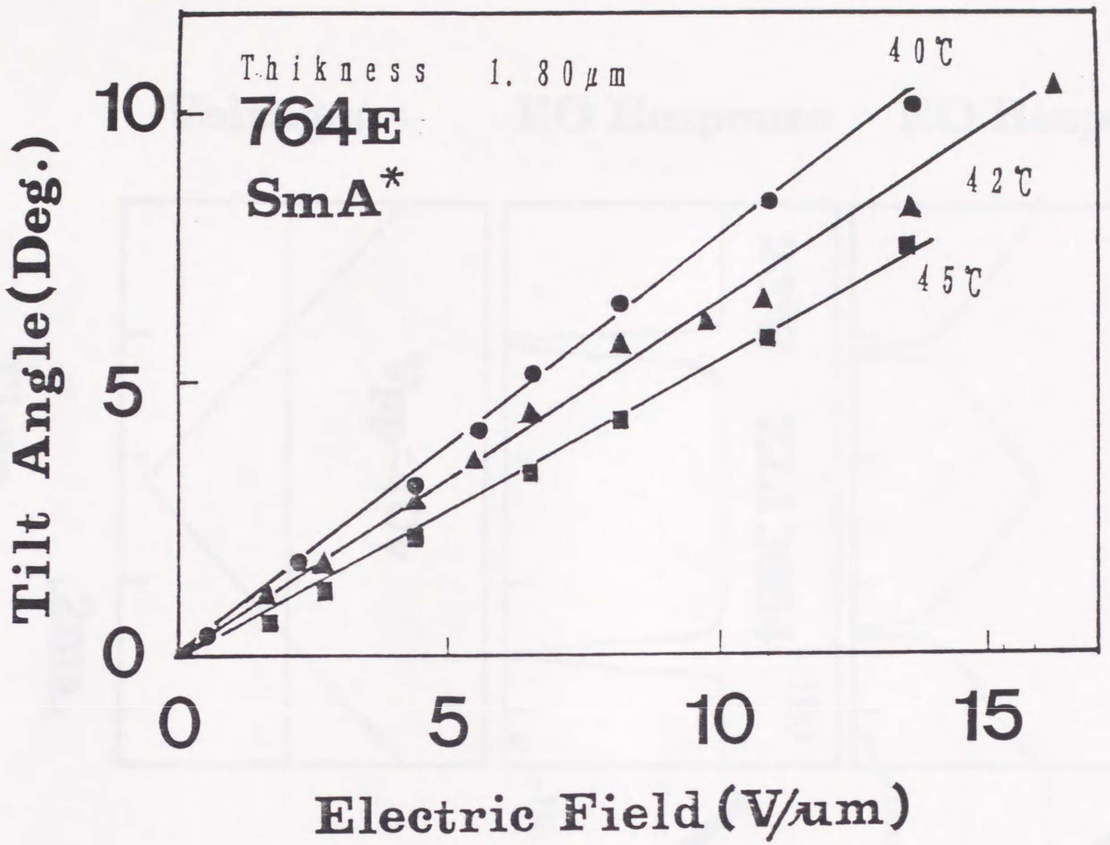

Fig.20b. The temperature dependence of the EC effect.

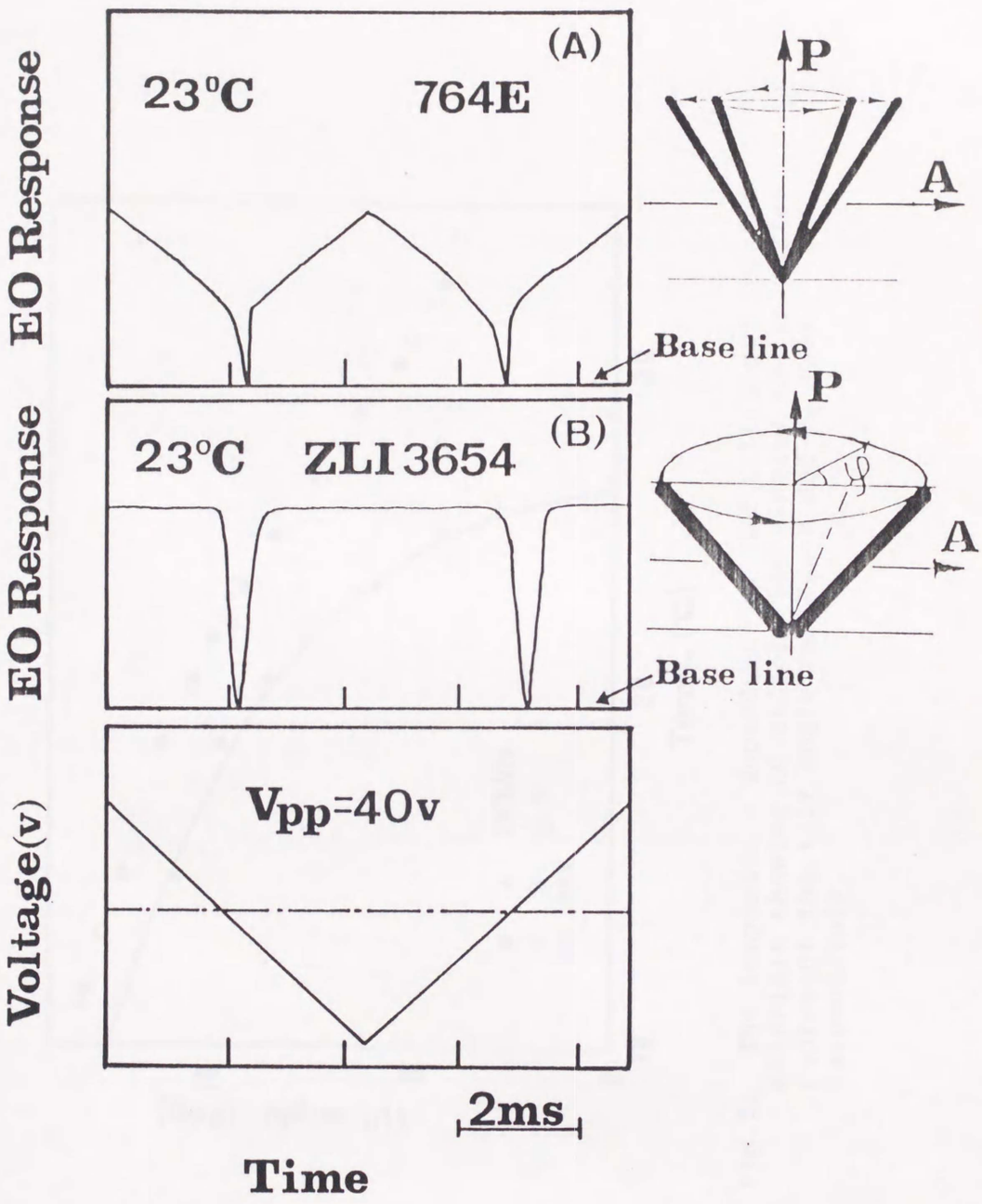

Fig.21. The transmission for the material showing EC effect and ordinary FLC material.

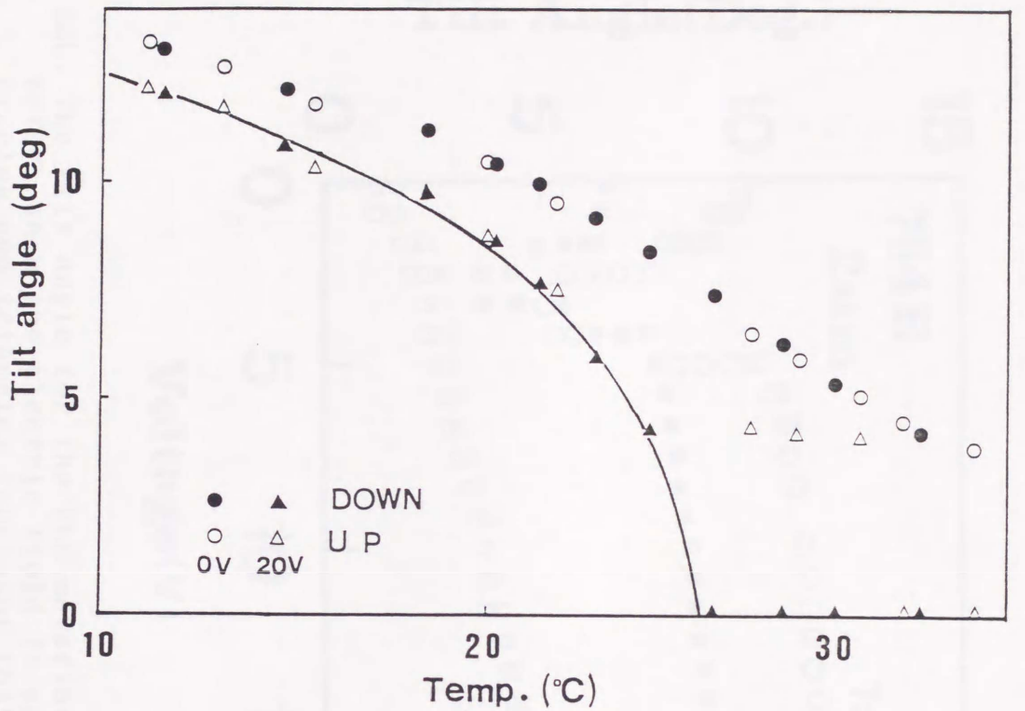

Fig.21. The temperature dependence of the tilt angle for the materials showing EC effect. The circles and triangles represent the tilt angle for V_{DC}=0 and V_{DC}=20v, respectively.

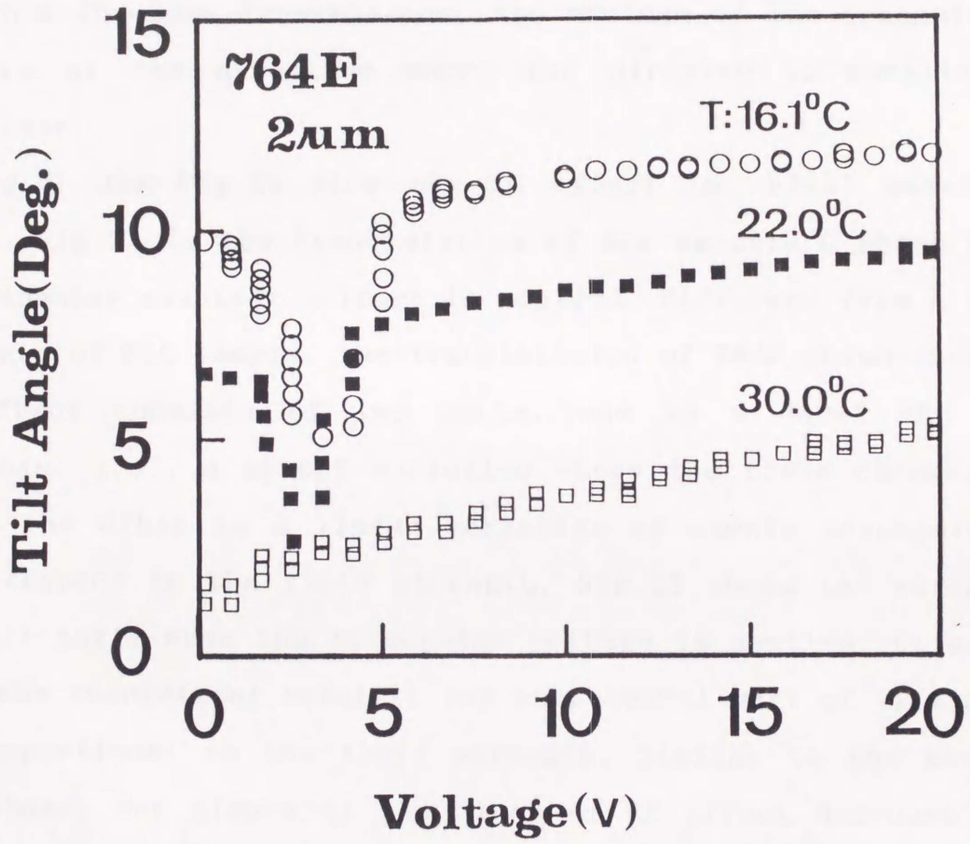

Fig.22b. The tilt angle for the FLC materials showing EC effect when the electric field is applied. The circles and triangles represent that in SmC* phase. The squares represent that of SmA phase.

The slopes of lines decrease with the increasing of the sample temperature.

Fig.20 shows the layout of the measuring system for the EC effect in the smectic C phase. In this system, the layer normal is parallel to polarizer direction. Two of the stable states of FLC show the same transmission, the minimum of the transmission appears at the direction where the director is parallel to polarizer.

Fig.21 and Fig.22 show the EC effect in chiral smectic C phase. Fig.21 is the transimission of the smectic C phase where a triangular electric voltage is applied. Different from a usual response of FLC sample, the transimission of 764E which shows EC effect consists of two parts, one is a usual FLC type response, i.e., a abrupt variation where the field changes its sign, the other is a linear variation of sample transimission with respect to the field strength. Fig.22 shows the variation of tilt angle when the triangular voltage is applied. Coincides with the theoretical results, the incremental part of tilt angle is proportional to the field strength. Similar to the case of SmA phase, the slopes of the lines of EC effect decrease with the decreasing of sample temperature far below the transition point.

Finally, Fig.23 illustrates the electroclinic coefficient as a function of temperature. To compare with formula (4.7) and (4.18), the reciprocal of K_{CE} and K_{AE} is taken as the spindle, instead of K_E itself. Good linearity had been found for K_E and (T-Tc). For absolute vakues, disagreements exist between the theoretical and experimental results for the relation of K_{CE} and K_{AE}. This is resulted from the influence of surface anchoring

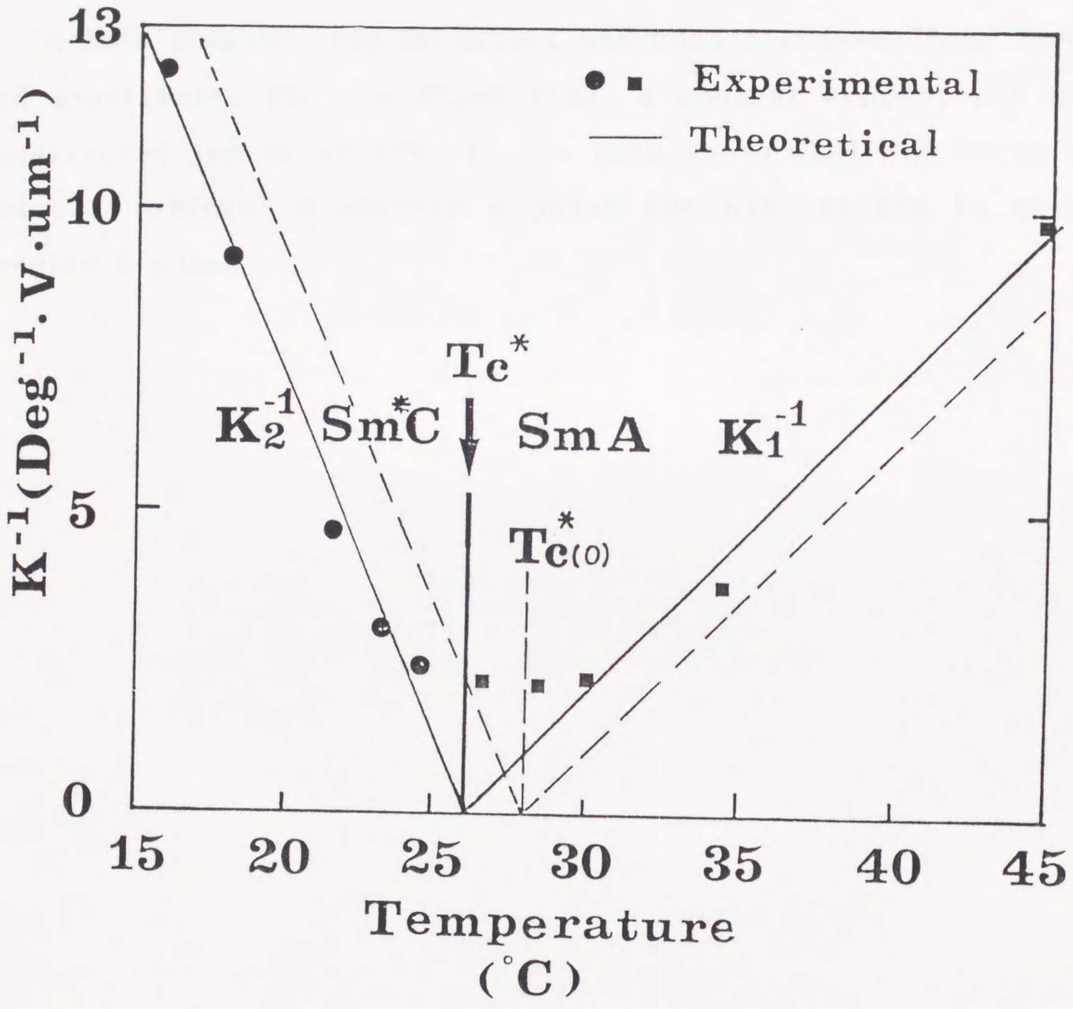

Fig.23. The temperature dependence of the reciprocal of the EC coefficient in the neighborhood of the transition point.

strength. Actually strong surface anchoring dependence of EC effect exists as will be dealed with in the next chapter.

§ 4.4 Conclusion

In this chapter, the EC effect has been discussed from theory and experiment. For the first time, a general concept has been constructed for EC effect. It has been shown that the EC effect not only exists in smectic A phase but also exists in chiral smectic C phase.

Chapter V PROPERTY OF ELECTROCLINIC EFFECT

It has been made clear that the EC effect not only exists in smectic A phase but also in chiral smectic C phase, in the last chapter. In this chapter, several basic properties of the EC effect, including the dielectric property, dynamic property and layer switching in EC effect will be discussed.

§5.1 The Dielectric Property of EC Effect

The dielectric responses of FLC materials are resulted from the rotations of LC molecules around their long and short axis, and intermolecular rotation and also from the reorientations of short axis and electronic polarization. Two large responses are from the Goldstone mode response[53] [54] and electroclinic response. The Goldstone mode response is the rotation of LC director around the short molecular axis on the cone structure. The EC effect response is resulted from the variation of the cone angle. The dielectric constant at arbitrary frequency ω can be written as

$$\varepsilon^* = \frac{\Delta\varepsilon_G}{1+(j\omega\tau_G)^2} + \frac{\Delta\varepsilon_E}{1+(j\omega\tau_E)^2} + \cdots \qquad (5.1)$$

Where $\Delta\varepsilon_G$ and $\Delta\varepsilon_E$ represent the perpendicular components of dielectric constant for Goldstone mode and EC effect. τ_G and τ_E are the relaxation times for Goldstone mode and EC effect. The relaxation frequencies of the Goldstone mode and EC effect are several 100s and near 1MHz, respectively. The response at

100Hz or even low frequency is resulted from all two responses of Goldstone mode and EC effect. However, the dielectric response for higher than 1kHz is resulted only EC effect. In this research the Goldstone mode and EC effect is basically distinguished by their frequency dependences.

In the homogeous FLC sample, because the restrict of the layer structure, the dielectric responses are only from the contributions from the perpendicular components of the dielectric constants.

① . Theoretical analysis

In the following, in all of the theoretical discussions, the dielectric constants will be restricted to the their static parts. The response without the variation of tilt angle are considered as that of Goldstone mode. The dielectric response induced by the variation of tilt angle is considered as that of EC effect.

As shown in the last chapter, the polarizations are state variables ont only in smectic C but also in smectic A phase. The discussion will be started from the simitaneous equation (5.2) about P and Θ. For the smectic C phase,

$$\frac{\partial F_g^C}{\partial \Theta} = A'\Theta + B\Theta^3 - C \cdot P = 0 \qquad (5.2a)$$

$$\frac{\partial F_g^C}{\partial P} = \chi^{-1} \cdot P - E - C \cdot \Theta = 0 \qquad (5.2b)$$

If E=0, a non-zero solution Ps exists for eq.(5.2). This

responses to the electric field, induces the Goldstone mode response. The solution for eq.(5.2) where E≠0 is presumed as Ps +δP(E), where Ps represents the spontaneous polarization, δP repersents the incremental part δP of the polarization because of the existance of electric field. This responses at high frequency, corresponding to the EC effect.

For the EC effect, (5.2) changes to

$$\{\chi^{-1}Ps - C\cdot\Theta_o\} + \{\chi^{-1}\delta P - E - C\cdot\delta\Theta\} = 0. \tag{5.3}$$

Because

$$\chi^{-1}Ps - C\cdot\Theta_o = 0, \tag{5.4}$$

The equation changes to

$$\chi^{-1}\delta P - E - C\cdot\delta\Theta = 0. \tag{5.5}$$

Its solution is

$$\delta P = \chi(E + C\cdot\delta\Theta) \tag{5.6}$$

According to the results in the last chapter

$$\delta P = \chi\left(E + C\cdot\frac{\chi C}{2a(T-Tc)}\cdot E\right) \tag{5.7}$$

$$= \left\{\chi + \frac{\chi^2 C^2}{2a(T-Tc)}\right\}\cdot E \tag{5.8}$$

This corresponds to the dielectric response of the EC effect in the smectic C phase. The corresponding dielectric constant is

$$\varepsilon_C{}^E = 1 + \chi + \frac{\chi^2 C^2}{2a(T-Tc)} \tag{5.9}$$

The dielectric constant for the smectic Λ phase can be obtained in the similar way,

$$\varepsilon_\Lambda{}^E = 1 + \chi + \frac{\chi^2 C^2}{a(T-Tc)}. \tag{5.10}$$

It is clear that the dielectric constants of the EC effect show similar temperature dependences to the electroclinic coefficient. Λ divergent peak exists at the transition point, but different from there, another constant term exists in the dielectric constants.

② .The experimantal results

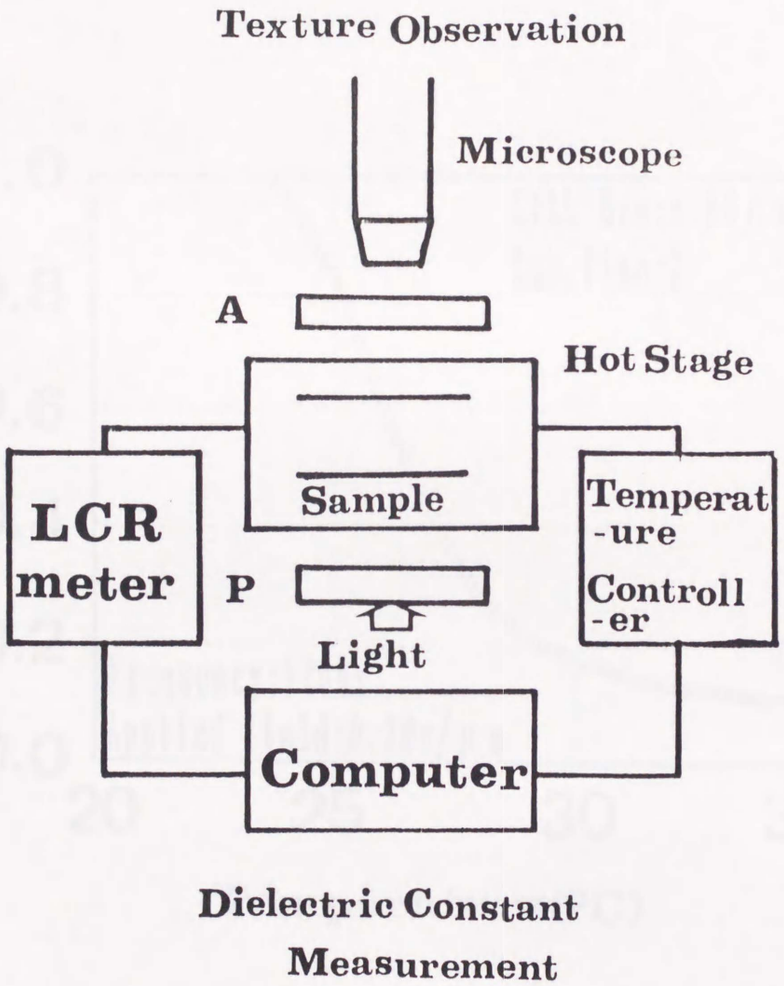

Fig.24. The layout of measuring system for the dielectric constant of the FLC materials

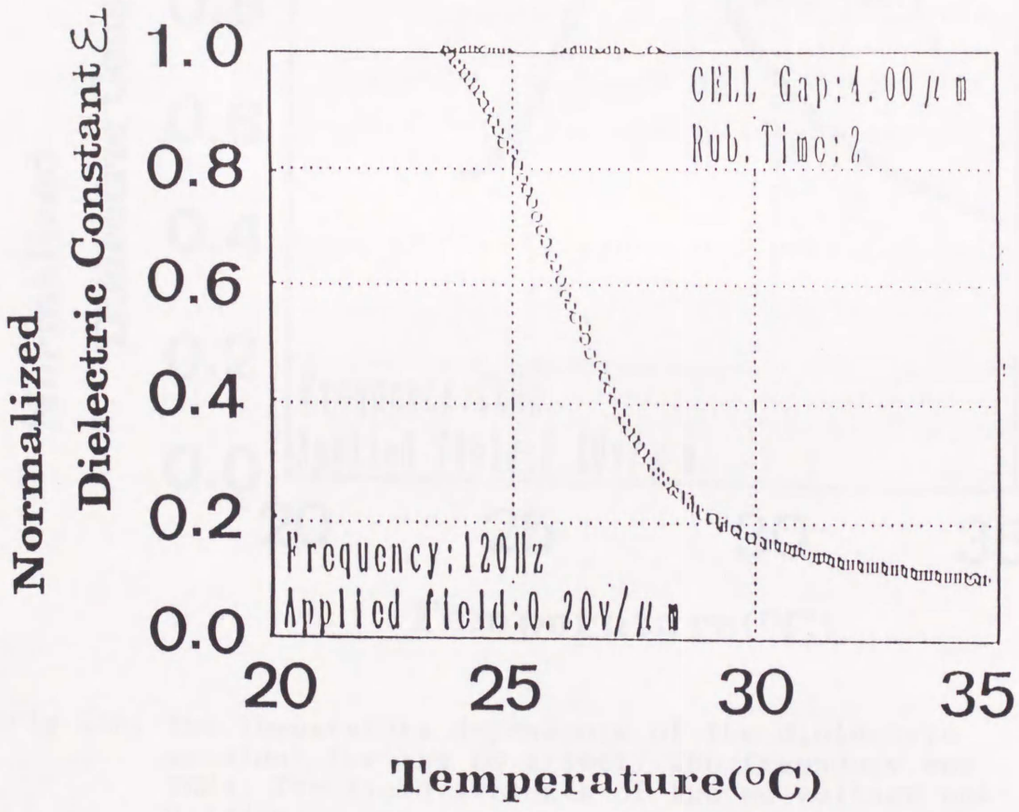

Fig.25a. The temperature dependence of the dielectric constant for the Goldstone mode. The frequency was 120 Hz. The field strength of the ac voltage was 0.2v/μm.

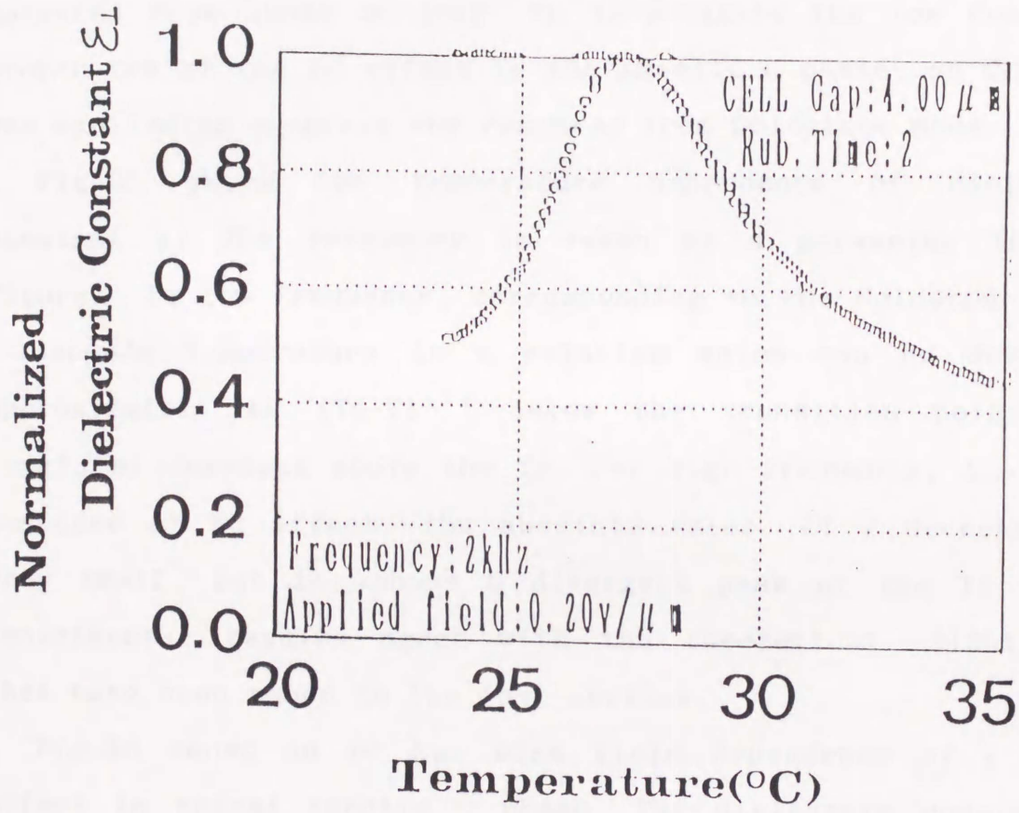

Fig.25b. The temperature dependence of the dielectric constant for the EC effect. The frequency was 2KHz. The field strength of the ac voltage was 0.2v/μm.

Fig.24 illustrates thelayout of the dielectric constant measuring system. The dielectric constant is measured with using LCR meter (YHP4974). The temperature is controlled with using precise hot-stage (Mettler 80). All of the equipments are controlled by microcomputer. The dielectric constant has been measured from 100HZ to 1MHZ. To investigate the low frequency properties of the EC effect in the smectic C phase, an DC field was applied to suppress the response from Goldstone mode.

Fig.25 shows the temperature dependence of dielectric constant ε. The frequency is taken as a parameter in this figure. In low frequency, corresponding to the Goldstone mode, ε depends temperature in a relation which can be described approximately as $(Tc-T)^{1/2}$ below the transition point, but remain as constant above the Tc. For high frequency, i.e., the response of EC effect, the absolute value of ε decreases to very small, but it shows a divergent peak at the Tc. These experimental results agree with the theoretical calculations that have been shown in the last section.

Fig.26 shows an DC E_{DC} bias field dependence of ε of EC effect in chiral smectic C phase. The dielectric constant in smectic C phase decreases with the increasing of the field strength E_{DC}. This means that the contribution from Goldstone mode is effectively diminished by E_{DC}.

For low frequency of the EC effect, only the response from the EC effect exists when the DC voltage exceeds 5v. While the most sharp peak at the Tc appears at 10KHZ where pure EC response exists, when an 5v DC field is applied. The EC effect response decreases with the increasing of DC field strength when the frequency of the AC field is fixed at 2KHZ, but the strength

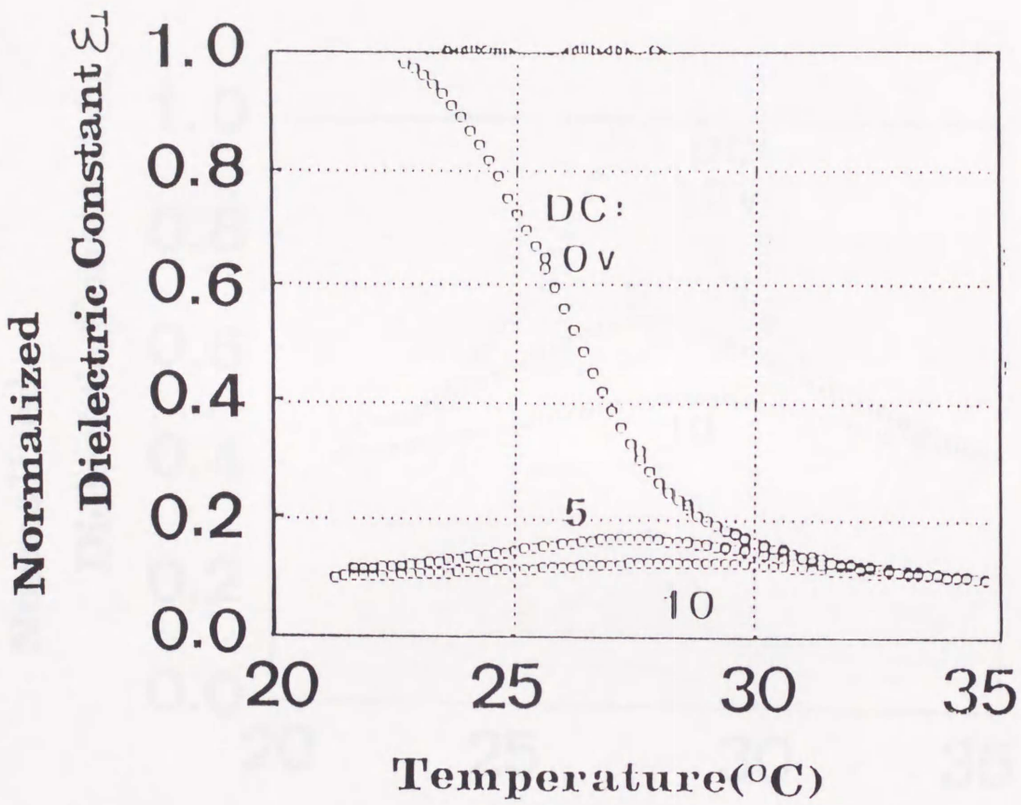

Fig.26 The influence of DC bias on the dependence of the dielectric constant including Goldstone mode and the response of the EC effect. The field strength of ac voltage was 0.2v/μm.

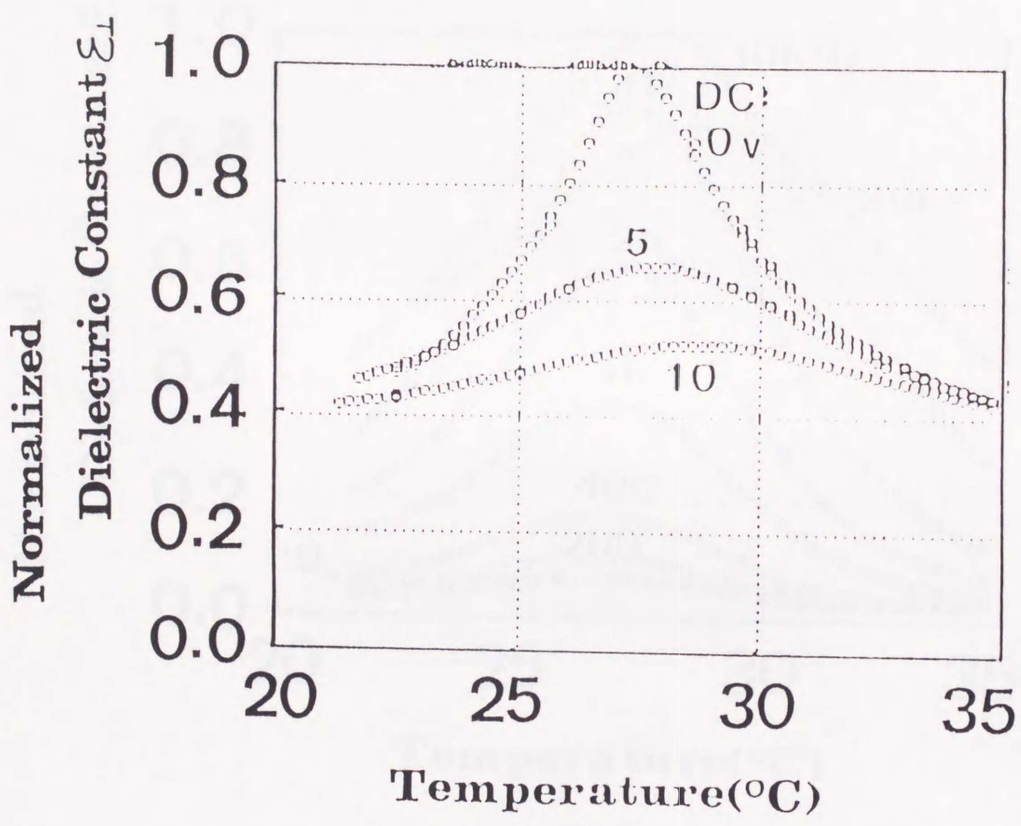

Fig.27 The influence of DC bias on the dependence of the dielectric constant for the response of the EC effect. The field strength of ac voltage was 0.2v/μm.

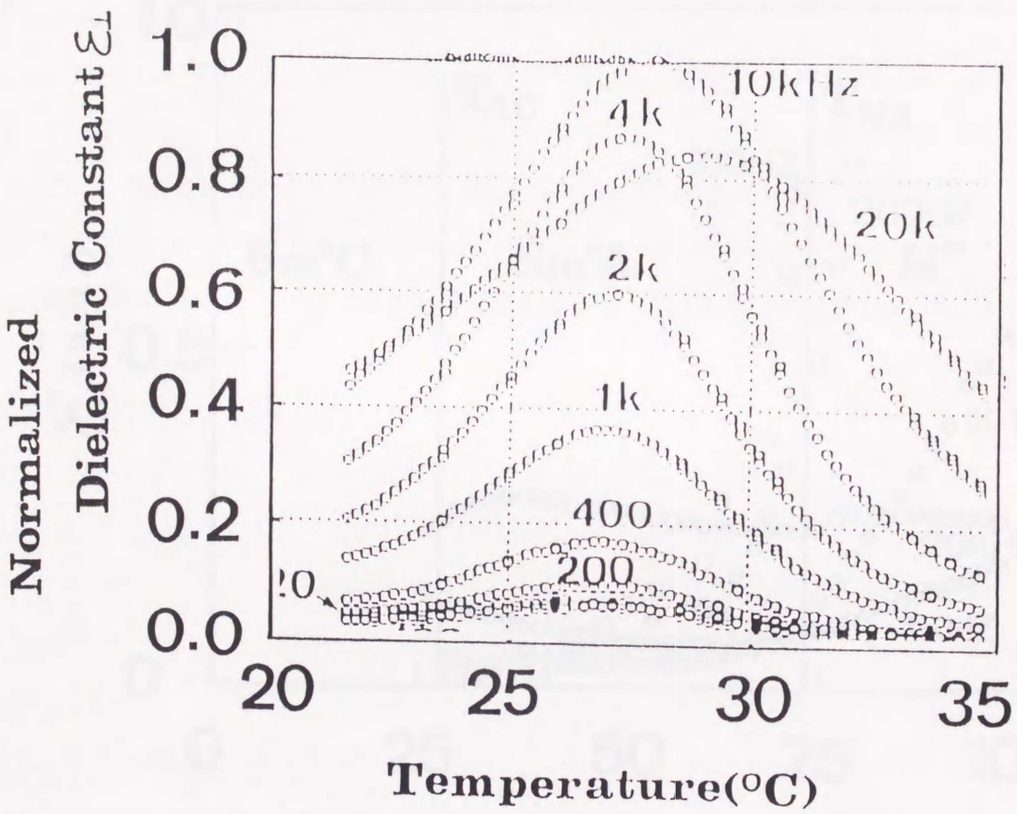

Fig.28a. The frequency dependence of the dielectric constant for the response of EC effect.

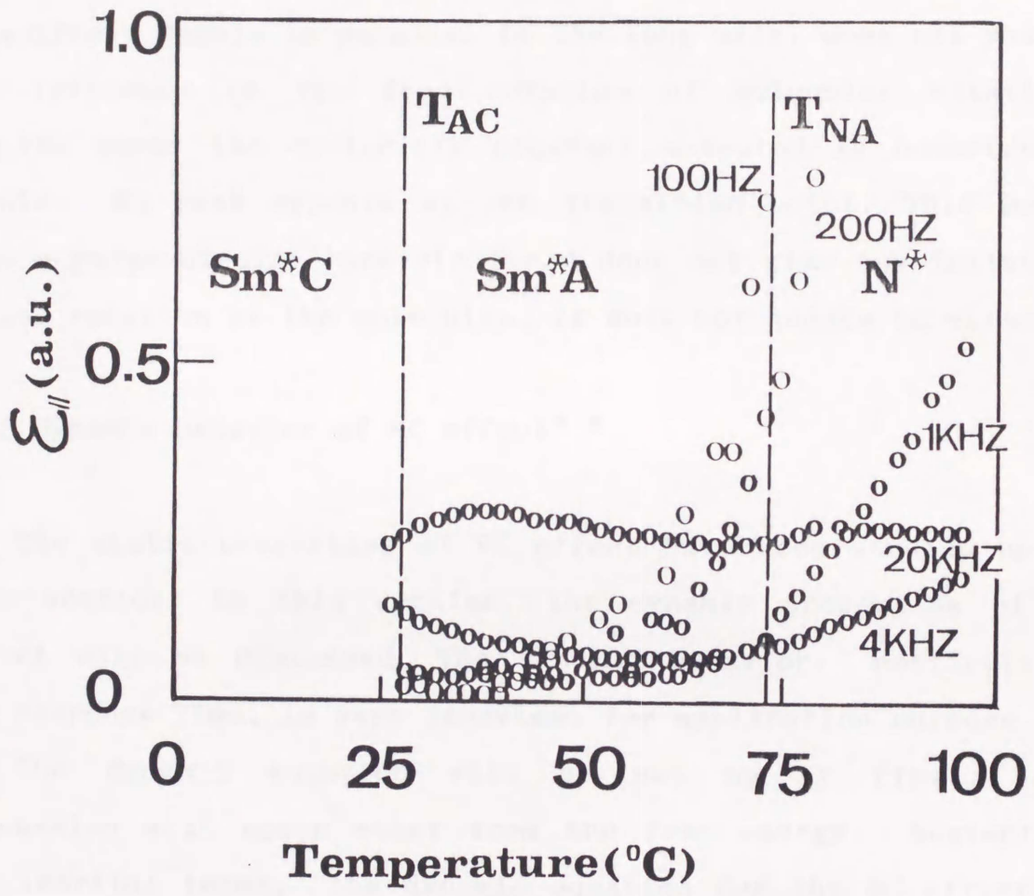

Fig.28b. The frequency dependence of the dielectric constant where the electric field is applied parallel to the long molecular axis.

of DC field is changed. This means that the EC effect response is also suppressed by the DC field.

The dielectric constants in homogeneous sample show the biasing of the free rotation of LC molecules around their short axis. Contrast to homogeneous sample, the electric field in homeotropic sample is parallel to the long axis, does not produce any influence to the free rotation of molecular rotation. Fig.28b shows the dielectric constant measured in homeotropic sample. No peak appears at the transition point. This means that a perpendicular electric field does not give any influence to the rotation of the molecules, it does not induce EC effect.

§5.3 Dynamic behavior of EC effect[8] [9]

The static properties of EC effect have been studied up to this section. In this section, the dynamic properties of EC effect will be discussed. The dynamic behavior, particularly the response time, is very important for application purpose.

The dynamic equation will be set up at first. The discussion will again start from the free energy. Neglecting the inertial terms, the dynamic equation for the EC effect in the smectic A phase is

$$\Gamma_{\Lambda} \cdot \frac{d\Theta}{dt} = - \frac{dF_{\Lambda}^{E}}{d\Theta} \qquad (5.11)$$

Where Γ is the tilting viscosity of LC director. Substituting F_{Λ}^{E} into (5.11) gives

$$\Gamma_A \cdot \frac{d\Theta}{dt} = (A' - \chi C^2) \cdot \Theta - \chi C \cdot E \qquad (5.12)$$

The solution is

$$\Theta = \left[1 - \frac{\chi C}{a(T-Tc)} \cdot E \right] \cdot \exp(-t/\tau_A) \qquad (5.13)$$

where τ_A is $\frac{\Gamma_A}{a(T-Tc)}$. This is the response time of EC effect in the smectic A phase. In smectic C phase, the response time of $\delta\Theta$ is also possible to be discussed in similar way. The dynamic equation for $\delta\Theta$ reads

$$\Gamma c \cdot \frac{d(\delta\Theta)}{dt} = -2(A' - \chi C^2) \cdot (\delta\Theta) - \chi C \cdot E \qquad (5.14)$$

The solution is

$$\delta\Theta = \left[1 - \frac{\chi C}{2a(T-Tc)} \cdot E \right] \cdot \exp(-t/\tau_C) \qquad (5.15)$$

The relaxation time is

$$\tau_C = \frac{\Gamma_C}{2a(T-Tc)}. \qquad (5.16)$$

From above discussion, it is clear that the response time of the

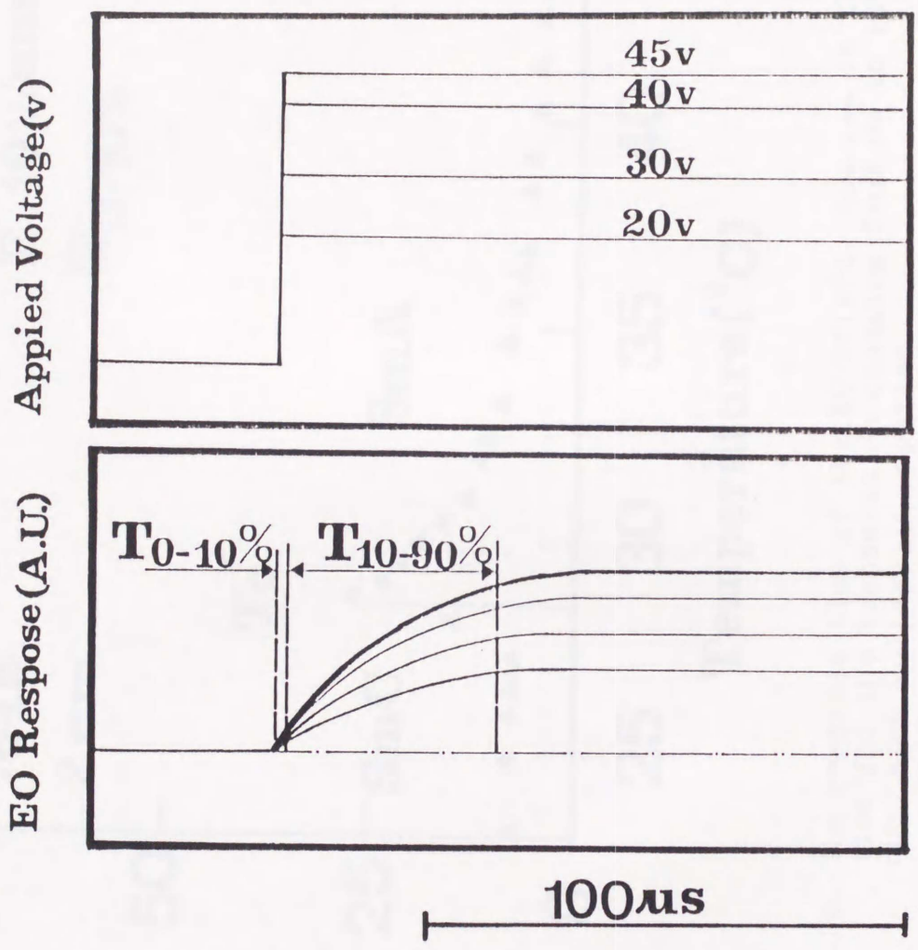

Fig.29. The variation of the transmission when step voltage is applied.

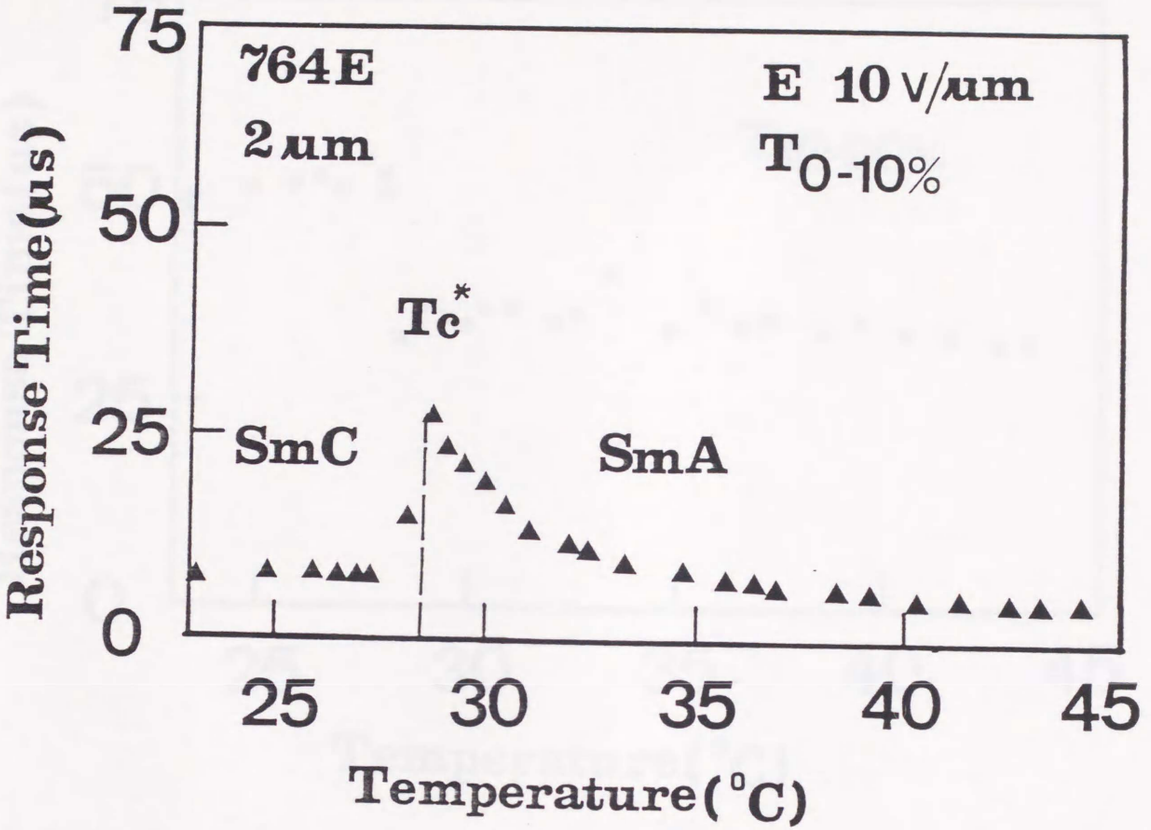

Fig.30. The response time of the EC effect. $\tau_{0\%-10\%}$ is the time for the transmission changing from 0% to 10%, when step voltage is applied.

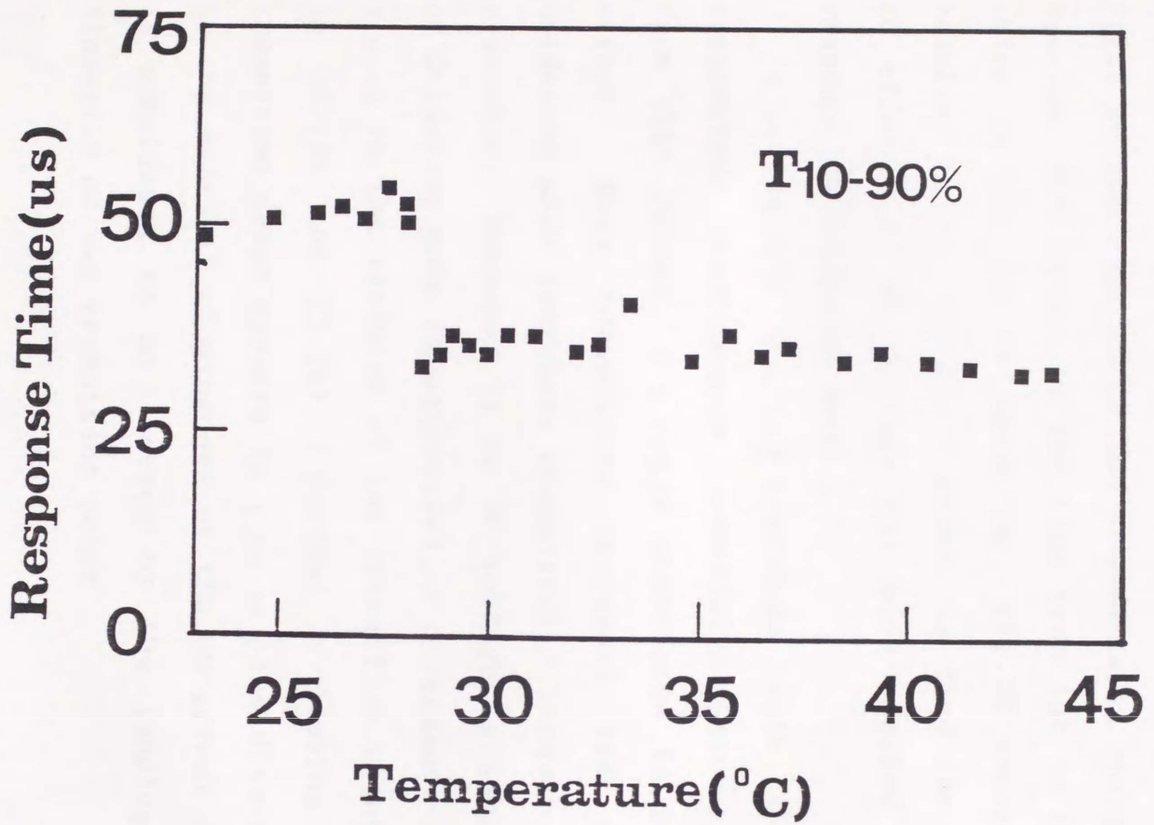

Fig.31. The response time of the EC effect. $\tau_{10\%-90\%}$ is the time for the transmission changing from 10% to 90%, when step voltage is applied.

EC effect shows divergent peak at the transition point.

The response time has been measured from the variation of transmission of the sample in crossed polarizers when a square voltage was applied. Three response times were defined, the first is the time where the transmission changes from 0% to 10% $\tau_{0\%-10\%}$, the second is the time from 10% to 90% $\tau_{10\%-90\%}$, the third is the sum of these two. Fig.29 shows the experimental results. In the smectic C phase, to find the real response for EC effect, an DC voltage has been applied to suppress the response fo Goldstone mode .

$\tau_{10-90\%}$ and $\tau_{0-10\%}$ increases with the decreasing of temperature continuously, especially below transition point. From this reason, $\tau_{0-10\%}$ is considered to be the time of EC effect. When temperature decreases the response time of Goldstone mode increases dramatically because the increasing of viscosity. However, if an DC voltage is applied, the response of Goldstone mode is suppressed, a divergence-like increasing of τ_{0-10} in the vicinity of the transition point appears as shown in (5.14) and (5.15). Further a jumping increase at the transition point appears in $\tau_{10-90\%}$. The divergence is attribute to the critical slowingdown of the EC effect at Tc. The jumping is considered to be caused by the jumping increase of the viscosity at the transition point.

§5.3. Layer switching in EC effect

The switching of the smectic layer is of interesting, because as shown in Fig.34, in the SmA phase two kinds of layer response can be considered for one kind of response of LC

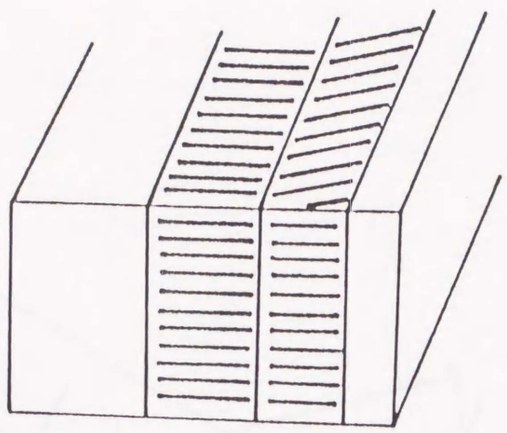

(a) The layer remains its direction but changes its direction.

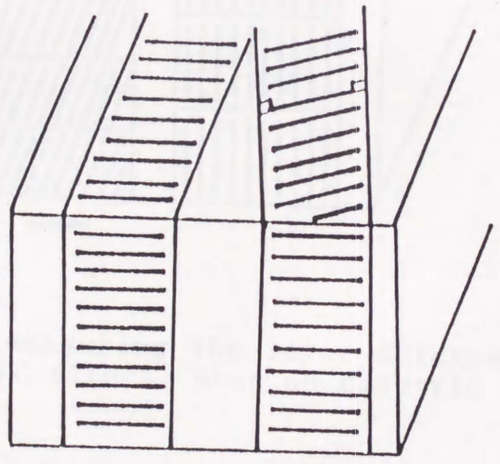

(b) The layer remains its thickness but changes its thickness.

Fig.33. Two models for the layer switching in the EC effect, when an electric field was applied.

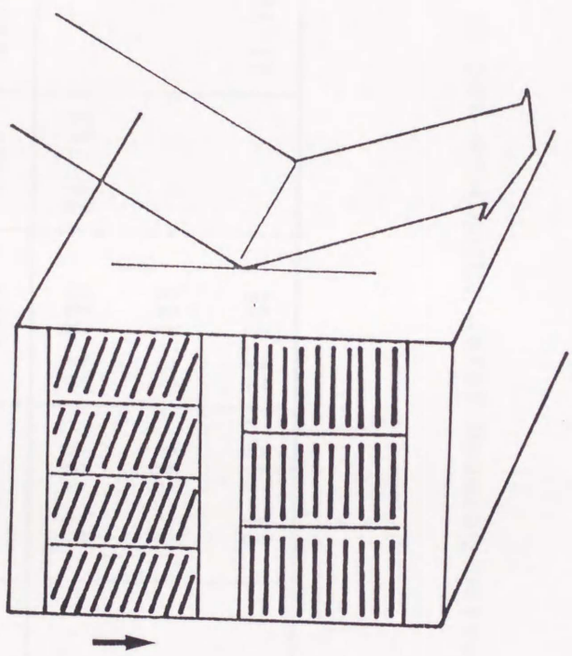

Fig.34. The geometry for measuring the layer thickness variation in the EC effect, when an electric field is applied.

d Volt. / Temp.	0v	150v	200v	250v	300v
26.3℃	24.799	24.799	24.743		
28.4℃	24.743	24.743			24.743
30.7℃	24.743	24.743		24.743	24.743

Table 1 The relation between layer thickness and DC field strength.

director in EC effet.

One is that the smectic layers keep their thickness constant but change their direction. The second is the layers keep their normal direction, produce a tilt between layer normal and director; but produce decreasing of layer thickness.

This was investigated by x-ray diffraction, in the following way. The homeotropic aligned sample was prepared by the substrates surface with silane. The smectic layers were parallel to the substrate . Array electrodes were made in the sample to produce a traverse electric field. This field would induce EC effect perpendicular to the substrate. The variations of the layer thickness can be detected by the X-ray incidenting into the sample as shown in Fig.33.

To get enough diffracting intensity of X-ray, the sample was made using up substrate of thickness 50μm. This thickness is enough to transparent for X-ray of 1.2KW. The temperature of the sample was controlled by a resistance heater made from ITO film on the glass substrate. The temperature was detected with using thermoelectric coupling.

Table.4-1 shows the results in the temperature from 26^{0}C to 60^{0}C. Three kinds ofelectric field strength were applied, 0, 200v/60μ, 300v/60μ. No variation of layer thickness has been found in this experiment. This results have confirmed that layer thickness do not change in the EC effect.

§5.4 Conclusion

In this chapter, several properties of EC effect have been discussed. At last, a interesting question about layer switching

in EC effect has been discussed. This will be discussed again in the next chapter.

Chapter VI THE SURFACE ANCHORING DEPENDENCE OF ELECTROCLINIC EFFECT

This chapter will deal primarily with the surface anchoring dependence of the electroclinic effect. Surface effects are important in LC research because the bulk properties of liquid crystals are influenced by the surface anchoring potential.

Since the beginning of this century, surface effects on nematic liquid crystals have drawn wide attention[55 56]. However, systematic researchs began in 1970, where many types of surface effects have been found. Among these are the anchoring of the molecular director parallel or perpendicular to the surface; The discovery of the polar and nonpolar anchoring, which are proportional to the odd and even power of the surface order parameter respectively.

In FLC materials, the molecular director has only two stable directions, thus the torque variation in an arbitrary direction in the switching process is difficult to obtain. For this reason, very few experiments on the surface anchoring of ferroelectric liquid crystals have been reported. In this research on FLC, the surface effect is treated by computer simulation where the surface anchoring of nematic LC was assumed. N.A Clark et. al[59 60], proposed a model, which coupled this to the deformation energy of FLC and interpreted the bistability of SSFLC. Nakagawa, et.al, presented another form where, instead of cos-sin functions and its power, an exponential factor containing sin-cos[61] was used to calculate the dynamic behavior in the switching process.

For the electroclinic effect, surface anchoring also has great

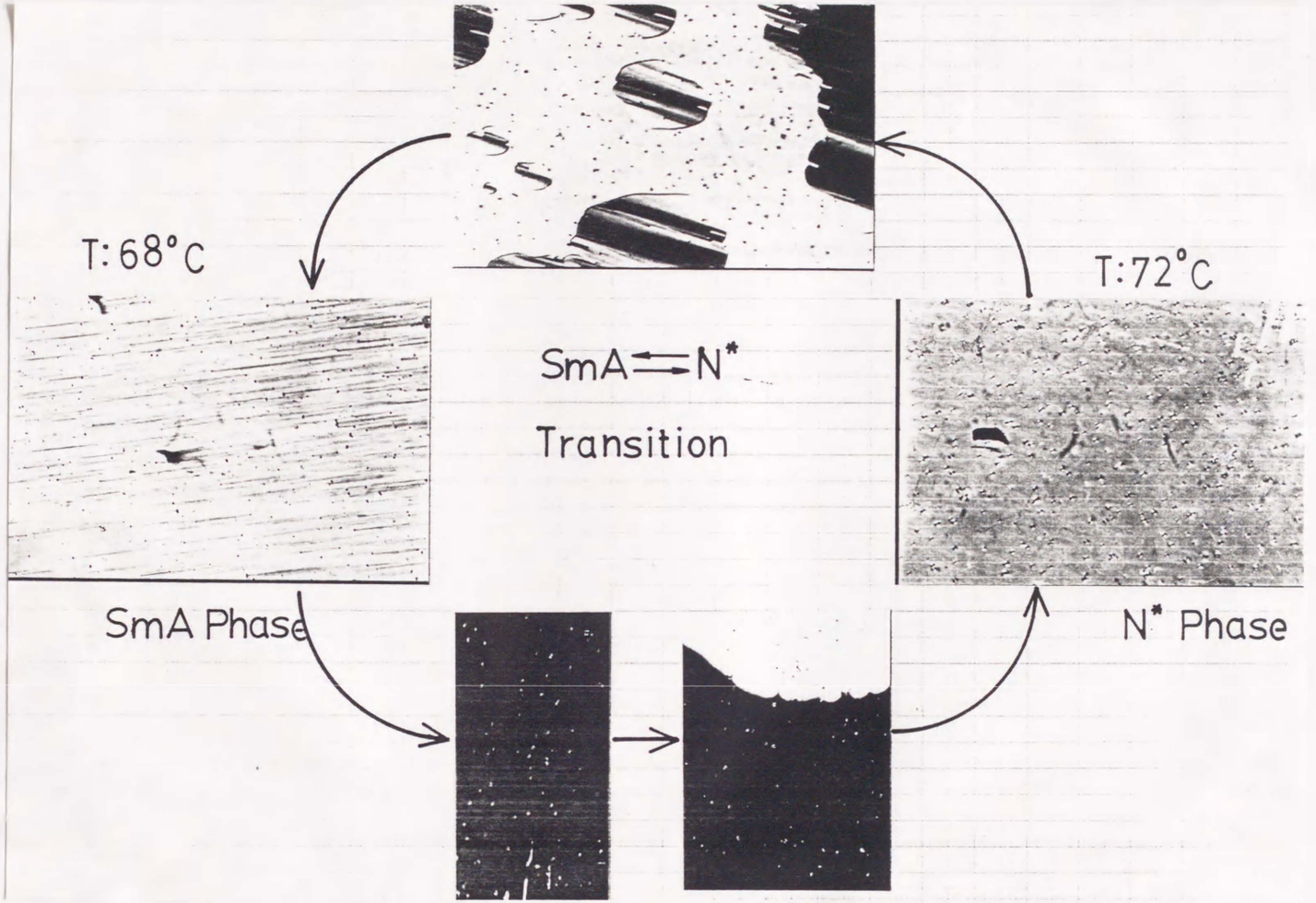

Fig.35. The variation of the defects in the smectic A phase in the neibourhood of the transition point from smectic A to the chiral nematic phase. The sample thickness is 1.8μm.

significance because the ordinary aligning film fixes the molecular director along one direction. If the surface anchoring therefor is very strong and the cell approaches a zero thickness, no EC effect can exist. On the contrary, if the cell is thick enough, the fundamental behavior of the EC effect can be observed. We also expect the surface anchoring of the EC effect to be able to provide some imformation on the surface effect in FLC. Surface anchoring strength in an arbitrary direction may be observed by investigating the balance between the torque of the electric field and surface anchoring. In EC effect, the rotation of the molecules is biased by a electric field and the microscopic states of molecules is very much like that in FLC. So the surface potential observed from ECE is also possibly adaptable for FLC.

§6.2 The experimental results showing the surface anchoring dependence of the electroclinic effect

In recent years, the electroclinic effect has been actively studied. However, no results about the influence of surface anchoring on EC effect have been reported. In this section, we will shows direct results of the influence of the surface.

① Texture variation

Fig.35 shows the texture of the SmA phase in the vicinity of the transition from chiral nematic to the smectic A phase. If the sample is very thick, the texture variation is constant whether the temperature is increasing or decreasing. This is the typical texture of the SmA phase with a layer undulations that

was discussed before. If the sample is thin enough, a new structure arises between the texture of smectic A and chiral nematic phase. In the heating process, at temperatures 2 to 3 degrees below the transition point, the undulation structure disappears. Instead, a very dark distinguishable director orientation in the cross polarizer appears due to the relaxation of defects by the surface torque. This state also shows an electroclinic effect, but much more weak than that in undulated state. Raising the temperature again, a new helicoidal structure of chiral nemetic phase arises at the ordinary transition point. In cooling the sample, the undulated structure of smectic A phase would appear directly from the chiral nematic structure. Texture variation depends strongly on the speed of cooling or heating. If we heat sample fast enough the undulated states get enough thermal energy, and changes directly to a helcoidal structure.

This result means that the director field and the layer structure are strongly affected by the surface anchoring energy.

§6.2 The influence of the electroclinic coefficient

1. The surface effect

Based on this result, we investigated the surface anchoring dependence of the electroclinic coefficient.

Before discussing the effect of the surface to EC effect, the change in the surface anchoring energy will be mentioned. As indicated above, many methods of producing different orientations of the molecular director at a solid surface have been formulared. These methods are divided into two types,

The first type, which includs the oblique deposition of SiO

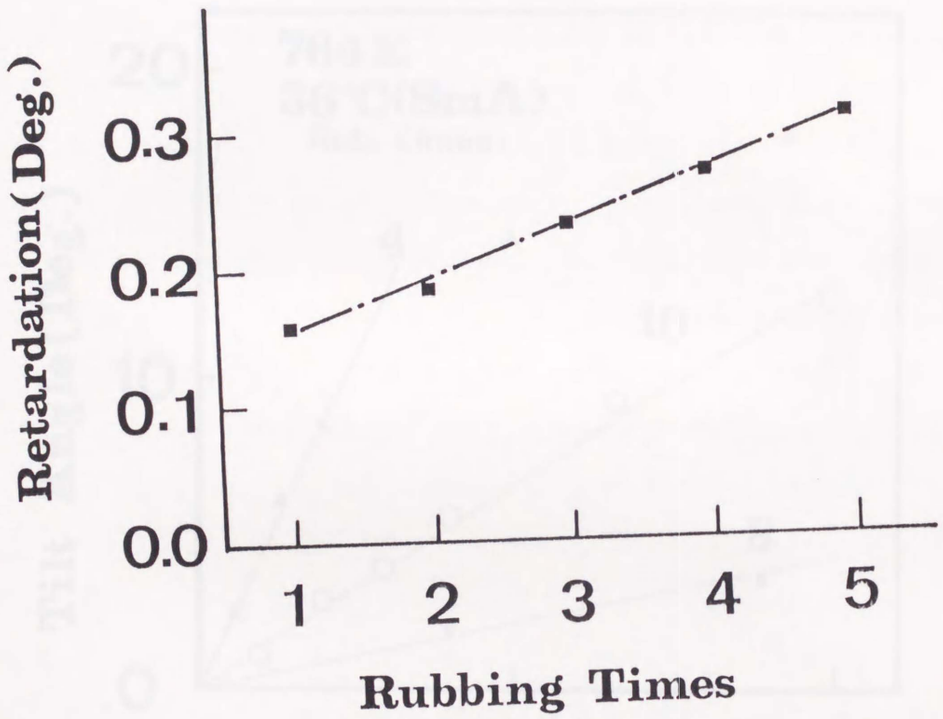

Fig.36. The relation between the induced optical retardation and rubbing number of PI surface.

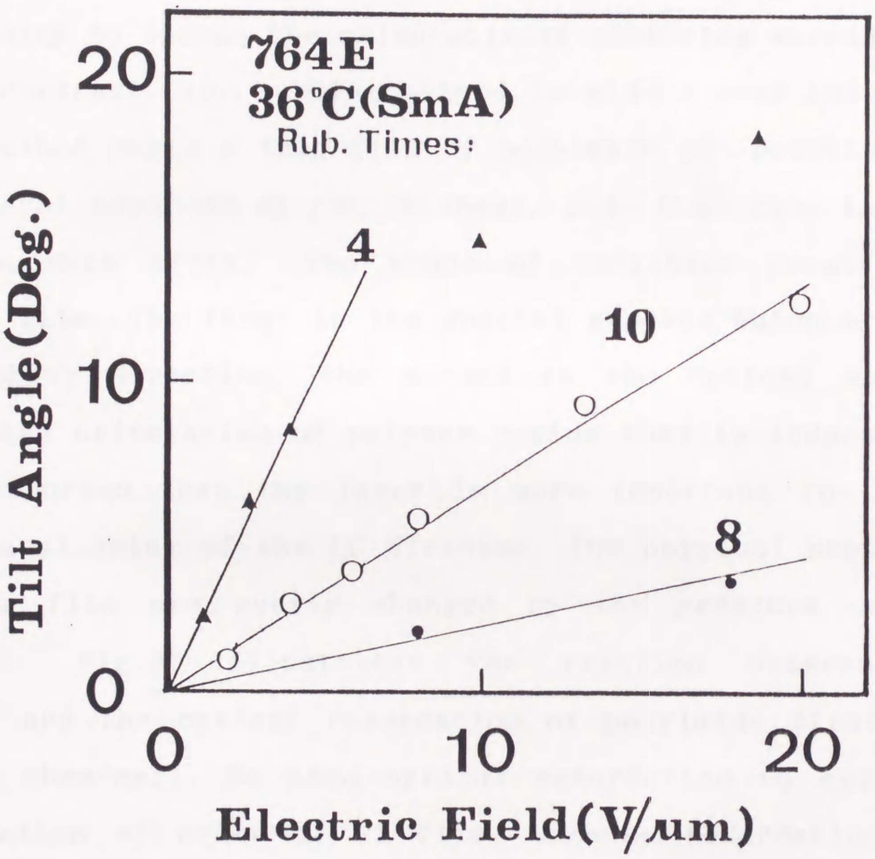

Fig.38. The influence of rubbing times of the aligning films to the EC effect.

or oblique sputtering of metal oxide, changes the surface roughness and produces micro grooves or columns (several hundreds angstrom) in a special direction. The LC molecular director would be orientated such that the material shows the smallest distortion. This method is widely used in research to produce a small sample with high pretilt angle. However, it is difficulty to change the orientational anchoring strength.

In contrast, the rubbing method is widely used industrially. This method coats a thin film of polyimide or polyvinylalchol, of several hundreds micron thikness, and then rubs the polymer surface with cloth. Two kinds of variation results in the rubbed film. The first is the special grooves which are induced in rubbing direction, the second is the optical anisotropy, i.e., the orientation of polymer chains that is induced. It has been reported that the later is more important for producing surface aligning of the LC director. The physical properties of rubbing film are easily changed by the pressure or rubbing number. Fig.36 illustrates the relation between rubbing number and the optical retardation of polyimide film(RN-305, Nissan chemical). We used optical retardation to estimate the orientation of order of PI film. Because retardation of the film can be written as $\Delta n \cdot d^*$, where d^* is the thickness of deformed part of the orientation film, Δn is the anisotropy of rubbed PI film and $\Delta n = S * \Delta n_o$. S represents the degree of orientation of the polymer chain, Δn_o is the anisotropy of the perfectly orientated PI film. From this result, it is possible to suggest that the order of polymer chain becomes higher as the rubbing pressure increases.

The surface anchoring of the molecular director increases

with the retardation as shown in Fig.37. From this result, if the retardation of the rubbing film can be changed, the anchoring strength of molecular director to the surface will likewise change. In this research, another method was used to change the retardation of the PI film.The retardation was changed by increasing the rubbing times.It was assumed that the retardation of film is proportional to the rubbing number. Fig.36 shows the experimental results based on assumption. A nearly linear relation was found between retardation and rubbing number. Hence, it can be inferred that there is a linear relation between rubbing number and surface anchoring strength.

In considering the the total energy of the sample, the bulk energy of the LC layer and surface energy are included. In general, the bulk energy is proportional to the size or the thickness of the sample. However, the surface energy is constant. So the ratio of the surface energy in the total energy may be changed by varying the sample thickness. This has been done in this research work.

② The variation of electroclinic effect

In the following section, the EC effect measured in several cells with different surface anchoring potential will be shown. Fig.38 shows one group of cells with the same thickness but different rubbing number, all other measuring conditions are the same in all of these data. It can be obtained from this graph that when the rubbing number increases, the slopes of Θ-E curve decrease. Hence the more the rubbing times, the stronger the surface anchoring strength. The sample with rubbing number of 11 shows a lower EC effect than a sample of rubbing number of 9. This can be interpreted by considering that if the rubbing

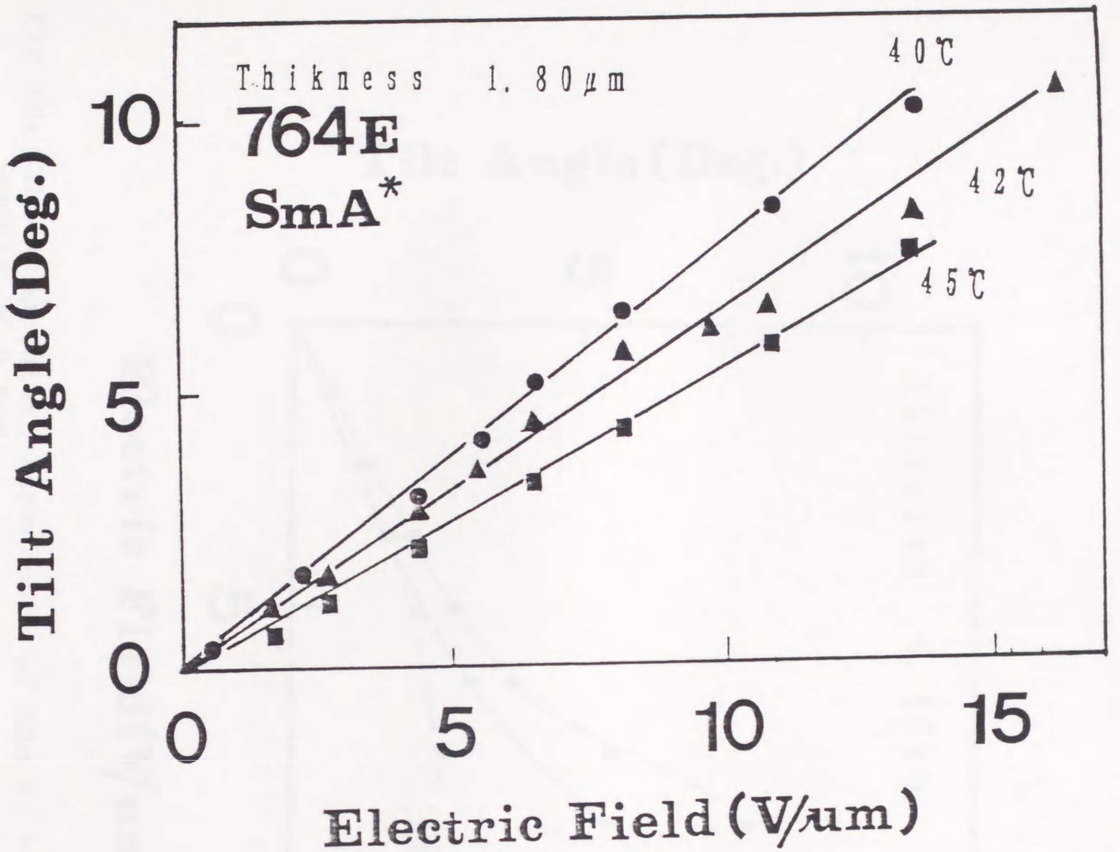

Fig.39a. The temperature dependence of the EC effect for the sample of 1.8μm.

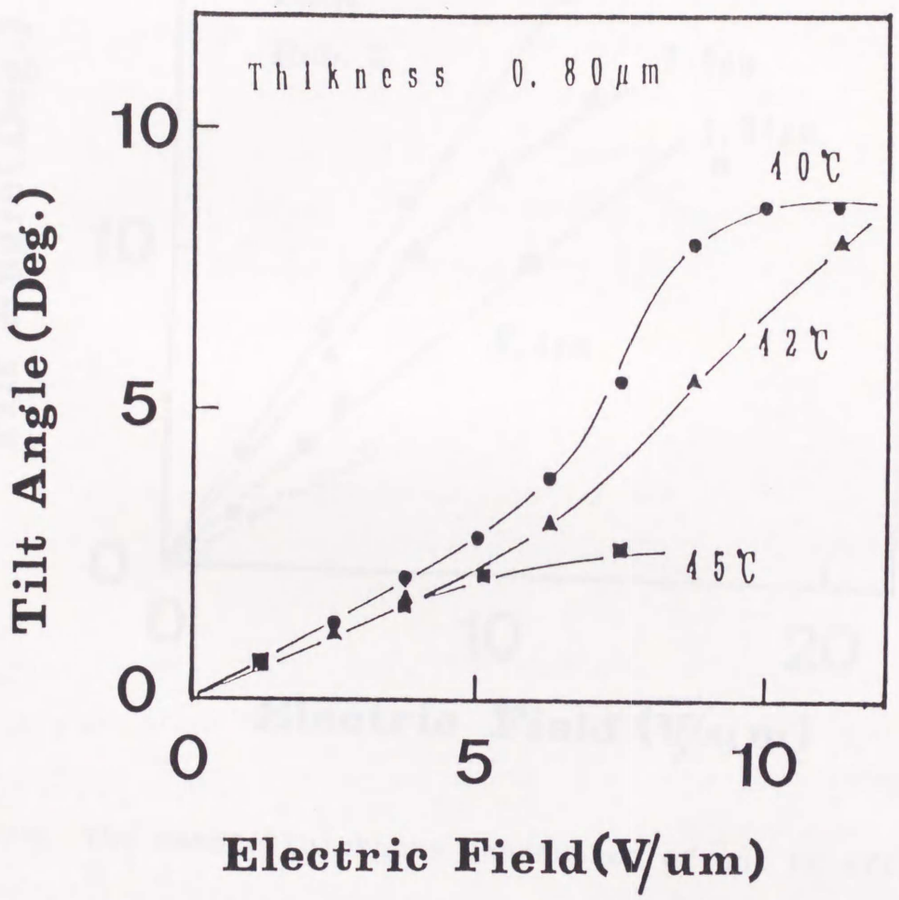

Fig.39b. The temperature dependence of the EC effect for the sample of 0.8μm.

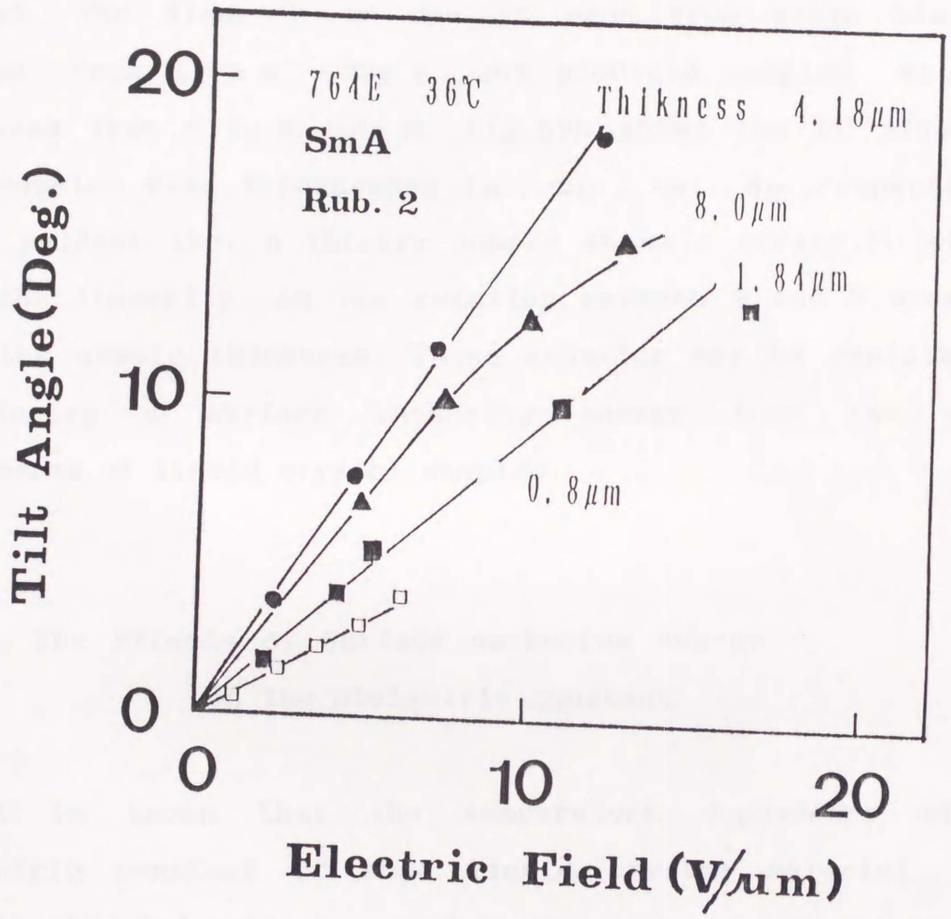

Fig.39c. The sample thickness dependence of the EC effect.

number exceeds a limit, the PI film would be scraped from the substrate surface, producing a lower surface strength.

Fig.39a shows a result where the LC medium thickness was changed. The diameter of spacers made from glass bias was changed, from 1.5μ m ~ 50μ m, and produced samples with the thickness from 0.7μ m~ 20μ m. Fig.39b shows the EC effect of four samples with thicknesses 1μ , 2μ , 4μ , 8μ ,respectively. It is evident that a thicker sample shows a larger EC effect. Also the linearity in the relation between Θ and E decreases with the sample thickness. These behavior may be explained by introducing a surface anchoring energy into the energy discussion of liquid crystal samples.

§ 6.3 The Effects of Surface Anchoring Energy on the Dielectric Constant

It is known that the temperature dependence of the dielectric constant of some liquid crystal material, which contain chiral dopant, measured at the soft mode frequency shows a divergent behavior at a critical temperature between SmA and SmC* phase[32]. This phenomenon can be explained by a theory parallel to Landau's theory of phase transitions[31 32].

However, no research has been done, on the effect of the surface anchoring potential on this transitional phenomenon.

In this section the effect of the surface potential on the phase transition phenomenon in smectic phase, in terms of the dielectric constants in the Goldstone mode at 100HZ and in the soft mode at 2KHZ wiil be reported. In the

temperature dependence of the dielectric constant in the soft mode, the phase transition temperature between SmA and SmC* phase measured from the divergent peak , and the width of the curves were shown to be strongly dependent on the surface potential.

The dependence of the dielectric constant both on the frequency and the temperature were measured with a system shown in Fig.24 consisting of YHP4274A LCR meter (5HZ- 100KHZ) and the temperature control unit and a precise hot stage (Mettler 80) which was controlled with a microcomputer. Fairly good temperature stability was achieved with an accuracy of ±0.01℃ during the data collection period. The collection of data was carried out for only the cooling process. The data of the capacitance and temperature were transferred to the microcomputer and then they were processed and the results were displayed on display unit.

The dielectric constant was measured in a freqency from 100HZ to 100KHZ. At 100HZ a dielectric response related to the Goldstone mode was obtained below the SmC*-SmA transition. To suppress dielectric response of Goldstone mode in SmC* phase, a DC field was applied through the samples.

The temperature variation of the dielectric constant is shown in Fig.25a. For low frequencies (a) corresponding to the Goldstone mode, ε_G increases with decreasing temperature of the samples below the transition point. However for high frequencies (b) corresponding to the soft mode, a frequency dependence of dielectric constant was discovered, a striking divergence was found at a region from 1-10KHZ. Considering that the transition from SmA to SmC* is a second order transition, then the divergent peak of the dielectric constant must be the

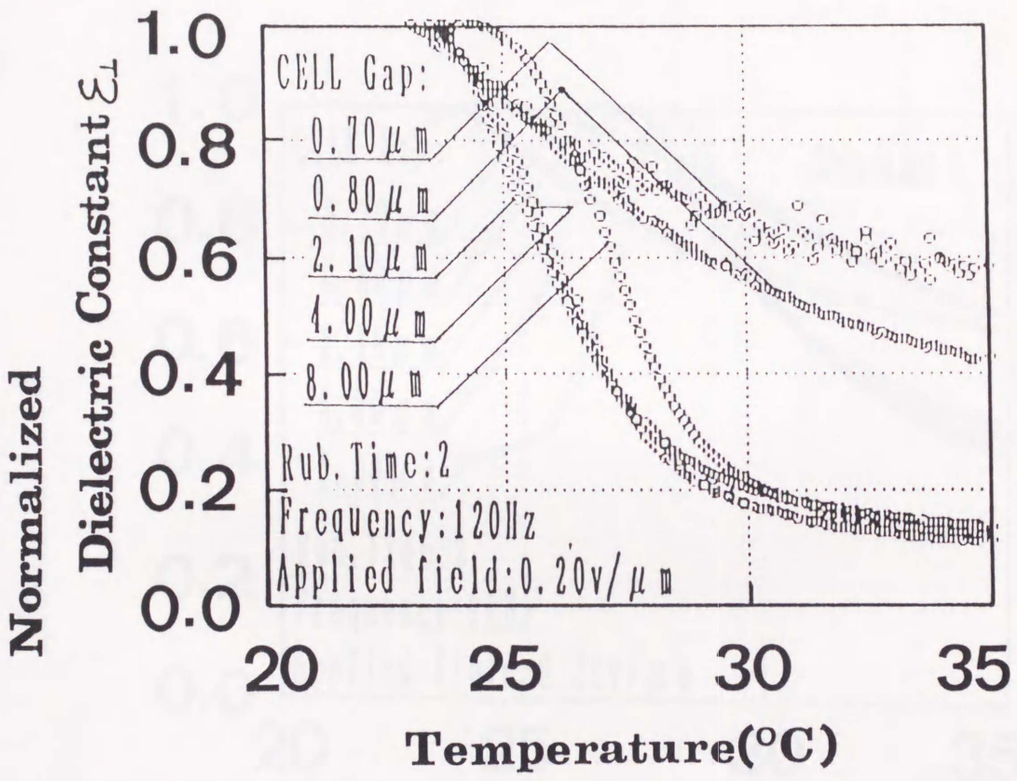

Fig.40.The influence of the sample thickness on the temperature dependence of the dielectric constants for the Goldstone mode (120HZ).

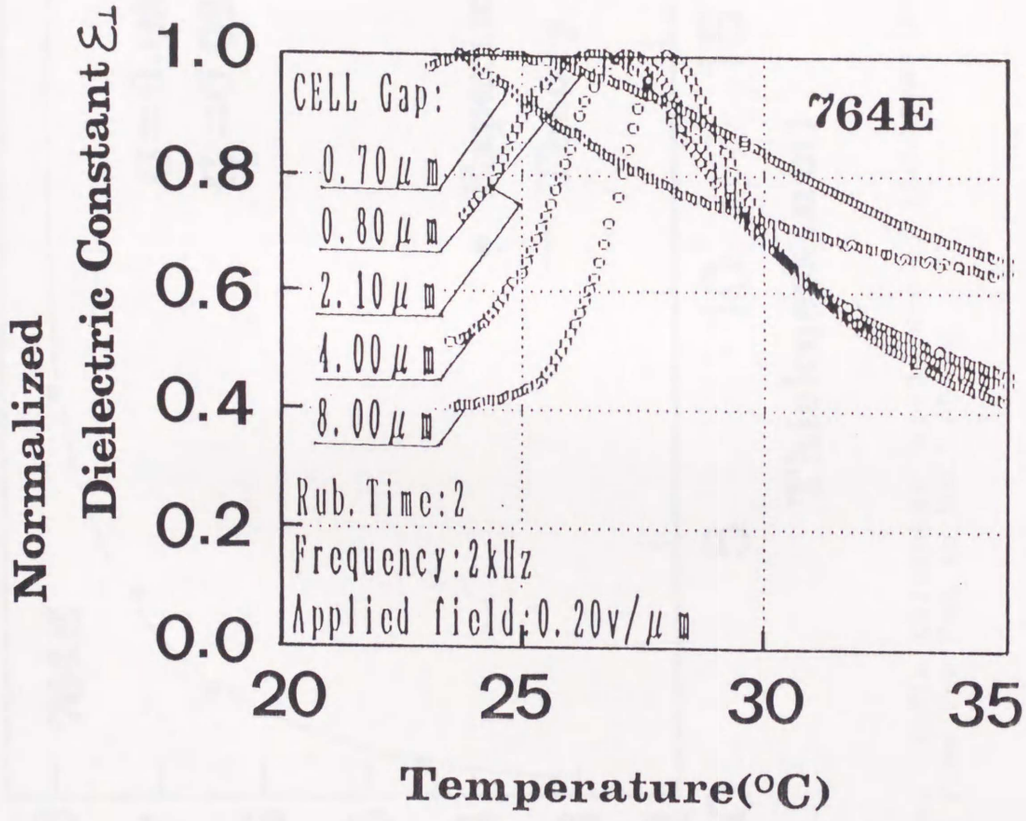

Fig.41. The influence of the sample thickness on the temperature dependence of dielectric constant for the EC effect(2KHZ).

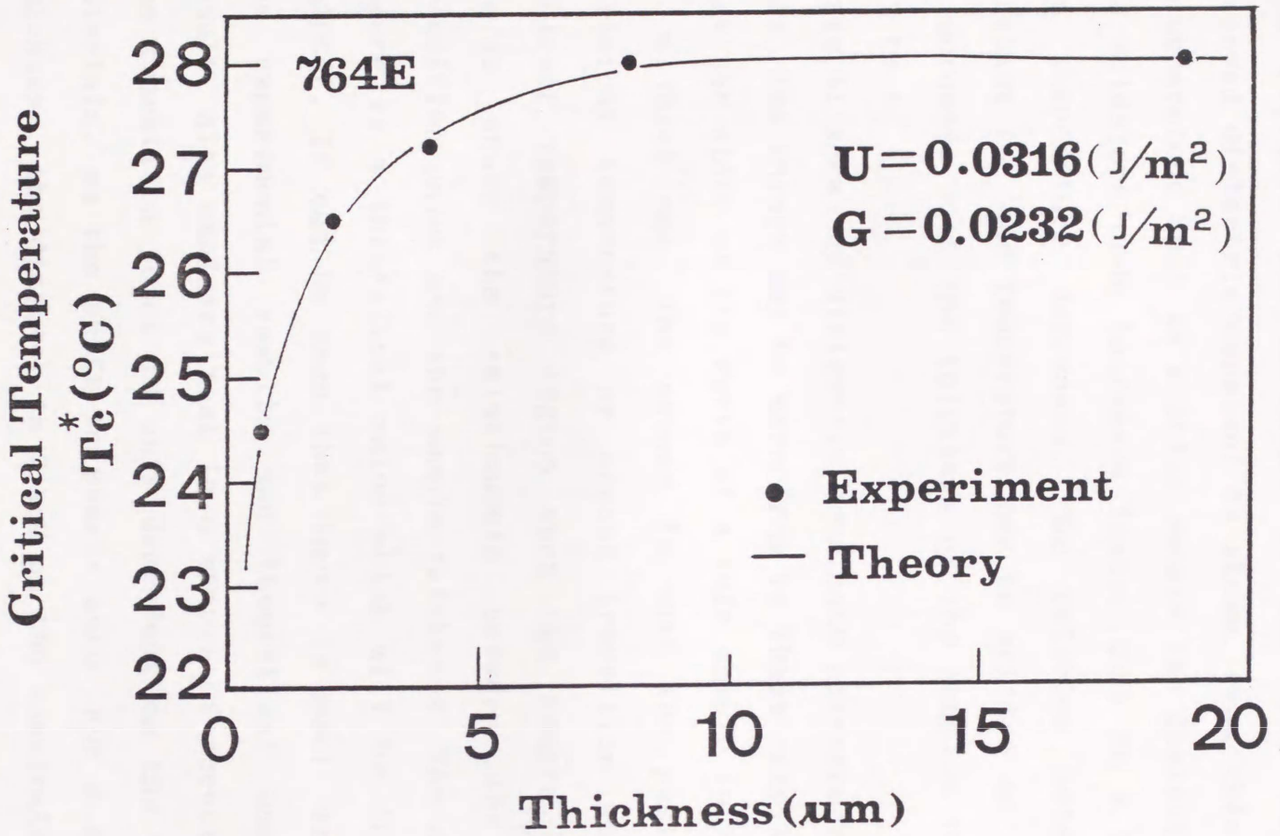

Fig.42. The sample thickness dependence of the transition point from the SmA to SmC* phase

transition point.

In Fig.40, the influence of the cell thickness on the observed dielectric constant is shown. From this result, it can be understood that in a thick sample the dielectric constant of the Goldstone mode increases faster than in a thin sample, as the temperature decreases. The relation between dielectric constant ε_G and temperature may be written as $(Tc-T)^n$, where n increases with the thickness of the samples in a region from 1/2 to 1.

Fig.41 show the dielectric constants corresponding to the soft mode. Two things may be seen from in these results. The first is that the width of the curve of a thin sample is larger than that of a thick one. The second is that the positions of peaks (critical temperature or second transition points) shift to thelower temperature region when the sample become thinner. Fig.42 shows the relationship between the second order transition point and the sample thickness. The dead line in the figure is a theoretical value which will be discussed in next chapter. It can be seen that there is good agreement between the experimental results and theoretical computations. The result also explains that in a sample of acceptable thickness, the transition point is only dependent on the property of the materials, so the shift is nearly zero. For a sample with zero thickness, the director is fixed on the substrate surface and no transition would be occur, even the temperature decreases.This means that the transition shift would be negative infinity.

To further investigate the influence of surface anchoring potential , the surface anchoring strength was controlled by

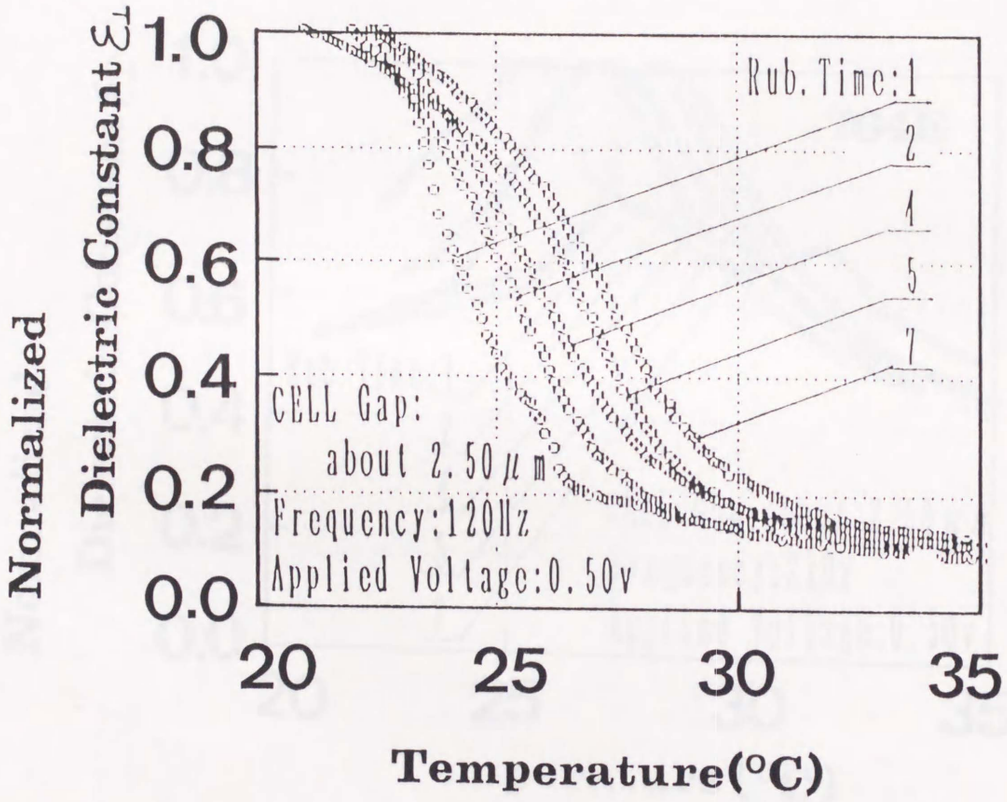

Fig.43. The influence of the rubbing number on the temperature dependence of dielectric constant for the Goldstone mode (120HZ).

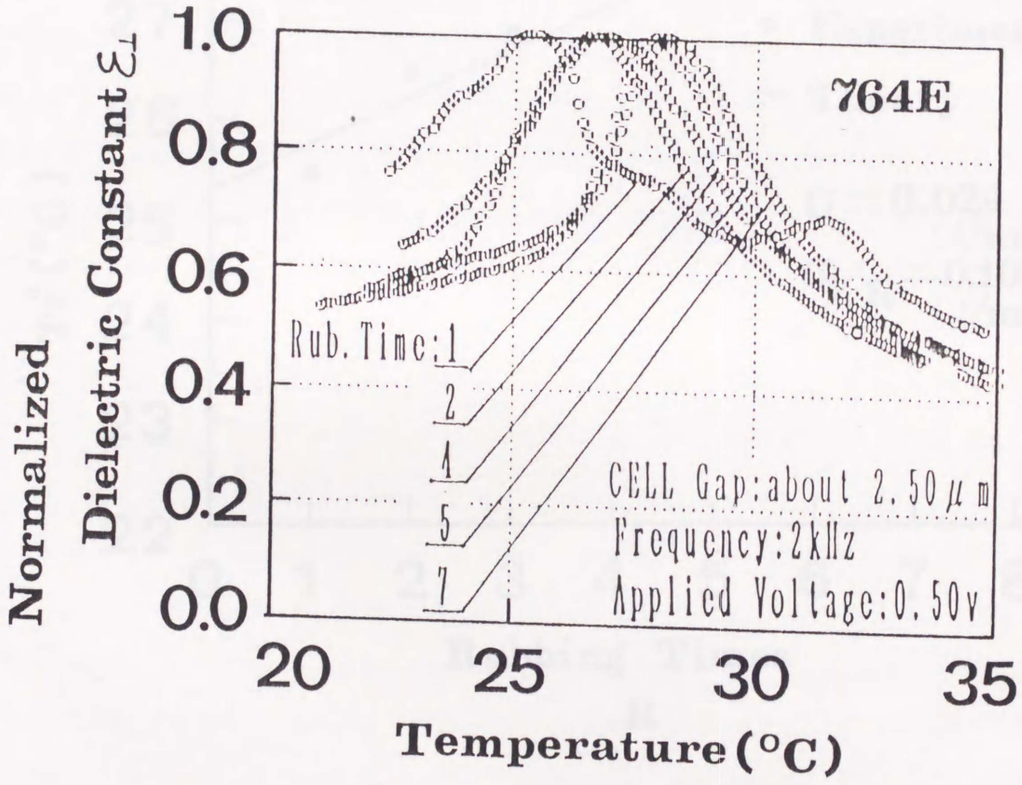

Fig.44. The influence of the rubbing number on the temperature dependence of dielectric constant for the EC effect(2KHZ).

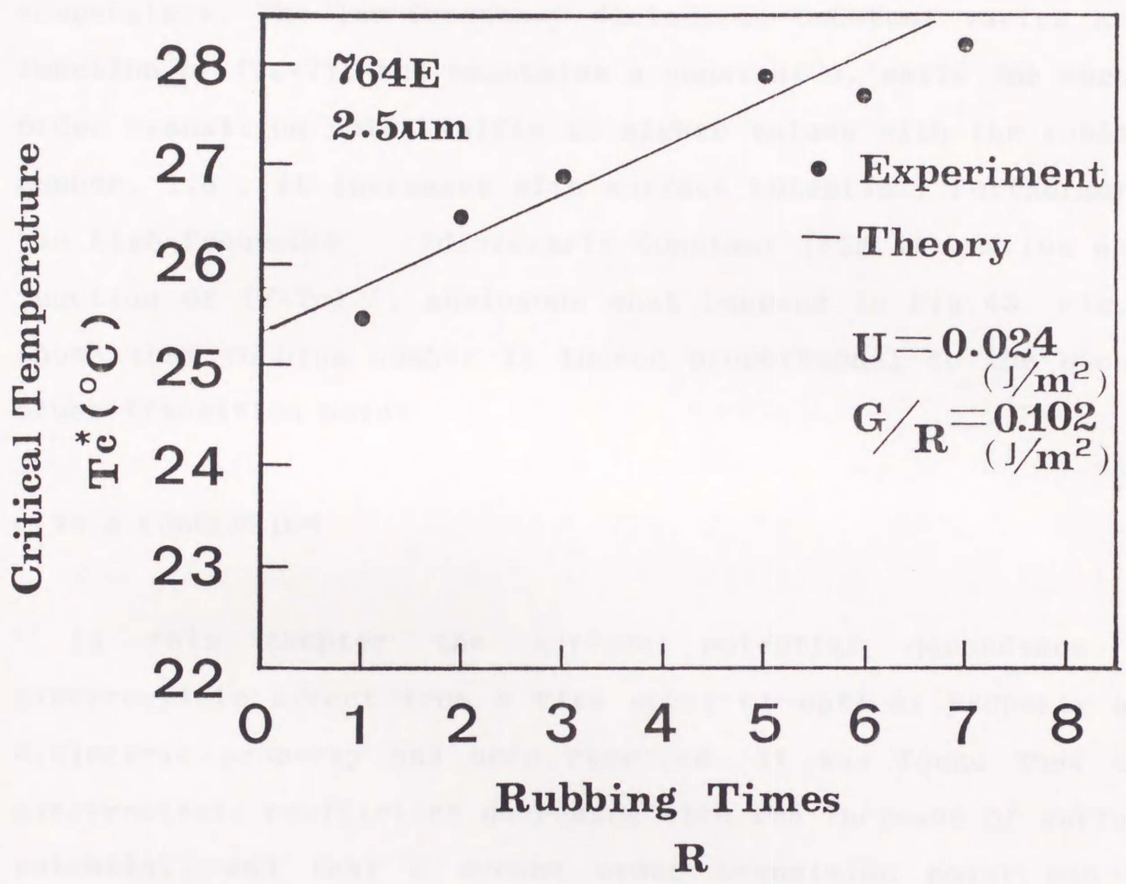

Fig.45. The rubbing number dependence of the transition point from the SmA to SmC* phase

changing the rubbing number of the polyimide orientation films. As mentioned before, the surface potential increases with the rubbing times. Fig. and Fig. show the dependence of the dielectric constant on the rubbing times as a function of temperature. The low-frequency dielectric constant varies as a function of (T_c-T), but maintains a constant n, while the second order transition point shifts to higher values with the rubbing number, i.e., it increases with surface potential. Furthermore, the high-frequency dielectric constant (Fig.44) varies as a function of $(T-Tc)^{-1}$, analogous what happens in Fig.43. Fig.44 shows that rubbing number is indeed proportional to the second order transition point.

§6.4 CONCLUSION

In this chapter the surface potential dependence of electroclinic effect from a view point of optical property and dielectric property has been reported. It was found that the electroclinic coefficient decreases with the increase of surface potential, and that a second order transition point can be shifted by a change in the surface potential. All of these results will be explained in the next chapter with the modified Landau theory.

Chapter VII A PHENOMENON THEORY OF SURFACE EFFECT IN ELECTROCLINIC EFFECT

In the last chapter it was reported that the electroclinic effect is strongly dependent on the surface potential. In this chapter the surface potential energy will be discussed with a modified Landau phenomenon phase transition theory.

§7.1 The surface potential energy

In this section a new model will be proposed to explain the surface effect observed in the electroclinic effect. As introduced in the last chapter, several models have been presented so far to interpret the surface effect in liquid crystal. A simple model whose surface potential energy consists of a polynomial expression will now be introduced.

The surface potential energy, may be divided into a polar part, which is described by odd power terms, and a non polar part, described by even power terms. For approximation, we ignored the higher order terms, and consider only the first and second orders. A similar discussion was used in the nemetic case, but a diveritive term was introduced to deal with the space variation of order parameter, that is not necessary here because the thickness of the smectic layer is hard to change by an external force as mentioned in the last chapter. Considering this factor, we get a surface potential in formula,

$$fs = -\{ U\cdot\Theta + 1/2 \cdot G\cdot\Theta^2\}\cdot\delta(z) \qquad (7.1)$$

where z is the sample thickness direction, Θ is the angle between the director, and the rubbing direction at the substrate surface. U and G are assumed to be positive constants independent on temperature and depend only on the property of the orientation films and the rubbing conditions. It is assumed that U and G are proportional to the rubbing times.

The discussion of the physical property of the smectic layer, when a surface potential is considered starts from the free energy density. The free energy density for the smectic A and the chiral smectic C phases may be written as

$$F_A^E = \frac{1}{2} A \Theta^2 + \frac{1}{2\chi} \cdot P^2 - P \cdot E - C\Theta P \tag{7.2}$$

$$F_C^E = \frac{1}{2} A \Theta^2 + \frac{1}{4} B\Theta^4 + \frac{1}{2\chi} \cdot P^2 - C\Theta P \tag{7.3}$$

The total energy of the sample can be written as

$$F_C^t = \int_0^d (F_C^E + f_s) \cdot dz \qquad F_A^t = \int_0^d (F_A^E + f_s) \cdot dz \tag{7.4}$$

Integrating F_C^t and F_A^t for z, a complete form of energy may be obtained, i.e.,

$$F_A{}^t = \left(\frac{1}{2} A'\Theta^2 + \frac{1}{2\chi} P^2 - P\cdot E - C\Theta P \right) \cdot d + \{ U\cdot\Theta + 1/2 \cdot G\cdot\Theta^2 \} \quad (7.5)$$

$$F_C{}^t = \left(\frac{1}{2} A'\Theta^2 + \frac{1}{4} B\Theta^4 + \frac{1}{2\chi} \cdot P^2 - C\Theta P \right) \cdot d + \{ U\cdot\Theta + 1/2 \cdot G\cdot\Theta^2 \} \quad (7.6)$$

From eqts. (7.6) and (7.7), the only variable is the tilt angle, while the sample thickness and temperature are two other parameter. Fig.46 illustrates the calculated results by (7.6) and (7.7), where the spindle represents the total energy and the abscissa represents the tilt angle. The temperature was taken as the third parameter. (a) shows a case where the surface potential was considered. Below the transition point, F shows two minimum with Θ, which decreases dramatically with temperature. The width of the minimum peak decreases with temperature. This means that the amplitude of the fluctuation at the minimum decreases with temperature, consequently the decrease of electroclinic effect. On the other hand, above transition point only one minimum appears in the curves. This means that in this region only smectic A is a stable state. The width of the minimums is the largest in the transition point, consequently the electroclinic effect is largest at the transition point.

Fig.47 and Fig.48 show the results where the surface potential is considered. Two parameter U and G were determined by fitting the shift of transition point. Note that G is helpful in producing a stable smectic C phase. and slightly change the EC effect. However U changes, the curves radically,

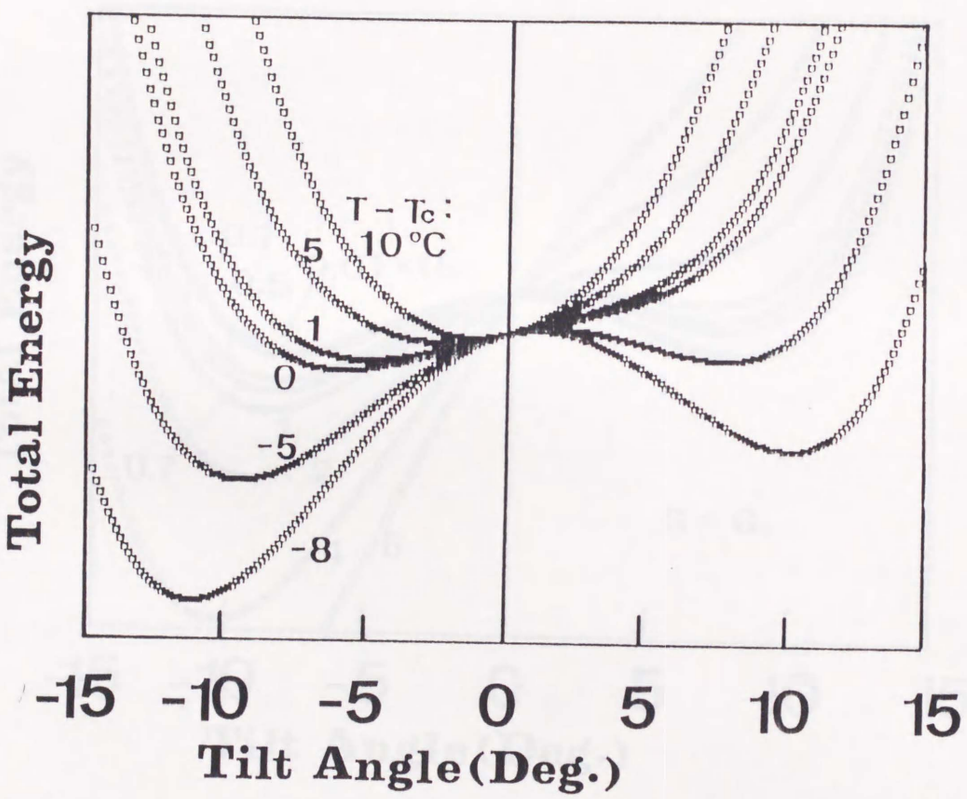

Fig.46. The total free energy for the sample of 2μm, where the surface potential parameters are U=0.0395 and G=0.232.

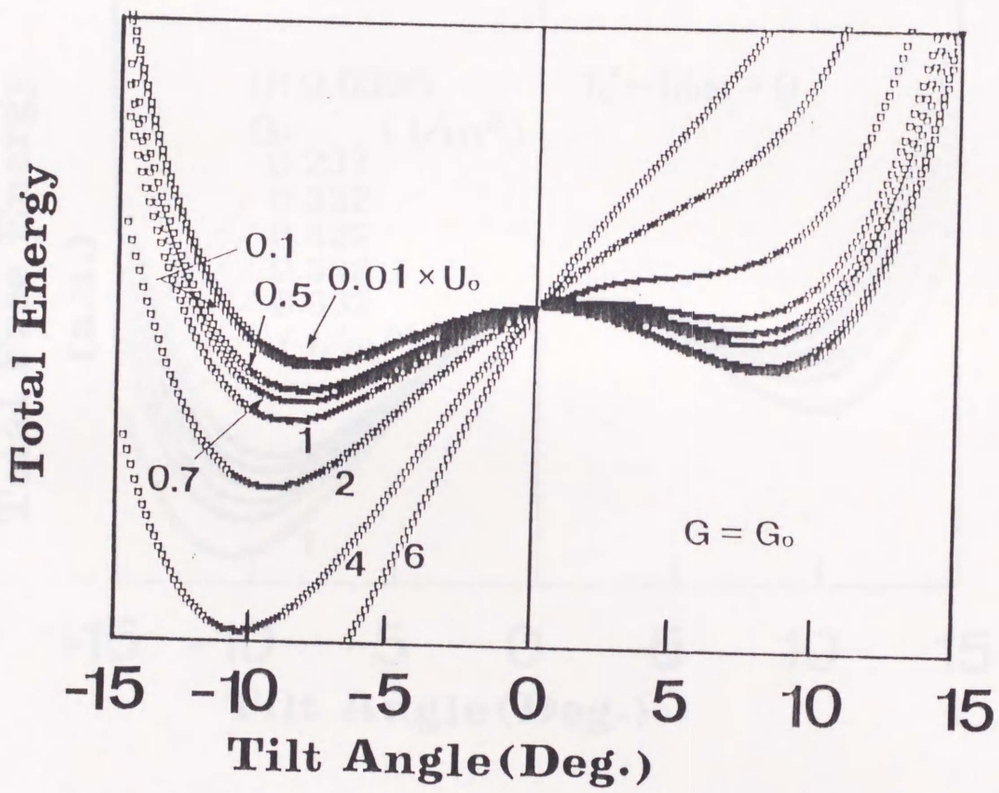

Fig.47. The total free energy for the sample of 2μm as a function of the tilt angle when the surface potential parameters is changed. where G=0.0232, ΔT=-5℃ .

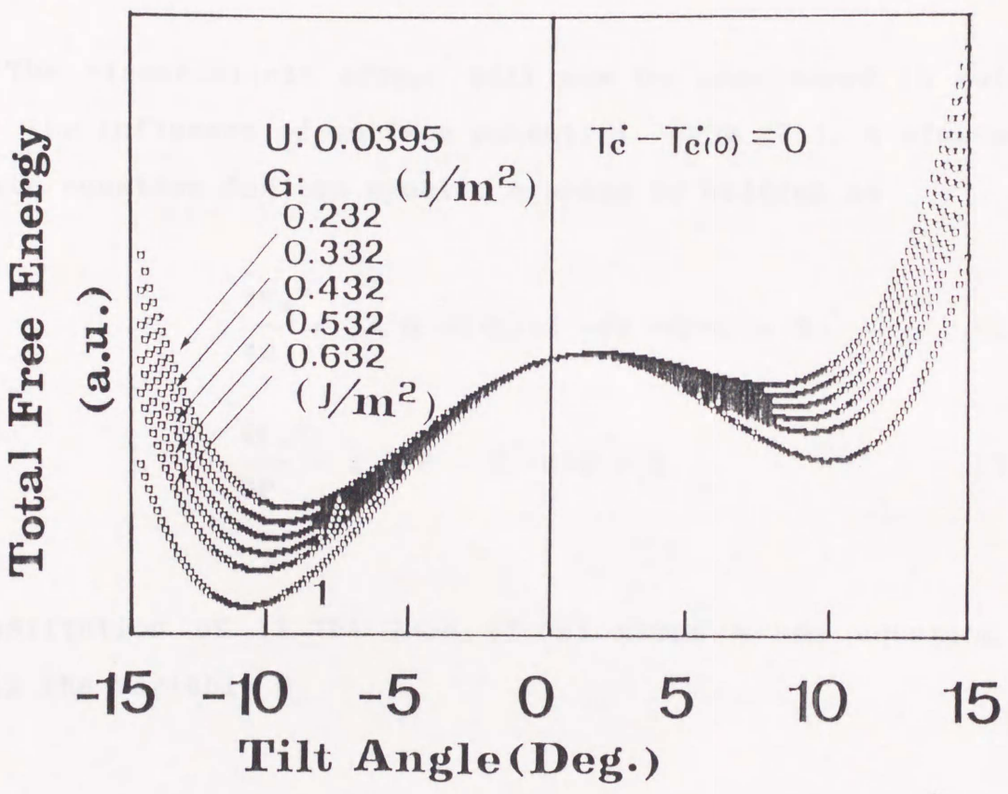

Fig.48. The total free energy for the sample of 2μm as a function of the tilt angle when the surface potential parameter is changed. where U=0.0395, ΔT=-5℃ .

showing only one stable state of the smectic phase even below the transition point. Simutaneously, U decreases the peak width of the minimum, producing a decrease of EC effect.

§7.2 In Smectic A Phase Electroclinic Coefficient and Dielectric Constant

The electroclinic effect will now be considered in relation to the influence of surface potential. From §7.1, a simutaneous state equation for the smectic A phase is written as

$$\frac{\partial F_g{}^c}{\partial \Theta} = (A\dot{}\Theta - C\cdot P)\cdot d - (U + G\cdot\Theta) = 0 \qquad (7.7a)$$

$$\frac{\partial F_g{}^c}{\partial P} = \chi^{-1}\cdot P - E - C\cdot\Theta = 0 \qquad (7.7b)$$

Substitution of (7.7b) into (7.7a) gives a new equation with only the variable Θ

$$(A\cdot\Theta - t\chi(E+t\cdot\Theta)) - \{ \frac{U}{d} + \frac{G}{d}\cdot\Theta \} = 0 \qquad (7.8)$$

The solution of (7.8) is

$$\Theta_\Lambda = \frac{\chi t}{\Lambda - \chi t^2 - G/d}\cdot E + \frac{U/d}{\Lambda - \chi t^2 - G/d} \qquad (7.9)$$

Clearly Θ_A consists of two parts; one is a spontaneous tilting induced by U, i.e.,

$$\Theta_A^{\circ} = \frac{U/d}{A - \chi t^2 - G/d} \tag{7.10}$$

This means that the introduction of a polar surface potential would necessarily produce a "small" spontaneous "incline" of the director, and hence a layer inclination as shown in Fig.48. Actually, research groups in CANNON Co.Ltd. and in Merck reported a tilting of smectic A phase.

The other one which is proportional to the strength of the applied field E, the latter being the contribution of EC effect. So if only the EC effect is considered, (7.9) can be rewritten as

$$\Theta_A = \frac{\chi t}{A - \chi t^2 - G/d} \cdot E \tag{7.11}$$

consequently the electroclinic coefficient gives

$$K_A^E = \frac{\chi t}{A - \chi t^2 - G/d} = \frac{\chi t}{a(T-Tc)} \tag{7.12}$$

Clearly, $Tc'' = Tc' + G/ad$, so a new result shows that if a non polar surface term is introduced, the phase transition point

would shift by a temperature G/ad. This is the first observation of shift of this type.

To find the dielectric behavior, Substitute eq.(7.10) back to eq.(7.6b), to obtain the polarization as

$$P = \left(\frac{\chi^2 t^2}{A - \chi t^2 - G/d} + \chi \right) \cdot E + \text{constant} \qquad (7.13)$$

Considering the relation between P and E, the dielectric constant may be written as

$$\varepsilon = (1+\chi) + \frac{\chi^2 t^2}{A - \chi t^2 - G/d} \qquad (7.14)$$

In conclusion, two new facts were revealed. One is that polar surface potential would induce a spontaneous incline in smectic A phase, the other is that the transition point would shift if a non-polar surface potential is considered.

§ 7.3 In Smectic C Phase

The smectic C phase will now be discussed. The state equation of the smectic C may be written as

$$\frac{\partial F_{g}{}^{c}}{\partial \Theta} = (A' \Theta + B \cdot \Theta^3 - C \cdot P) \cdot d - (U + G \cdot \Theta) = 0 \qquad (7.16a)$$

$$\frac{\partial F_g^c}{\partial P} = \chi^{-1}\cdot P - E - C\cdot\Theta = 0 \qquad (7.16b)$$

If no electric field exists in z direction, (b) becomes

$$Ps = \chi t\Theta_o \qquad (7.17)$$

substituting (7.17) into (7.16a) gives a new equation about Θ, i.e.,

$$B\cdot\Theta^3 + (A' - \chi t^2 - G/d)\cdot\Theta - U/d = 0 \qquad (7.18)$$

which may be written as

$$\Theta^3 + \frac{a}{B}(T-Tc')\cdot\Theta - \frac{U}{Bd} = 0 \qquad (7.19)$$

where $Tc' = Tc + \chi t^2/a + G/ad$. Let $3\alpha = \frac{a}{B}(T-Tc')$, $\beta = -\frac{U}{Bd}$, we get a new cubic equation

$$\Theta^3 + 3\alpha\Theta + \beta = 0 \qquad (7.19)$$

If two other variables are defined

$$\mu,\ \nu = \frac{1}{2}\{-\beta \pm \sqrt{\beta^2 + 4\alpha^3}\} \tag{7.20}$$

Under the condition $\beta^2 + 4\alpha^3 < 0$. Eq.(7.20) has two solutions

$$\Theta 0 = \sqrt[3]{\mu} \pm \sqrt[3]{\nu}. \tag{7.21}$$

To find the relation between Θ_o, temperature and surface potential, note that since $\beta^2+4\alpha^3<0$, so μ, ν can be written as

$$\mu,\ \nu = \frac{1}{2}\{-\beta \pm j\sqrt{-(\beta^2 + 4\alpha^3)}\} = L*\exp(\pm j\phi) \tag{7.22}$$

where

$$L = \frac{1}{2}\sqrt{\beta^2+\{-(\beta^2+4\alpha^3)\}}$$

$$= \sqrt{a^3(Tc`-T)^3} \qquad T<Tc` \tag{7.23}$$

$$\cos(\phi) = \frac{U}{Bd}\ \frac{1}{a(Tc`-T)} \tag{7.24}$$

so the solutions are now given by

$$\Theta_o = 2\sqrt{a(Tc`-T)}\cdot\cos\left(\frac{\phi+\pi}{3}\right)$$

(7.25)

$$\Theta_o = 2\sqrt{a(Tc`-T)}\cdot\cos\left(\frac{\phi-\pi}{3}\right) \tag{7.26}$$

$$\cos(\phi) = \frac{U}{Bd}\,\frac{1}{a(Tc`-T)} \tag{7.27}$$

From the above discussion, we get another phase transition condition is imposed

$$\beta^2 + 4\alpha^3 < 0 \tag{7.28}$$

Tc` indicated that above Tc` only smectic A is stable. Another transition shift $\Delta T`$ may be proposed because of the existence of the polar surface potential U

$$\left(\frac{U}{Bd}\right)^2 + 4\left(\frac{a}{3B}\right)^3\cdot(-\Delta T`)^3 = 0 \tag{7.29}$$

$$\Delta T` = 3/a\ \sqrt[3]{U^2B}\ \cdot\ 1/d^{2/3} \tag{7.30}$$

so the real transition temperature can be written as

$$Tc`` = Tc` - \Delta T`$$

$$=Tc + \frac{\chi^2 t}{a} + \frac{G}{ad} - \frac{3}{a*d^{2/3}}\sqrt[3]{U^2B} \qquad (7.31)$$

From (7.30) the transition temperature shifts to higher values when G increases. When d decreases, there two possibilities, when d is large Tc`` shifts to lower temperature.

The electroclinic effect will now be considered in relation with the surface potential. As in chapter V , the form for Θ and P when a electric field is applied may be written as

$$\Theta = \Theta_o + \delta\Theta(E) \qquad (7.32a)$$

$$P = Ps + \delta P(E) \qquad (7.32b)$$

substituting all of Θ and P into (7.7), a new equation reads

$$B\cdot(\Theta+\delta\Theta)^3 + (A`-\chi t^2 - G/d)\cdot(\Theta+\delta\Theta) - U/d = 0 \qquad (7.33)$$

$$(P+\delta P) = \chi\{E + t(\Theta+\delta\Theta)\} \qquad (7.34)$$

Neglecting higher order of δΘ, the solution is given by

$$\delta\Theta = \frac{\chi t}{A` - \chi t^2 - G/d + 3B\Theta_o^2} E \qquad (7.35)$$

$$\delta P = \chi + \frac{\chi^2 t^2}{A` - \chi t^2 - G/d + 3B\Theta o^2} E \qquad (7.36)$$

where Θ_o is the spontaneous tilt of the smectic C phase. From this formula, we can get the electroclinic coefficient and the dielectric constant

The transition point observed in the smectic A phase does not depend on U. This meanst that the transition point shift to higher temperature when d decreases, In contrast to this, the transition temperature from smectic C phase is strongly affected by U, such that Tc shifts to low temperatures when d decreases. These two factors imply that the width of dielectric curve increases with the decrease of sample thickness. This has been confirmed in the last chapter.

§7.4 The Surface Potential Dependence of The Transition Point

In this section the transition point will be discussed briefly. The transition temperature is determined by

$$Tc`` = Tc + \frac{\chi^2 t}{a} + \frac{G}{ad} - \frac{3}{a * d^{2/3}} \sqrt[3]{U^2 B} \qquad (7.37)$$

Some simulation results will be shown.

Fig.49,50 show the relation between the shift of the transition temperature and the sample thickness. In this graph, the value of U and G were determined to make good fitting to the experimental results. The best values are 0.0395 and 0.232 respectively. It is clear that the theoretical results agree

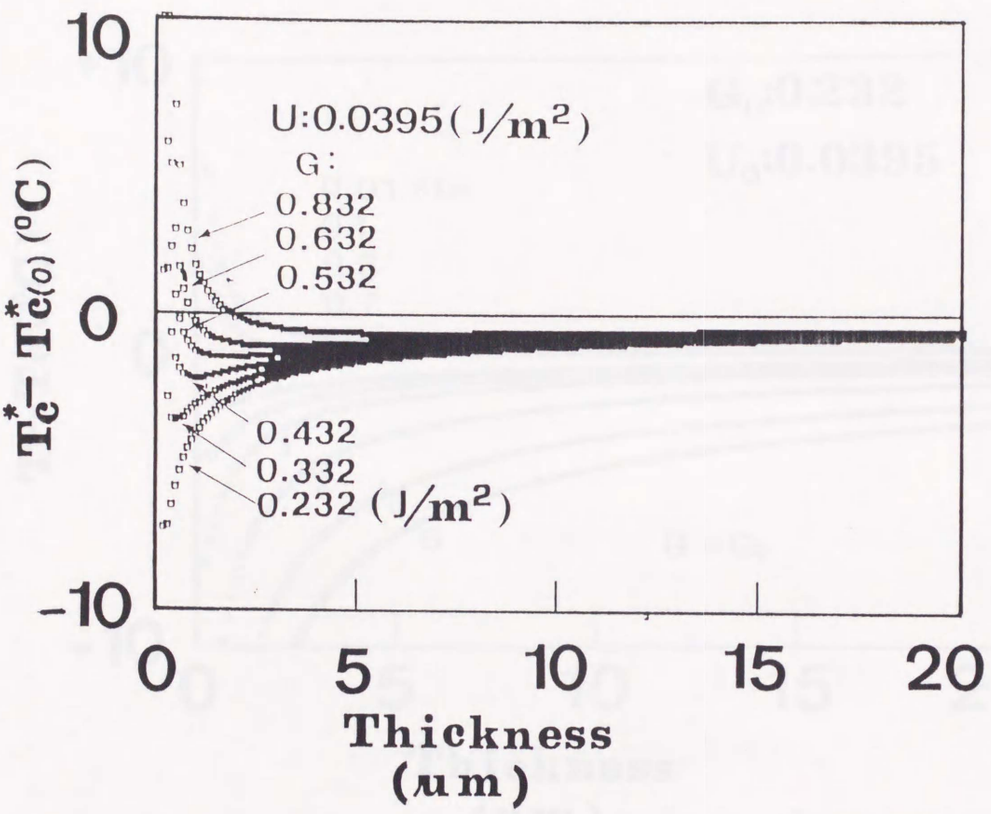

Fig.49. The shift of the transition point when changing the sample thickness. Where surface potential parameter is G=0.232.

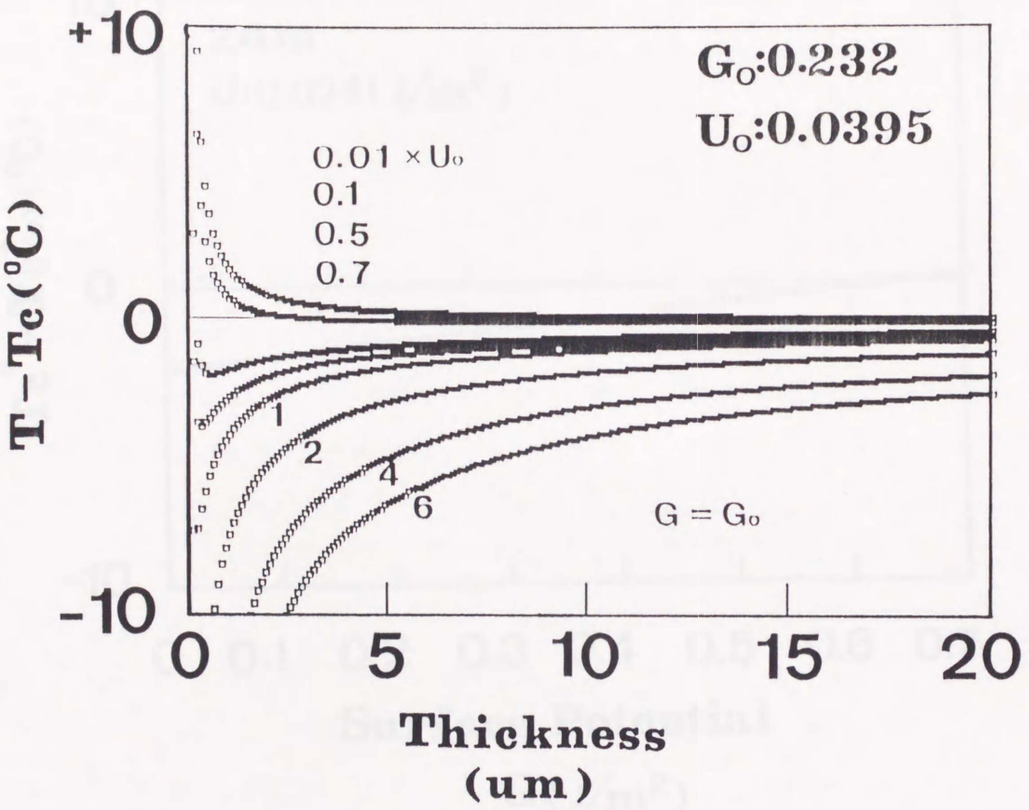

Fig.50. The shift of the transition point while changing the polar surface potential parameter U. Where G_o=0.232, U_o=0.0395

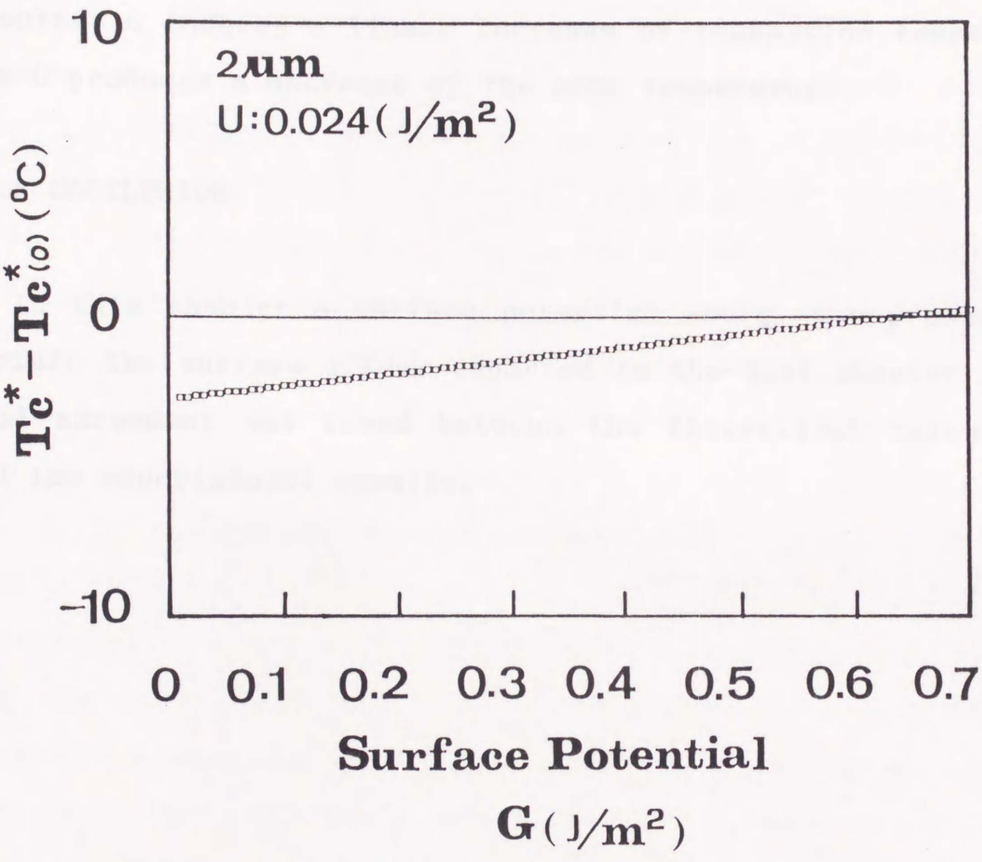

Fig.51. The shift of the transition point while changing the nonpolar surface potential parameter. Where G_o=0.232, U_o=0.0395

with the experimental results very well. If the value of U and G are changed, the relation with the transition temperature d can be found as shown in Fig. 50,51.

For the case where the sample thickness is constant, but the surface potential is varied, Fig.50,51 show the calculated results. G induces a linear increase of transition temperature. but U produces a decrease of the same temperature.

§7.5 CONCLUSION

In this chapter a surface potential energy was presented to explain the surface effect reported in the last chapter. A very good agreement was found between the theoretical calculations and the experimental results.

Chapter VIII CONCLUSION

The basic properties of the EC effect have been studied systematically from experiment and theory.

Several new experimental results have been obtained. It has been made clear that the EC effect exists not only in smectic A phase but also in chiral smectic C phase or chiral nematic phase. The critical properties of the EC effect have been studied in detail. The divergences at the transition point, for the physical properties of LC materials, which charaterize the second type phase transition have been confirmed in EC coefficient, dielectric constant and response time. It has been discovered for the first time that the EC effect is strongly dependent on the surface anchoring properties of the sample. The transition point, from the smectic A to chiral smectic C phase, is strongly dependent on the surface anchoring strength and the sample thickness.

Chapter 2 discussed the phases of liquid crystal materials and their basical physical properties, especially the E-O properties which are very important in application, has been introduced briefly. It is shown that the EC effect exhibits the highest response speed in the E-O effect of LC materials.

Chapter 3 discussed the ferroelectric liquid crystals. The FLC has been discussed by modifying Landau phase transition theory to the transition from the SmA to the SmC* phase. A detail comparison of FLC properties, between the material with EC effect and one without EC, has been made. Anomalous FLC behaviors were found in the temperature dependence of the tilt angle and polarization for the FLC materials showing EC effect.

The EC effect has been discussed in chapter 4. The EC effect

has been studied by applying Landau phase transition theory to the transition from smectic A to smectic C phase. The EC effect which is discovered in chiral smectic C is explained successfully. The surface dependence of the EC effect and the transition point have interpreted by introducing surface anchoring potential, which consists of the powers of the tilt angle, into the free energy of the LC material.

The EC coefficients K_Es have been studied in detail by measuring the birefringence of the LC sample. In the temperature dependence, K_E is found to be $(T-T_c)^{-1}$ in the SmA phase, i.e., $T>T_C$, $(T_C-T)^{-1}$ in the SmC* phase, i.e., $T<T_C$. The ratio between K_E^A and K_E^C is found to be 2.36. This value is near the prediction 2 of Landau phase transition theory.

The other physical properties of EC materials have been discussed in chapter 5. The dielectric property, dynamic property, i.e., the response time, and layer switching have been discussed. It has been shown that the dielectric constant and response time for EC effect show divergent peak at the transition point. Their temperature dependence are shown to be $(T-Tc)^{-1}$. It has shown that in EC effect, the smectic layers preserve their thickness by turning their normals around the short axis of the LC molecules.

The surface anchoring dependence of the EC effect has been discussed in chapter 6 and chapter 7. It has been shown that the EC coefficient K_E decreases with the increasing of surface potential or the decreasing of the sample thickness. The temperature dependence of the dielectric constant for EC effect is found to be strongly affected by surface anchoring. The value of the dielectric constants decreases with the increasing of the surface anchoring strength. The divergent peak, which is

referred as the transition point between SmA and SmC*, shifts to high temperature while the surface anchoring potential increases, and shifts to low temperature while the sample thickness decreases. The half width of the dielectric constant-temperature curve increases with the decreasing of the sample thickness.

The theoretical discussion on the surface anchoring dependence has been done in chapter 7. The surface potential, which exists only at the physical surfaces, consist of the two terms formula on the powers of the tilt angle. The surface potential is divided in polar and nonpolar part. The tilt angle and the polarization, when an electric field is applied, has been calculated from the condition where the total free energy takes its minimum. The theoretical discussion shows that the transition point is dependent on both surface anchoring strength and sample thickness. Quatatitive agreement between the theoretical model and experiment, has been confirmed by computer simulations. The surface anchoring dependence of the transition point shows that the rubbing treatment only changes the nonpolar part of the surface potential, does not induce any variation in polar surface potential.

This thesis only dealled with the pure physical properties of the EC effect. The EC effect is expected to find wide applications in display and optical processing. Much work has to be done on the alignment of the smectic A phase and its display properties, such as viewing angle and colour properties.

REFERENCE

1.C.M.Gomes,S.Tsujigawa,H.Maeda,H.Sekine,T.Yamazaki,M.Sakamoto, F.Okumura and S.Kobayashi, Jpn.J.Appl.Phys.30,L386(1991)

2.R.B.Meyer,L.Liebert,L.strzelecki and P.Keller, J.Physique(Lett.),36,L-69(1975).

3 N.A.Clark and S.T.Lagerwall,Appl.Phys.Lett.36,899(1980).

4 S.Garoff and R.B.Meyer, Phys.Rew.Lett.,38,848(1977).

5 S.Garoff and R.B.Meyer, Phys.Rew.Lett.A 19,338(1979).

6 G.Andersson,I.Dahl,P.Keller,W.Kuczynski,S.T.Lagerwall K.Skarp and B.Stebler,Appl.Phts.Lett. 51,640(1987).

7 S.Nishiyama,Y.Ouchi,H.Takezoe and A.Fukuda, Jpn.J.Appl.Phys., 26,L1787(1987).

8 Sin-Doo Lee and J.S.Patel,Appl.Phys.Lett.,54,1653(1989).

9 Sin-Doo Lee and J.S.Patel,Appl.Phys.Lett.,55,122(1989).

10 C.V.Raman and T.M.K.Nedungadi,Nature,145,147(1940).

11 L.A.Berensev,L.M.Blinov,M.A.Osipov and S.A.Pikin, Mol.Cryst. Liq.Cryst.158A,3(1988).

12 CH Bahr and G.Heppke,Liq.Cryst.2,825(1987).

13 R.Qiu,J.T.Ho and S.K.Hark,Phys.Rew.A 38,1653(1988).

14 C.Rosenblatt and J.D.Litster,Phys.Rew.A,26,1809(1982).

15 C.C.Huang and J.M.Viner,Phys.Rew.a 25,3385(1984).

16 Zili Li and Charles Rosenblatt,Phys.Rew.A,39,1594(1989)

17 CH Bahr,G.Heppke,and N.K.Sharma,Ferrelectrics,76,221(1987)

18 J.Pavel,M.Glogarova,Ferroelectrics,84,241(1987).

19 K.Yoshino,T.Uemoto,and Y.Inuishi,Jpn.J.Appl.Phys., 16,571(1977).

20 J.Hoffman,W.Kuczynski and J.Malecki,Mol.Cryst.Liq.Cryst., 44,287(1978).

21 B.I.Ostrovskii,A.Z.Rabinovich,A.S.Sonin and E.A.Strukov;

Sov.Phys.JEPT,47,912(1979).

22a A.Levstik,B.Zeks,I.Levsyik,R.Blink and C.Fillipic,J.Phys., 40, C3-303(1979).

22b A.Levstik,B.Zeks,I.Levsyik,R.Blink and C.Fillipic, Mol. Cryst.Liq. Cryst.Lett.,56,145(1980).

23 de Genns, "The Physics of Liquid Crystal" (Clarendon Press, Oxford, 1974).

24 R.Williams,J.Chem.Phys., 39,384(1963).

25 R. Williams,G.H.Heilmeier, J.Chem. Phys.,44, 638(1966).

26 G.H.Heilmeier, L.A.Barton and L.A.Zanoni,Appl.Phys. Lett.,13,46(1968).

27 G.H.Heilmeier,L.A.Zanoni and L.A.Barton Pro.IEEE56, 1162(1968).

28 G.H.Heilmeier and J.E.Goldmacher,Pro.IEEE,57,34(1969).

29 J.L.Fergason U.S. Patent3,731,986(1973).

30a M.Schadt W.Helfrich,Appl.Phys.Lett.,18,127(1971).

30b S.A.Pikin and V.L.Indenbom,Usp.Fiz.Nank.125,251(1978).

31 Ph.Martinot-Lagarde and G.Gurand,J.Phys.42,269(1981).

32 B.Zeks,Mol.Cryst.Liq.Cryst.,114,259(1984).

33 Ph.Martinot-Lagarde J.Phys.(Paris) Lett.38,17(1977).

34 V.Dvorak,Ferroelectrics 7,1(1974).

35 R.Blink,Phys.Status Solidi B70,K29(1975).

36 D.Cabib and L.Benguigui,J.Phys.(Paris)38,419(1977).

37 A.Michelson,D.Cabib and L.Benguigui,J.Phys.(Paris)38, 961(1977).

38 T.P.Rieker,N.A.Clark,G.S.Smith,D.S.Parmar,E.B.Sirota and C.R.Safinya,Phys.Rew.Lett.59,2658(1987).

40 K.Skarp,I.Dahl,S.T.Lagarwall and B.Stebler,Mol.Cryst.Liq. Cryst., 114,283(1984).

41 K.Miyasato,S.Abe,H.Takezoe,A.Fukuda and E.Kuze,Jpn.J.Appl.

Phys., 22,L661(1983).

42 L.M.Blinov,L.A.Beresnev,N.M.Shtykov and Z.M.Elashvili, J.Physique, 40,C3-269(1979).

43 W.J.Merz,Phys.Rew.,95,690(1954).

44 A.M.Biradar,S.S.Bawa,S.B.Samanta and S.Chandra,Phys.Stat. Solidi (a)97,427(1986).

45 K.Kondo,Y.Sato,H.Takezoe,A.Fukuda and E.Kuze,Jpn.J.Appl. Phys.,20,L871(1981).

46 K.Kondo,H.Takezoe,A.Fukuda and E.Kuze,Jpn.J.Appl.Phys., 21,224(1982).

47 S.A.Rozanski,Phys.Stat.Sol.(a),79,309(1983).

48 K.Skarp,K.Flatischler,K.Kondo,Y.Sato,K.Miyasato,H.Takezoe A.Fukuda and E.Kuze,Jpn.J.Appl.Phys.,22,566(1983).

49 K.Kondo,H.Takezoe,A.Fukuda and E.Kuze,Jpn.J.Appl.Phys., 21,224(1982).

53 R.Blink,S.Lugomer and B.Zeks,Phys.Rew.A,9,2214(1974).

54 Ph.Martinot-Lagarde and G.Gurand,Ferroelectrics,24, 89(1980).

58 M.A.Handschy,N.A.Clark,Ferroelectrics,59,69(1984).

59 Xue Jin-Zhi,M.A.Handschy and N.A.Clark,Ferroelectrics,73, 305(1987).

60 M.Odamura,S.Nonaka,K.Kondo,M.Isogai and K.Anjyo Proceeding of the SID Meeting in San Diego,1985,P.228.

List of Publication

1. Y.B. Yang, N.Nakamura, A.Mochizuki and S.Kobayashi:
   "Electric-Field-Dependence of Tilt (Cone) Angle in a Chiral Smectic C Liquid Crystal Showing Electroclinic Effect in the Smectic A Phase"
   Jpn. J. Appl. Phys. 30 (1991) ppL612-615.

2. Y.B.Yang, T.Bang, A.Mochizuki and S.Kobayashi:
   " The Surface Anchoring Dependence of the Dielectric Constant of an FLC Material Showing Electroclinic Effect"
   FERROELECTRICS,Vol.121 pp113-125.

3. Y.B.Yang, T.Bang and S.Kobayashi:
   "The Surface Anchoring Dependence of Electroclinic Effect"
   Submitted to Mol.Cryst.Liq.Cryst. for Publication.

4. Y.B.Yang, T.Bang and A.Mochizuki and S.Kobayashi:
   "The smectic Layer Deformation in Electroclinic Effect"
   Submitted to Jpn. J. Appl. Phys. for Publication.

Presentations

1. Y.B. Yang, A.Mochizuki, T.Ban and S.Kobayashi:
   "The orientation film dependence of the structure of SmA phase and electroclinic effect"
   Presented at FLC'91 Internal. Conference
   (Colorado University, Colorado, USA)

2. Y.B.Yang, N.Nakamura and S.Kobayashi:
   " The Electroclinic Effect in SmC* Phase"
   Presented at the applied physics synposium '1990
   (Morioka University, Morioka, Japan) (in Japanese)

3. Y.B.Yang, T.Bang and S.Kobayashi:
   "The surface anchoring dependence of the dieletric constant of ferroelectric liquid crystal showing electroclinic effect"
   Presented at the industrial chemics synposium'1991
   (Hokkaido University, Sapporo, Japan) (in Japanese)